THE MOLECULAR GENETIC ANALYSIS OF THE ARABIDOPSIS *ACTIN DEPOLYMERIZING FACTOR* GENE FAMILY: EXPRESSION PATTERNS AND ISOVARIANT FUNCTIONS

by

DANIEL RAYMOND RUZICKA

(Under the Direction of Richard B. Meagher)

ABSTRACT

The actin cytoskeleton plays an essential role in many cellular processes, and its diverse functions include cytoplasmic organization, establishment of cell polarity, cell elongation, endocytosis, intracellular trafficking, cytokinesis, and nuclear activities. Essential to these functions is the dynamic organization and remodeling of actin filaments by a suite of actin binding proteins (ABPs). One such ABP, Actin Depolymerizing Factor (ADF), severs and depolymerizes actin filaments creating new small polymers and re-supplying the G-actin pool, thereby increasing the dynamic remodeling capacity of the actin cytoskeleton. In *Arabidopsis thaliana*, ADF is encoded by an eleven-member gene family with four anciently conserved subclasses. We hypothesize that Arabidopsis ADFs have evolved specific expression patterns and isovariant functions enhancing the complexity of the actin cytoskeleton's regulation and function. We explored the expression pattern of each Arabidopsis ADF with multiple techniques and classified their expression into vegetative, root-hair specific, and pollen-

specific groups. We explored the functions of two ADF isovariants, ADF5 and ADF11, by way of mutant and RNA interference silencing studies. We identified ADF5 to be an important regulator of organ and cell development and a repressor of freeze tolerance. The CBF cold-response transcription factors are de-repressed and the chromatin of the CBF1 promoter is significantly altered in the *adf5-1* mutant. Complementation experiments over-expressing *ADF7* or *ADF9* in the *adf5-1* mutant were unable to restore wild-type freeze tolerance, demonstrating functional non-redundancy among some ADF isovariants. RNAi silencing of subclass II *ADF11* resulted in severe morphological and F-actin root hair phenotypes, indicating ADF11 is required for proper root hair development. Over-expression of subclass II *ADF8* or *ADF10* was able to restore normal root hair development, demonstrating that the subclass II ADFs have a conserved function. However, over-expression of subclass I *ADF4* or subclass III *ADF9* could not complement the loss of *ADF11*. In conclusion, the Arabidopsis *ADF* gene family members display a diverse range of expression patterns, including ubiquitous and cell-type specific, and a diverse range of isovariant functions, including gene regulation and F-actin remodeling, supporting our hypothesis.

INDEX WORDS: *Arabidopsis thaliana*, Actin Cytoskeleton, Actin Depolymerizing Factor, ADF, Gene Family, Subfunctionalization, Freeze Tolerance, Root Hair Development

THE MOLECULAR GENETIC ANALYSIS OF THE *ACTIN DEPOLYMERIZING FACTOR* GENE FAMILY IN ARABIDOPSIS: EXPRESSION PATTERNS AND ISOVARIANT FUNCTIONS

by

DANIEL RAYMOND RUZICKA

B.S., University of Missouri, 2003

A Dissertation Submitted to the Graduate Faculty of The University of Georgia in Partial Fulfillment of the Requirements for the Degree

DOCTOR OF PHILOSOPHY

ATHENS, GEORGIA

2008

THE MOLECULAR GENETIC ANALYSIS OF THE *ACTIN DEPOLYMERIZING FACTOR* GENE FAMILY IN ARABIDOPSIS: EXPRESSION PATTERNS AND ISOVARIANT FUNCTIONS

by

DANIEL RAYMOND RUZICKA

Major Professor: Richard B. Meagher

Committee: Michael Bender
Sarah Covert
Nancy Manley
Michelle Momany

Electronic Version Approved:

Maureen Grasso
Dean of the Graduate School
The University of Georgia
May 2008

DEDICATION

I dedicate this to my wife Kristin and to my family who have supported me throughout my education and nurtured my scientific curiosity from day one.

ACKNOWLEDGEMENTS

Many thanks to my committee members, Dr. Michael Bender, Dr. Sarah Covert, Dr. Nancy Manley, and Dr. Michelle Momany for their support, advice, and questions. A profound thanks goes to my major professor, Dr. Rich Meagher, for guiding me throughout this experience and for being a great mentor at every step along the way. Thanks to Libby McKinney and Dr. Kandasamy for giving me the best molecular and cell biology training anyone could ask for. Thanks also to everyone else in the Meagher Lab, past and present, but especially to Roger Deal and Lori King-Reid. Graduate students are the foundation of Academic research and I have been lucky to be surrounded by the best. Thanks to Judith Mank for convincing me that evolutionary genetics is useful and at times even fun. I want to give a special thanks to my family back in St. Louis for supporting my education and giving me the foundation to which I could build this endeavor on. Finally, I would like to thank my wife Kristin for her support, encouragement, strength, and love.

TABLE OF CONTENTS

LIST OF TABLES

Page

LIST OF FIGURES

Page

CHAPTER 1

INTRODUCTION AND LITERATURE REVIEW

The Actin Cytoskeleton

The actin cytoskeleton plays an essential role in many cellular processes, and its diverse functions include cytoplasmic organization, establishment of cell polarity, cell elongation, cell motility, endocytosis, intracellular trafficking, cytokinesis, and several newly evident nuclear activities (Meagher and Williamson, 1994; Pollard et al., 2000). At the cellular level, the actin cytoskeleton is comprised of actin polymer filaments (F-actin) and free globular actin monomers (G-actin) assembled and organized into a cross-linked network by a suite of actin binding proteins. Actin contains two protein domains that form its highly conserved tertiary structure. Between the two domains lies the actin fold: a hinge region containing the nucleotide-binding site. In this conserved fold, actin monomers bind ATP thus keeping the fold in its open state. Upon hydrolysis of ATP to ADP, the actin fold closes and traps the ADP nucleotide inside. Hydrolysis of ATP on actin filaments occurs at the older, “pointed ends” of filaments causing a

decrease in their stability thus conferring a polarity to the decay and turnover of actin filaments (Pollard et al., 2000).

To function as a coordinated network that can respond to multiple cellular activities, filaments are dynamically reorganized and remodeled by a suite of actin binding proteins (ABPs). Actin binding proteins including CAP1, Arp2/3, tropomyosin, fimbrin, villin, profilin, actin depolymerizing factor, and AIP1 are highly conserved across eukaryotes and their functions include filament severing, monomer depolymerizing, monomer sequestering, filament polymerizing, filament and network stabilizing, filament branching and cross-linking, and filament end-capping (Borisy and Svitkina, 2000; dos Remedios *et al.*, 2003; Paavilainen *et al.*, 2004). Each ABP is coordinately regulated to remodel the actin cytoskeleton in a process termed cytoskeleton dynamics. For example, profilin and ADF coordinate to treadmill actin filament growth in one direction during polar cell elongation by promoting actin polymerization and depolymerization. Conversely, the activation of ADF, AIP1, and gelsolin and inhibition of profilin and Arp2/3 together facilitate the rapid disassembly of the filament network during cell stress (Borisy and Svitkina, 2000; Cooper and Schafer, 2000).

Isovariant Dynamics

Higher plants and animals share the complex problems associated with multicellular development. The increase in organ and tissue complexity of plants compared to unicellular organisms correlates with an increase in cytoskeletal complexity as well (Meagher and Fechheimer, 2003). Unlike *Saccharomyces cerevisiae's* single

actin gene, *Arabidopsis* actin is encoded by an eight member gene family consisting of two anciently conserved subclasses (McDowell et al., 1996). The Arabidopsis actins phylogenetically group into ancient vegetative and reproductive categories, and isovariant differences have evolved between the two subclasses resulting in non-redundant protein functions (Kandasamy *et al.*, 2002; Kandasamy *et al.*, 2007).

In addition to the added complexity at the level of the actin gene family, the regulation of the actin cytoskeleton is also multi-layered. First termed isovariant dynamics, Meagher hypothesized that the multi-gene families of the cytoskeleton proteins confer an expansion of the plant's responses as a result of the simultaneous expression and interaction of multiple isovariants. This hypothesis of isovariant dynamics requires that the co-expressed isovariants be functionally distinct in at least one activity, but allows for their core functions to remain overlapping (Meagher et al., 1999).

An extension of the isovariant dynamics theory was proposed to explain the co-evolution of dozens of ABP gene families as well. The isovariant dynamics among the actin multi-gene family members and members of each ABP multi-gene family create a combinatorial number of interactions. Taken together with the complex model of cytoskeleton dynamics, multicellular Eukaryotes such as *Arabidopsis* have a more tightly regulated and highly buffered actin cytoskeleton. Furthermore, this system provides an interesting opportunity to study gene evolution because the spatial and temporal separation of cytoskeletal protein isovariants could allow for the evolution of novel functions or interactions (Kandasamy *et al.*, 2007).

The role of actin depolymerizing factor (ADF) in the cytoskeleton:

ADF/cofilin is a small (130-145 amino acids) actin binding protein conserved across Eukaryotes. Its primary functional role is to bind ADP-actin filaments at or near the older, pointed end. Upon ADF binding, the steric hindrance of the ADF-actin interaction causes a slight helical twist in the actin filament (McGough et al., 1997). The additive effect of multiple ADF molecules bound to a filament results in the severing of the last few actin molecules as a small polymer(Hawkins et al., 1993; Moon and Drubin, 1995). These severed polymers subsequently serve as new barbed ends for profilin-mediated actin polymerization, thus increasing the filament growth capacity of the cell (Chan et al., 2000; Ghosh et al., 2004).

Alternatively, ADF-decorated actin filaments can undergo depolymerization of actin-ADF heterodimers that re-supply the G-actin monomer pool. Upon dissociation from ADF, the actin monomers can undergo ADP-ATP nucleotide exchange and subsequently undergo polymerization onto the growing barbed ends of filaments by profilin (Carlier et al., 1997; Theriot, 1997). In summary, ADF facilitates two major processes of actin remodeling, severing and depolymerization, and the outcomes of these processes include shortening of the filaments at their pointed ends, increasing the number of small filaments available for actin polymerization at their barbed ends, and increasing the concentration of the monomeric G-actin pool.

ADF regulation

ADF's function as a high-level regulator of cytoskeleton dynamics stems from its own regulation by multiple co-factors. ADF's activity is directly regulated by its phosphorylation state (Agnew et al., 1995; Moriyama et al., 1996). ADF is phosphorylated at its N-terminal serine, which is also required for both F-actin and G-actin binding (Lappalainen et al., 1997; Blondin et al., 2001). The regulation of this serine-phosphorylation is facilitated by the LIM-kinase family of proteins, which are activated by upstream effectors ultimately regulated by the RhoGTPases. This complex upstream regulation of ADF protein activity allows for the tight regulation of ADF-actin remodeling in response to a variety of extra-cellular and intra-cellular signals (Moon and Drubin, 1995).

Another regulatory mechanism of ADF activity is intracellular pH. At lower pH's (below 7.0), ADF is held in its inactive state and cannot bind-to, nor depolymerize/sever actin filaments. A subsequent increase in pH restores ADF's actin binding and remodeling functions. *In vivo*, this is likely a combination of direct effects of pH on the conformation of the ADF protein, and indirect effects on ADF through upstream effectors such as the RhoGTPases and LIM kinases (Yonezawa et al., 1985; Hawkins et al., 1993; Hayden et al., 1993).

The RhoGTPases also regulate the production and localization of phosphatidyl inositol phosphate (PIP) and phosphatidyl inositol 4,5-bisphosphate (PIP_2), two key regulators of ADF. PIP_2 acts as an inhibitor of ADF activity, whereby an increase in the concentration of PIP_2 leads to the dissociation of ADF from actin. The actin and PIP_2

binding sites on ADF are overlapping, thus high concentrations of PIP_2 out-compete actin for ADF binding, resulting in a decrease in cytoskeletal remodeling (Moon and Drubin, 1995). Lastly, although the mechanism of ADF dephosphorylation is unknown, it results in the activation of ADF. ADF activators include calcium, growth factors, and cAMP (Moon and Drubin, 1995). In summary, multiple upstream pathways and cellular signals tightly and coordinately regulate ADF activity. This regulation results in changes in actin cytoskeleton organization and remodeling.

Nuclear functions of ADF

Previous studies have characterized the subcellular localization of ADF/cofilin as both cytoplasmic and nuclear in a range of Eukaryotes (Matsuzaki *et al.*, 1988; Ohta *et al.*, 1989; Iida *et al.*, 1992; Abe *et al.*, 1993; Nebl *et al.*, 1996; Ruzicka *et al.*, 2007). Nuclear phenotypes such as alterations in gene regulation have been characterized in hypo- and hyper-morph ADF alleles in a variety of organisms (Dong *et al.*, 2001c; Ruegg *et al.*, 2004). ADF may affect gene regulation via cytoplasmic or nuclear functions, but the function of nuclear ADF is a subject of debate and of limited empirical evidence. Hypothesized roles include the nuclear import of actin monomers, nuclear remodeling of actin rods, actin and actin related protein (Arp) binding in nuclear protein complexes, and novel ADF functions.

Considering a nuclear import role, Nebl *et al* demonstrated that ADF/cofilin is required for the nuclear localization of actin. ADF contains a nuclear localization sequence, and pre-incubation of cells with anti-cofilin antibody inhibited the nuclear

import of actin. Alternatively, ADF may remodel nuclear actin rods in a mechanism similar to ADF-actin cytoskeletal remodeling in the cytosol (Nishida *et al.*, 1987). With either of these roles, ADF activity would alter the concentration of actin monomers in the nucleus. Nuclear actin binds transcription factors thus affecting their activity, nuclear actin is a component in chromatin remodeling complexes, and nuclear actin is required for RNA polymerase I, II, and III activity (Dong *et al.*, 2001b; Hofmann *et al.*, 2004; Hu *et al.*, 2004; Philimonenko *et al.*, 2004; Posern *et al.*, 2004) (See review in (Miralles and Visa, 2006)). Therefore, it is possible that ADF could indirectly affect these nuclear processes via its role in actin transport or actin dynamics in the nucleus. Furthermore, the nuclear actin-related proteins (Arps) function exclusively in nuclear protein complexes including chromatin remodeling machinery, and share modest sequence identity with the conventional actins (Blessing *et al.*, 2004; Meagher *et al.*, 2007). It is therefore plausible that ADFs could bind Arps and affect their participation in these complexes.

To consider the possibility that ADF affects gene regulation via cytoplasmic functions, there are now multiple examples of actin cytoskeleton dynamics altering gene regulation through the nuclear import of G-actin-transcription factor complexes (Miralles *et al.*, 2003; Ruegg *et al.*, 2004; Vartiainen *et al.*, 2007). These actin-TF complexes and their localization are modulated by the ratio of F-actin to G-actin, a process directly controlled by ADFs. To complicate the picture even further, the nuclear localization of these actin-TF complexes may depend on ADF given its role in transporting actin into

the nucleus. In summary, ADF has numerous roles that could affect gene regulation either in the cytoplasm, the nucleus, or through the nuclear localization of actin.

ADF in the plant kingdom

Vertebrate, invertebrate, and plant genomes all encode multiple ADF gene members. A phylogeny of the ADF gene family across all eukaryotes resulted in each kingdom having a single monophyletic clade, indicating that the multi-gene families have independent origins and do not predate the evolution of the kingdoms. Species in the plant kingdom contain an especially large number of ADF genes, which have been grouped into at least four subclasses (Maciver and Hussey, 2002). Land plants have undergone multiple polyploidization events in their ancient history (Simillion et al., 2002), and early whole genome duplications could have created the ancient subclasses while subsequent polyploidization events and individual gene duplications would have expanded the number of genes in each subclass.

Gene duplications frequently lead to gene dosage problems and redundant genes are silenced through mutations and heterochromatin establishment, but plants have slower rates of silencing and can maintain duplicates longer as reviewed in (Moore and Purugganan, 2005). Ohno wrote that over evolutionary time, gene duplicates were either lost via silencing or gained new functions (neofunctionalization) (Ohno, 1970). More recently however, genomic evidence supports a third outcome for gene duplicates termed subfunctionalization. Subfunctionalization is the accumulation of function-altering, but complementary, mutations that modify one or more subfunctions in the duplicate genes (Lynch and Force, 2000). The organism does not experience a net

gain or loss of functions, but instead divides the existing functions of the original gene member between the multiple new members. This process allows for tighter regulation and the evolution of more complex (specialized) mechanisms. Considering the ADF gene family, subfunctionalization could be responsible for the evolution of tissue specific expression or unique actin-ADF protein interactions. Given that the plant actins also form a large gene family including eight functional isovariants in Arabidopsis, we hypothesize that ABPs such as ADF co-evolved isovariant-specific interactions with different actins, thus selecting for the co-expansion of the actin and ADF gene families and for their maintenance in the genome.

Based on the phylogeny of ADF proteins across many plant species, Maciver proposed that the ADF subclasses could be grouped into vegetative and reproductive-specific clades. This type of subfunctionalization into specific expression patterns could be partially responsible for the ADF gene family's conservation (Maciver and Hussey, 2002). However, because of limited gene-specific expression data for the ADFs in their phylogenetic study, tissue-specific expression data from monocot *Zea mays* (corn) ADFs 1, 2, and 3 and dicot *Arabidopsis* ADFs 1, 5, and 6 were relied upon to classify these two expression pattern clades (Lopez et al., 1996).

For the *Z. mays* ADF gene members, antibodies specific to the ADF isovariants were used on a western blot to probe for protein localization within a variety of tissues. From this characterization, they concluded that *Z. mays* ADF3 was localized to vegetative tissues while *Z. mays* ADF1 and ADF2 were reproductive specific (Lopez et al., 1996). The major limitation to this study was the lack of a complete *Z. mays*

genome sequence and thus a complete *Z. mays* ADF gene family. Without a complete genome sequence to query, it can be assumed that there are additional ADF gene members in *Z. mays* that could further resolve their phylogenetic and expression-pattern relationships. Also, the anti-ADF antibodies used to characterize ZmADF 1, 2, and 3 localization could have cross-reacted with unknown ADF isovariants and given the appearance of broader tissue specificity for ADFs 1, 2, and 3. Further evidence for the limitations of this study comes from the monocot *Oryza sativa*. The *Oryza sativa* genome has been completely sequenced and contains eleven putative ADF gene members, indicating that there are likely more than three *Zea mays* ADFs (Yuan et al., 2003). There are no previous studies of the expression patterns of the *ADF* gene family in *Oryza* however, so the resolution of the *ADF* gene family is still very limited in the monocots. Additional studies on plant ADFs have characterized the function of *Lilium longiforum* (lily) and *Nicotiana tabacum* (tobacco) ADFs (Allwood et al., 2002; Chen et al., 2003). These studies focused on ADF's role in polar tip growth, RhoGTPase signaling pathways, and the regulation of ADF by N-terminal serine phosphorylation.

Arabidopsis ADF

Previous work on the *ADF* gene family in *Arabidopsis* partially characterized *ADF* expression patterns, but recent studies in petunia identified an important enhancer element missing from the Arabidopsis studies. Dong *et al* initially dissected the expression patterns of *Arabidopsis ADF1*, *ADF5*, and *ADF6* (Dong et al., 2001a) using a transcriptional fusion of the *GUS* reporter gene to the respective *ADF* promoter. By assaying for GUS protein activity, they analyzed the tissue specificity of each of the

three *ADF* genes. *ADF1* and *ADF6* were weakly expressed in vascular bundles and other vegetative tissues while *ADF5* expression localized exclusively to the root-tip meristem. Most Arabidopsis *ADF* gene family members exhibit a conserved gene structure where the first intron directly follows the ATG start codon. Additionally, this first intron is significantly larger than the average Arabidopsis intron size. Mun *et al* used GUS studies of the petunia *PtADF1* promoter to demonstrate that the first intron is essential for replicating expression level and localization characteristics of the endogenous locus (Mun et al., 2000; Mun et al., 2002).

In addition to the expression pattern studies, *Arabidopsis* ADF1 has also been studied from a more functional perspective (Dong *et al.*, 2001b). ADF1 was constitutively expressed under the 35S tobacco mosaic virus promoter (35S) in both the sense and anti-sense direction. From this, they correlated a range of phenotypes with the over-expression or reduced expression of *ADF1*. Overexpression of *ADF1* caused irregular cellular and tissue development, and an overall reduced growth rate. Reduced expression resulted in a delay in flowering time, increased cell expansion, and an increased growth rate. The anti-sense sequence of the *ADF1* coding region was highly expressed to create a knockdown allele, but there was significant off-target *ADF* gene silencing as well. Without further characterization of which *ADF* genes were affected, the phenotypes characterized in this study can only be interpreted as *ADF* gene family defects and cannot be assigned to specific gene members.

In conclusion, at the initiation of this study, the literature dissecting the *Arabidopsis ADF* gene family was limited and disjointed. This thesis aims to thoroughly characterize the *Arabidopsis* ADF gene family in regard to both expression patterns and

isovariant functions. We have developed a range of tools for dissecting ADF functions including antibodies, GUS-reporter transgenes, and T-DNA and RNA interference alleles. Chapter 2 of the dissertation will detail the analysis of the expression patterns and subcellular localization of the entire Arabidopsis *ADF* gene family. Furthermore, we show that subclass II *ADFs* have undergone subfunctionalization of expression patterns in the Arabidopsis lineage when compared to the subclass II ADFs of the anciently related monocot *Oryza sativa*. Chapter 3 focuses specifically on the function of ADF5 and details its role in organ and cellular proliferation and also its role in the repression of the cold-response transcription factors *CBF1, 2*, and *3*. Furthermore, through paralogous complementation experiments we show that other ADF isovariants cannot complement the *adf5-1* mutant defect, arguing that the Arabidopsis ADFs are functionally distinct. This chapter presents a strong case for an ADF5 gene regulation activity, and begins to dissect what mechanisms this function may entail. Chapter 4 details the characterization of ADF11, a root hair specific ADF. ADF11 is required for proper root hair growth and its knockdown grossly affects the organization of the actin cytoskeleton in root hair cells. Interestingly, experiments testing the paralogous complementation of the ADF11 knockdown phenotypes show that subclass II ADF8 and ADF10 can at least partially complement the root hair defects. In addition to these chapters, this thesis includes an appendix where the candidate was co-first author. In appendix A, we detail the functional characterization of Arabidopsis ADF9 as an important regulator of flowering time through changes in the expression of high-level

regulators including the floral repressor *FLC*, furthering our understanding of the diverse Arabidopsis ADF gene family.

REFERENCES

Abe, H., Nagaoka, R. and Obinata, T. (1993) Cytoplasmic localization and nuclear transport of cofilin in cultured myotubes. *Exp Cell Res*, **206**, 1-10.

Agnew, B.J., Minamide, L.S. and Bamburg, J.R. (1995) Reactivation of phosphorylated actin depolymerizing factor and identification of the regulatory site. *J Biol Chem*, **270**, 17582-17587.

Allwood, E.G., Anthony, R.G., Smertenko, A.P., Reichelt, S., Drobak, B.K., Doonan, J.H., Weeds, A.G. and Hussey, P.J. (2002) Regulation of the pollen-specific actin-depolymerizing factor LlADF1. *Plant Cell*, **14**, 2915-2927.

Blessing, C.A., Ugrinova, G.T. and Goodson, H.V. (2004) Actin and ARPs: action in the nucleus. *Trends Cell Biol*, **14**, 435-442.

Blondin, L., Sapountzi, V., Maciver, S.K., Renoult, C., Benyamin, Y. and Roustan, C. (2001) The second ADF/cofilin actin-binding site exists in F-actin, the cofilin-G-actin complex, but not in G-actin. *Eur J Biochem*, **268**, 6426-6434.

Borisy, G.G. and Svitkina, T.M. (2000) Actin machinery: pushing the envelope. *Curr Opin Cell Biol*, **12**, 104-112.

Carlier, M.-F., Laurent, V., Santolini, J., Melki, R., Didry, D., Xia, G.-X., Hong, Y., Chua, N.-H. and Pantaloni, D. (1997) Actin depolymerizing factor (ADF/cofilin) enhances the rate of filament turnover: Implication in actin-based motility. *J Cell Biol*, **36**, 1307-1323.

Chan, A.Y., Bailly, M., Zebda, N., Segall, J.E. and Condeelis, J.S. (2000) Role of cofilin in epidermal growth factor-stimulated actin polymerization and lamellipod protrusion. *J Cell Biol*, **148**, 531-542.

Chen, C.Y., Cheung, A.Y. and Wu, H.M. (2003) Actin-depolymerizing factor mediates Rac/Rop GTPase-regulated pollen tube growth. *Plant Cell*, **15**, 237-249.

Cooper, J.A. and Schafer, D.A. (2000) Control of actin assembly and disassembly at filament ends. *Curr Opin Cell Biol*, **12**, 97-103.

Dong, C.H., Kost, B., Xia, G. and Chua, N.H. (2001a) Molecular identification and characterization of the *Arabidopsis AtADF1*, *AtADFS* and *AtADF6* genes. *Plant Mol Biol*, **45**, 517-527.

Dong, C.H., Xia, G.X., Hong, Y., Ramachandran, S., Kost, B. and Chua, N.H. (2001b) ADF proteins are involved in the control of flowering and regulate F- actin organization, cell expansion, and organ growth in *Arabidopsis*. *Plant Cell*, **13**, 1333-1346.

Dong, C.H., Xia, G.X., Hong, Y., Ramachandran, S., Kost, B. and Chua, N.H. (2001c) ADF proteins are involved in the control of flowering and regulate F-actin organization, cell expansion, and organ growth in Arabidopsis. *Plant Cell*, **13**, 1333-1346.

dos Remedios, C.G., Chhabra, D., Kekic, M., Dedova, I.V., Tsubakihara, M., Berry, D.A. and Nosworthy, N.J. (2003) Actin binding proteins: regulation of cytoskeletal microfilaments. *Physiol Rev*, **83**, 433-473.

Ghosh, M., Song, X., Mouneimne, G., Sidani, M., Lawrence, D.S. and Condeelis, J.S. (2004) Cofilin promotes actin polymerization and defines the direction of cell motility. *Science*, **304**, 743-746.

Hawkins, M., Pope, B., Maciver, S.K. and Weeds, A.G. (1993) Human actin depolymerizing factor mediates a pH-sensitive destruction of actin filaments. *Biochemistry*, **32**, 9985-9993.

Hayden, S.M., Miller, P.S., Brauweiler, A. and Bamburg, J.R. (1993) Analysis of the interactions of actin depolymerizing factor with G- and F-actin. *Biochemistry*, **32**, 9994-10004.

Hofmann, W.A., Stojiljkovic, L., Fuchsova, B., Vargas, G.M., Mavrommatis, E., Philimonenko, V., Kysela, K., Goodrich, J.A., Lessard, J.L., Hope, T.J., Hozak, P. and de Lanerolle, P. (2004) Actin is part of pre-initiation complexes and is necessary for transcription by RNA polymerase II. *Nat Cell Biol*, **6**, 1094-1101.

Hu, P., Wu, S. and Hernandez, N. (2004) A role for beta-actin in RNA polymerase III transcription. *Genes Dev*, **18**, 3010-3015.

Iida, K., Matsumoto, S. and Yahara, I. (1992) The KKRKK sequence is involved in heat shock-induced nuclear translocation of the 18-kDa actin-binding protein, cofilin. *Cell Struct Funct*, **17**, 39-46.

Kandasamy, M.K., McKinney, E.C. and Meagher, R.B. (2002) Functional non-equivalency of actin isovariants in Arabidopsis. *Mol Biol Cell*, **13**, 251-261.

Kandasamy, M.K., Burgos-Rivera, B., McKinney, E.C., Ruzicka, D.R. and Meagher, R.B. (2007) Class-specific interaction of profilin and ADF isovariants with actin in the regulation of plant development. *Plant Cell*, **19**, 3111-3126.

Lappalainen, P., Fedorov, E.V., Fedorov, A.A., Almo, S.C. and Drubin, D.G. (1997) Essential functions and actin-binding surfaces of yeast cofilin revealed by systematic mutagenesis. *Embo J*, **16**, 5520-5530.

Lopez, I., Anthony, R.G., Maciver, S.K., Jiang, C.J., Khan, S., Weeds, A.G. and Hussey, P.J. (1996) Pollen specific expression of maize genes encoding actin depolymerizing factor-like proteins. *Proc. Natl. Acad. Sci., U.S.A.*, **93**, 7415-7420.

Lynch, M. and Force, A. (2000) The probability of duplicate gene preservation by subfunctionalization. *Genetics*, **154**, 459-473.

Maciver, S.K. and Hussey, P.J. (2002) The ADF/cofilin family: actin-remodeling proteins. *Genome Biol*, **3**, reviews3007.

Matsuzaki, F., Matsumoto, S., Yahara, I., Yonezawa, N., Nishida, E. and Sakai, H. (1988) Cloning and characterization of porcine brain cofilin cDNA. Cofilin contains the nuclear transport signal sequence. *J Biol Chem*, **263**, 11564-11568.

McDowell, J.M., Huang, S., McKinney, E.C., An, Y.-Q. and Meagher, R.B. (1996) Structure and Evolution of the Actin Gene Family in Arabidopsis thaliana. *Genetics*, **142**, 587-602.

McGough, A., Pope, B., Chiu, W. and Weeds, A. (1997) Cofilin changes the twist of F-actin: implications for actin filament dynamics and cellular function. *J Cell Biol*, **138**, 771-781.

Meagher, R.B. and Williamson, R.E. (1994) The Plant Cytoskeleton. In *Arabidopsis*, Vol. 38 (Meyerowitz, E. and Somerville, C., eds). Cold Spring Harbor: Cold Spring Harbor Laboratory Press, pp. 1049-1084.

Meagher, R.B., McKinney, E.C. and Kandasamy, M.K. (1999) Isovariant dynamics expand and buffer the responses of complex systems: the diverse plant actin gene family. *Plant Cell*, **11**, 995-1006.

Meagher, R.B. and Fechheimer, M. (2003) The Cytoskeletal Proteome of *Arabidopsis*. In *Arabidopsis*, Vol. www.aspb.org/publications/arabidopsis/toc.cfm (Meyerowitz, E. and Somerville, C., eds). Cold Spring Harbor, NY: Cold Spring Harbor Laboratory Press.

Meagher, R.B., Kandasamy, M.K., Deal, R.B. and McKinney, E.C. (2007) Actin-related proteins in chromatin-level control of the cell cycle and developmental transitions. *Trends Cell Biol*, **17**, 325-332.

Miralles, F., Posern, G., Zaromytidou, A.I. and Treisman, R. (2003) Actin dynamics control SRF activity by regulation of its coactivator MAL. *Cell*, **113**, 329-342.

Miralles, F. and Visa, N. (2006) Actin in transcription and transcription regulation. *Curr Opin Cell Biol*, **18**, 261-266.

Moon, A. and Drubin, D.G. (1995) The ADF/cofilin proteins: stimulus-responsive modulators of actin dynamics. *Mol Biol Cell*, **6**, 1423-1431.

Moore, R.C. and Purugganan, M.D. (2005) The evolutionary dynamics of plant duplicate genes. *Curr Opin Plant Biol*, **8**, 122-128.

Moriyama, K., Iida, K. and Yahara, I. (1996) Phosphorylation of Ser-3 of cofilin regulates its essential function on actin. *Genes Cells*, **1**, 73-86.

Mun, J.H., Yu, H.J., Lee, H.S., Kwon, Y.M., Lee, J.S., Lee, I. and Kim, S.G. (2000) Two closely related cDNAs encoding actin-depolymerizing factors of petunia are mainly expressed in vegetative tissues. *Gene*, **257**, 167-176.

Mun, J.H., Lee, S.Y., Yu, H.J., Jeong, Y.M., Shin, M.Y., Kim, H., Lee, I. and Kim, S.G. (2002) Petunia actin-depolymerizing factor is mainly accumulated in vascular tissue and its gene expression is enhanced by the first intron. *Gene*, **292**, 233-243.

Nebl, G., Meuer, S.C. and Samstag, Y. (1996) Dephosphorylation of serine 3 regulates nuclear translocation of cofilin. *J Biol Chem*, **271**, 26276-26280.

Nishida, E., Iida, K., Yonezawa, N., Koyasu, S., Yahara, I. and Sakai, H. (1987) Cofilin is a component of intranuclear and cytoplasmic actin rods induced in cultured cells. *Proc Natl Acad Sci USA*, **84**, 5262-5266.

Ohta, Y., Nishida, E., Sakai, H. and Miyamoto, E. (1989) Dephosphorylation of cofilin accompanies heat shock-induced nuclear accumulation of cofilin. *J Biol Chem*, **264**, 16143-16148.

Paavilainen, V.O., Bertling, E., Falck, S. and Lappalainen, P. (2004) Regulation of cytoskeletal dynamics by actin-monomer-binding proteins. *Trends Cell Biol*, **14**, 386-394.

Philimonenko, V.V., Zhao, J., Iben, S., Dingova, H., Kysela, K., Kahle, M., Zentgraf, H., Hofmann, W.A., de Lanerolle, P., Hozak, P. and Grummt, I. (2004) Nuclear actin and myosin I are required for RNA polymerase I transcription. *Nat Cell Biol*, **6**, 1165-1172.

Pollard, T.D., Blanchoin, L. and Mullins, R.D. (2000) Molecular mechanisms controlling actin filament dynamics in nonmuscle cells. *Annu Rev Biophys Biomol Struct*, **29**, 545-576.

Posern, G., Miralles, F., Guettler, S. and Treisman, R. (2004) Mutant actins that stabilise F-actin use distinct mechanisms to activate the SRF coactivator MAL. *Embo J*, **23**, 3973-3983.

Ruegg, J., Holsboer, F., Turck, C. and Rein, T. (2004) Cofilin 1 is revealed as an inhibitor of glucocorticoid receptor by analysis of hormone-resistant cells. *Mol Cell Biol*, **24**, 9371-9382.

Ruzicka, D.R., Kandasamy, M.K., McKinney, E.C., Burgos-Rivera, B. and Meagher, R.B. (2007) The ancient subclasses of Arabidopsis Actin Depolymerizing Factor genes exhibit novel and differential expression. *Plant J*, **52**, 460-472.

Simillion, C., Vandepoele, K., Van Montagu, M.C., Zabeau, M. and Van de Peer, Y. (2002) The hidden duplication past of Arabidopsis thaliana. *Proc Natl Acad Sci U S A*, **99**, 13627-13632.

Theriot, J.A. (1997) Accelerating on a treadmill: ADF/cofilin promotes rapid actin filament turnover in the dynamic cytoskeleton [comment]. *J Cell Biol*, **136**, 1165-1168.

Vartiainen, M.K., Guettler, S., Larijani, B. and Treisman, R. (2007) Nuclear actin regulates dynamic subcellular localization and activity of the SRF cofactor MAL. *Science*, **316**, 1749-1752.

Yonezawa, N., Nishida, E. and Sakai, H. (1985) pH control of actin polymerization by cofilin. *J Biol Chem*, **260**, 14410-14412.

Yuan, Q., Ouyang, S., Liu, J., Suh, B., Cheung, F., Sultana, R., Lee, D., Quackenbush, J. and Buell, C.R. (2003) The TIGR rice genome annotation resource: annotating the rice genome and creating resources for plant biologists. *Nucleic Acids Res*, **31**, 229-233.

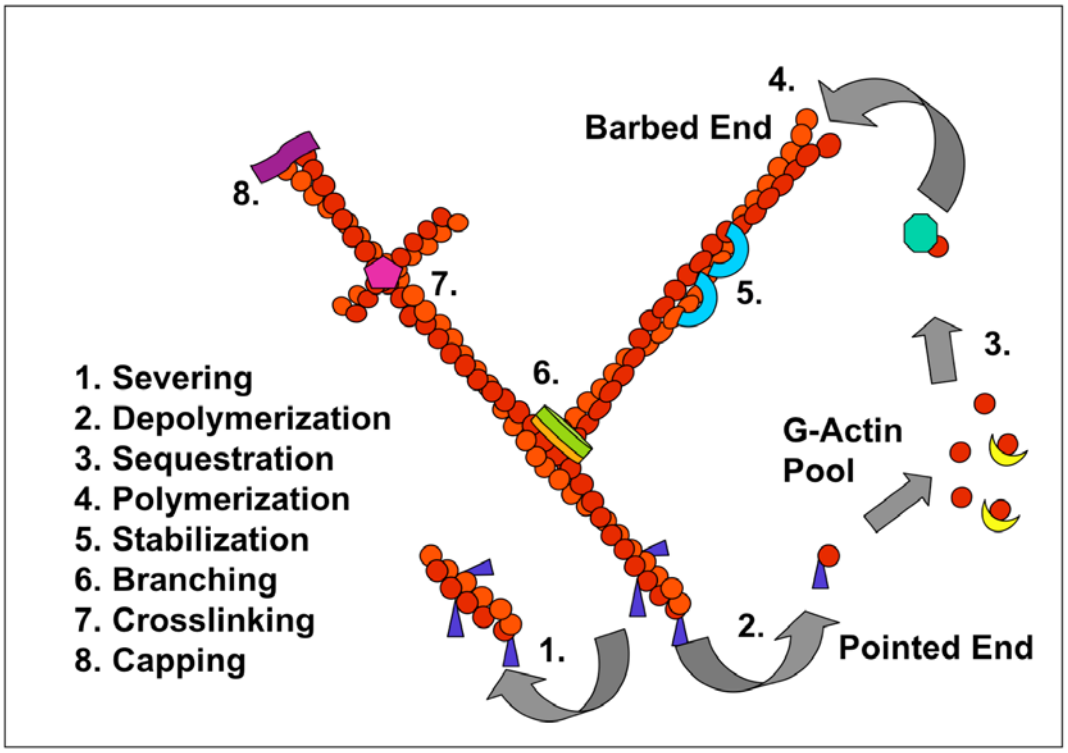

Figure 1.1 Actin cytoskeletal dynamics are mediated by a variety of processes controlled by actin binding proteins. Severing and depolymerization (1 and 2) are mediated by actin depolymerizing factor (ADF), while polymerization is promoted by profilin (4). Other actin binding protein functions such as sequestration, stabilization, branching, and capping, all involve various other actin binding proteins, and effect filament dynamics and remodeling.

CHAPTER 2

THE ANCIENT SUBCLASSES OF ARABIDOPSIS *ACTIN DEPOLYMERIZING FACTOR* GENES EXHIBIT NOVEL AND DIFFERENTIAL EXPRESSION[1]

[1] Ruzicka, DR., MK Kandasamy, EC McKinney, B Burgos-Rivera, and RB Meagher 2007 The Plant Journal 52: 460-472 Reprinted here with permission of the publisher

ABSTRACT

The *Actin Depolymerizing Factor (ADF)* gene family of *Arabidopsis thaliana* encodes eleven functional protein isovariants in four ancient subclasses. We report the characterization of the tissue-specific and developmental expression of all *Arabidopsis* ADF genes and the subcellular localization of several protein isovariants. The four subclasses exhibited distinct expression patterns as examined by qRT-PCR and histochemical assays of a GUS-reporter gene under the control of individual *ADF* regulatory sequences. Subclass I *ADFs* were expressed strongly and constitutively in all vegetative and reproductive tissues except pollen. Subclass II *ADFs* were expressed specifically in mature pollen and pollen tubes or root epidermal trichoblast cells and root hairs, and these patterns evolved from an ancient dual expression pattern comprised of both polar tip-growth cell-types, still observed in the monocot *Oryza sativa*. Subclass III *ADFs* were expressed weakly in vegetative tissues, but were strongest in fast growing, and/or differentiating cells including callus, emerging leaves, and meristem regions. The single Subclass IV *ADF* was constitutively expressed at moderate levels in all tissues including pollen. Immunocytochemical analysis with subclass-specific monoclonal antibodies demonstrated that subclass I isovariants localize to both the cytoplasm and the nucleus of leaf cells, while subclass II isovariants predominantly localize to the cytoplasm at the tip region of elongating root hairs and pollen tubes. The distinct expression patterns of the *ADF* subclasses support a model of ADFs co-evolving with the ancient and divergent actin isovariants.

INTRODUCTION

The actin cytoskeleton plays an essential role in many cellular processes, and its diverse functions include cytoplasmic organization, establishment of cell polarity, cell elongation, polar tip growth, intracellular trafficking, and cytokinesis (Meagher and Williamson, 1994; Pollard *et al.*, 2000; Staiger, 2000; Wasteneys and Galway, 2003). To function as a coordinated network that rapidly responds to multiple cellular activities, actin filaments are dynamically reorganized and remodeled by multiple actin binding proteins (ABPs) (Borisy and Svitkina, 2000; Paavilainen *et al.*, 2004). In higher plants, the actin cytoskeleton is comprised of multiple actin isovariants phylogenetically grouped into two ancient subclasses (McDowell *et al.*, 1996), whose vegetative and reproductive members predate the origin of angiosperms (Meagher *et al.*, 1999a; Meagher *et al.*, 1999b). More than a dozen ABPs are in similarly encoded diverse and ancient families (Klahre *et al.*, 2000; Deeks *et al.*, 2002; Kandasamy *et al.*, 2002a; Meagher and Fechheimer, 2003; Cvrckova *et al.*, 2004) suggesting a remarkable complexity of networked interactions surrounding the ancient actins. The hypothesis of isovariant dynamics proposes that differences in gene regulation and protein structure among co-expressed family members increase the dynamic capacity of the actin cytoskeleton (Meagher *et al.*, 1999a). Support for this comes from the functional non-equivalency of the ancient classes of *Arabidopsis* actins demonstrated by the dramatic phenotypes created by the ectopic expression of a reproductive actin in vegetative tissues (Gilliland *et al.*, 2002; Kandasamy *et al.*, 2002b). It is likely ABP gene families

also demonstrate equivalent specialization and divergence of expression patterns and functions (Kovar *et al.*, 2000; Hussey *et al.*, 2002).

The ABP Actin Depolymerizing Factor (ADF) is a small (~17 kDa) protein that is moderately conserved across eukaryotes. ADF, and its close relative in vertabretes, cofilin, functions in the remodeling of the actin cytoskeleton by promoting the severing and depolymerization of actin at the pointed end of filaments in response to a wide variety of environmental and physiological cues (Bamburg, 1999). These filament degredation products subsequently serve as new filament initiation sites or re-supply the monomeric actin pool. Thus, ADF acts to increase the dynamics of the F-actin cytoskeleton (Theriot, 1997; Chan *et al.*, 2000; Ghosh *et al.*, 2004). The *Arabidopsis ADF* gene family contains eleven expressed members that group phylogenetically into four ancient subclasses as shown in Figure 2.1 (Rhee *et al.*, 2003; Feng *et al.*, 2006). The expression patterns of multiple plant ADFs from *Zea mays*, *Lilium longiforum*, and *Nicotiana tabacum* have been studied previously and classified as constitutive or pollen-specific (Kim *et al.*, 1993; Lopez *et al.*, 1996; Jiang *et al.*, 1997; Allwood *et al.*, 2002; Chen *et al.*, 2002). These data point to the differential regulation of plant ADFs, and provide a framework for a model where the differentially expressed actins and ABPs co-evolved in specific organs, tissues, and cells. As part of this model, the size and diversity within the plant ADFs increases the likelihood of their contributing to isovariant dynamics.

To further explore this model, we have undertaken a thorough analysis of the entire *ADF* gene family in *Arabidopsis*. We characterized the organ- and tissue-specific

expression patterns of the 11 *ADFs* by quantifying transcript levels and studying translational fusions to the *GUS* reporter gene. We examined the subcellular localization of two subclasses of isovariants using anti-ADF monoclonal antibodies. Lastly, to refine our understanding of the evolution of expression patterns in the *ADF* gene family, we explored the origin of the conserved expression patterns of subclass II *ADFs* using evolutionarily distant plant species including *Oryza sativ*a. We have shown that the four subclasses of *Arabidopsis ADFs* are expressed in various patterns and tissues, and evidence from subcellular localization indicates functional differences in their cytoskeletal role. The majority of these expression patterns and proposed functional differences predate the divergence of monocots and eudicots, altogether supporting the hypothesis of isovariant dynamics-driven co-evolution within the plant actin cytoskeleton.

RESULTS

ADF Protein Phylogeny

To characterize the relatedness of the ADF protein sequences, we assembled an alignment of all eleven *Arabidopsis* ADFs and subclass-representative rice (*Oryza sativa*) and poplar (*Populus trichocarpa*) ADF sequences using ClustalW (Supplemental Figure 2.S1). We created a neighbor joining phylogenetic tree from this alignment as described in Experimental Procedures (Figure 2.1) (Rhee *et al.*, 2003; Tuskan *et al.*, 2006; Ouyang *et al.*, 2007). The *Arabidopsis* ADFs group into four ancient subclasses supported by the existence of homologous ADF protein sequences from each subclass

in the eudicot poplar and the monocot rice. For example, PtADF13 and OsADF5 are significantly more related in protein sequence to *Arabidopsis* ADF5 and ADF9 in subclass III than to other poplar or rice ADF genes. Poplar and rice have not shared a common ancestor with *Arabidopsis* for approximately 110 and 145 million years, respectively (Chaw *et al.*, 2004; Tuskan *et al.*, 2006). This phylogeny revealed significant divergence among members within subclasses as well. For example, ADF5 and ADF9 form a distinct and divergent clade, and yet they were only 80% identical. Sequence identity comparisions among the four Arabidopsis ADF subclasses were generally between 48 and 75%. To put this in perspective, human ADF/Cofilin 1 and 2 (NP005498; NP619579) are 75-78% identical to ADFs from Zebra fish and Fugu (*Danio rerio* NP 998806; *Tetraodon nigroviridis* CAG09787). Humans have not shared a common ancestor with these two vertabrete fish for over 450 million years (Blair Hedges and Kumar, 2003). Hence, the divergence levels among the Arabidopsis ADF isovariants are striking, and are likely to be functionally significant. These data suggest the gene diversity among *Arabidopsis* ADFs predates the common ancient ancestry of the three plant species and infers that functional differences have evolved among the 11 ADF isovariants and particularly across the four ancient subclasses. Moreover, additional information about the differential expression of the various family members could reveal more about plant ADF function and co-evolution with the differentially expressed actins and other ABPs.

Organ, Tissue, and Cell Specific Expression of ADF Transcripts and Reporter Cassettes

The ancient diversity of the plant *ADF* gene family combined with the diverse expression patterns of other cytoskeleton gene families suggested there might be functional significance to the expression patterns of the *Arabidopsis ADF* members. First, we quantified the expression of the 11 *Arabidopsis ADF* transcripts with quantitative reverse transcriptase-mediated real time PCR (qRT-PCR) using RNA from various organs and tissues (Livak and Schmittgen, 2001). The 11 *ADF* genes showed a 500-fold range in their relative expression levels among the various tissues as shown in Table 2.1. The relative *ADF* expression levels presented at the Genevestigator microarray database support our results, although these microarray data appear to have significantly underestimated quantitative differences in ADF expression levels among plant samples (Zimmermann *et al.*, 2004).

To further explore the expression patterns of the individual ADF genes at a tissue and cell-specific level, we examined reporter fusions of all eleven *Arabidopsis ADFs*. Previous work explored transcriptional fusions of *Arabidopsis ADF1*, *ADF5* and *ADF6* promoter sequences to the *beta-glucuronidase* reporter gene (*GUS*) in transgenic plants. These constructs showed weak expression patterns in vascular tissue, root tip meristem, and vascular tissue, respectively (Dong *et al.*, 2001). More recent work on a *Petunia hybrida ADF1* homolog has indicated that its relatively large first intron has important enhancer functions for high-level tissue-specific expression (Mun *et al.*, 2000; Mun *et al.*, 2002; Jeong *et al.*, 2007), and this intron was not included in previous

Arabidopsis studies. Therefore, we used the *GUS* reporter gene to assay *ADF* expression patterns by transforming plants with a translational fusion of the promoter (1000bp); the 5´UTR; the first intron with potential enhancer elements; the first 1-9 codons of each *ADF* gene member fused in frame to the coding region of the *beta-glucoronidase* gene; and the *nopthaline synthatase* 3´UTR and poly(A) signal as described in Experimental Procedures (Jefferson *et al.*, 1987).

Expression of Subclass I: Subclass I *ADFs* include *ADF1, 2, 3* and *4* (Figure 2.1). Transcripts for these four *ADFs* were strongly expressed in a wide range of tissues including root, seedling, mature leaves, and the flowers based on qRT-PCR as shown in Figure 2.2. Our GUS reporter assay data support and further refine this expression analysis. *ADF1p::GUS* staining was strongest in the hypocotyl and cotyledons, mature roots, adult leaves, and stamen filaments (Figure 2.2b, c, d, e). It was weaker in young root, sepals, anthers, stigma, and stem tissue, and absent from the carpel and pollen. *ADF2p::GUS* staining was similar to *ADF1p::GUS*, but was stronger in younger root and sepals (Figure 2f, g, h, i). *ADF3p::GUS* staining was the strongest among all 11 ADFs, in agreement with our qRT-PCR data. Analysis of *ADF3p::GUS* plants was limited to samples stained only 4 hours because longer staining times resulted in over-stained black tissue. *ADF3p::GUS* staining was similar in pattern and localization to, but always stronger than, *ADF1p::GUS* and *ADF2p::GUS*, with notable exceptions (Figure 2.2j, k, l, m). *ADF3p::GUS* staining was strong in the entire stigma, and significant staining was evident in petals (Figure 2.2m). At this short staining time, only pollen, carpel, and stem

did not stain strongly. *ADF4p::GUS* staining was strong in the root tip, mature leaves, the stigma, and stamen filaments, but was weak in the hypocotyl, cotyledons, stems, and anthers (Figure 2.2n, o, p, q). Combining both GUS expression and transcript level data, *ADF3* is the most strongly expressed subclass I member followed by the moderately expressed *ADF1, ADF2,* and the more weakly expressed *ADF4*. Subclass I is therefore characterized as constitutively expressed in all organs and tissues except pollen, with only minor variation of expression patterns among its family members.

Expression of Subclass II: The four sequences comprising *Arabidopsis* subclass II ADFs can be viewed as two phylogenetically distinct clades, IIa (ADF7 and 10) and IIb (ADF8 and 11) (Figure 2.1). Based on qRT-PCR data, the two clades differ dramatically in expression pattern, with clade IIa *ADFs* expressed in reproductive tissue and clade IIb *ADFs* expressed in root tissue (Figure 2.3a). Histochemical staining of clade IIa GUS-fusions *ADF7p::GUS* and *ADF10p::GUS* was restricted to, and very strong in, mature pollen grains (Figure 2.3d, e, f, j, k). No staining was observed for either reporter fusion in seedlings, root or leaf tissue in agreement with the qRT-PCR data (Figure 2.3b, c, d, g, h, i). More specifically, these lines only showed staining of mature pollen grains on anthers after dehiscence indicating that *ADF7* and *ADF10* are late-pollen specific *ADFs* similar to the reproductive class of actins and profilins (Figure 2.3j) (Kandasamy *et al.*, 1999, 2002a) and may have a cytoskeletal role in the polar tip growth of elongating pollen tubes.

In contrast to the pollen specific expression of *ADF7* and *ADF10*, clade IIb constructs, *ADF8p::GUS* and *ADF11p::GUS,* exhibited staining that was restricted to root epidermal cell files comprised primarily of the trichoblasts and mature root hairs (Figure 2.3l, m, p, q). Staining was strongest in epidermal trichoblasts adjacent to the elongation zone, indicating that *ADF8* and *ADF11* are distinctly expressed in young root hair cells, and may have a cytoskeletal role in the polar tip growth of emerging root hairs (Figure 2.3m). No staining was observed for clade IIb *ADF GUS* fusions in mature pollen as was with clade IIa, confirming their non-overlapping expression patterns (Figure 2.3o, s). Together, subclass IIa and IIb are therefore classified as tip-cell specific ADFs with a division of expression patterns of the two clades between mature pollen and root trichoblasts, respectively.

Expression of Subclass III: Transcripts encoding the subclass III ADFs, *ADF5* and *ADF9*, were expressed differentially in a wide variety of tissues including roots, shoots, and flowers and showed distinct expression differences between each other based on qRT-PCR as shown in Figure 2.4a, left. Analysis of *ADF5p::GUS* plants showed strong staining in cotyledons, root vascular tissue, the root tip meristem, and emerging leaves (Figure 2.4b, c, d, e). *ADF5p::GUS* staining was weak in reproductive tissue, adult leaves, and mature roots indicating its differential expression in vegetative tissue. Analysis of *ADF9p::GUS* plants showed strong staining in young seedlings, the root tip meristem, the root elongation zone, root vascular tissue, the apical meristem, the edges of leaves, trichomes, the style, and anther/stamens (Figure 2.4f, g, h, i). *ADF9p::GUS*

expression was absent from root epidermal cells, carpal, stigma, papillae, and pollen. It is clear that together *ADF5* and *ADF9* were expressed in both overlapping and unique tissues and cells in agreement with the qRT-PCR data. Compared with the remaining 9 *ADFs*, *ADF5* and *ADF9* were expressed most weakly based on both qRT-PCR and *GUS* fusions. The only exception to this observation was in callus tissue, where *ADF9* mRNA levels were the highest of all eleven *ADFs* (Table 2.1 and Figure 2.4a). Preliminary GUS staining of callus tissue regenerated from various *ADF9p::GUS* plant organs confirmed these high expression levels in multiple callus cell types (data not shown). Subclass III is therefore classified as being broadly expressed in multiple organs and tissues including meristem regions, but also contains non-overlapping patterns between its two members.

Expression of Subclass IV: In *Arabidopsis*, *ADF6* is the only subclass IV member and its transcripts were found at detectable levels in all tissues analyzed by qRT-PCR as shown in Figure 4a, right. *ADF6p::GUS* reporter staining was strongest in the root tip, root vascular tissue, and cotyledons; was moderate in filaments, anthers, pollen, stigma, and vegetative epidermal tissue; and was weak in carpel, sepal, and hypocotyl tissue (Figure 2.4j, k, l, m, n). Unlike subclass I *ADF* expression patterns, *ADF6p::GUS* also showed staining in the pollen grains indicating it to be truly constitutively expressed (Figure 2.4n). This data confirmed the constitutive expression pattern observed with qRT-PCR, but compared to the similarly expressed subclass I *ADFs*, *ADF6's* expression was moderate to weak. Subclass IV *ADF6* is therefore classified as having a weak

constitutive expression pattern including both male and female reproductive tissue. This distinguished it from any previous vegetative or constitutive cytoskeletal gene characterization that lacked pollen expression.

Subclass I ADF isovariants localize to the cytoplasm and nucleus

In order to address the possible functional differences among the 11 ADF isovariants proposed from their phylogeny, a monoclonal antibody, mAbADF4a, was raised from mice immunized with recombinant ADF4 protein. mAbADF4a reacted on a western blot with seven recombinant Arabidopsis ADFs representing subclass I and II (ADF1, 2, 3, 4, 7, 10, and 11), and not with the remaining four ADF proteins as shown in Figure 2.5a. Equal amounts of total protein from callus, root, 7 day-old seedling, 14 day old seedling, mature leaf, immature flower bud, mature flower, pollen, and silique tissue were seperated by SDS-PAGE. Western blot analysis with mAbADF4a showed bands of 14-17 kDa for all tissues (Figure 2.5b). Based on the expression patterns of the seven ADF isovariants with which mAbADF4a reacts, the band in the pollen sample was due to a reaction with ADF7 and ADF10 protein. Similarly in root tissue, mAbADF4a detected root trichoblast specific ADF11 and the constitutive ADF1, 2, 3, and 4. The bands in the remaining tissue samples were from ADFs 1, 2, 3, and 4, given their near-constitutive expression patterns. The Coomassie staining of protein bands on duplicate SDS-PAGE gels run in parallel demonstrate relatively equal loading, except for pollen, in which less was loaded to adjust for an excessive immuno-chemical signal (Figure 2.5b, bottom).

We immunolabeled ADF protein in paraformaldehyde-fixed and dissociated leaf cells with the mAbADF4a, and investigated subcellular localization patterns (see Experimental Procedures). Of the seven ADFs that react with mAbADF4a, only subclass I ADFs are expressed in leaf, and thus this antibody can be used to specifically examine the subcellular localization of this class of isovariants. In leaf cells, the mAbADF4a localized subclass I ADFs to both the cytoplasm and nucleus, with the majority of the cells exhibiting both subcellular localization patterns (Figure 2.5c, e, f, and g). In addition, ADF immunolocalization with mAbADF4a was performed by the cryofixation method to preserve actin filament structure (Baskin *et al.*, 1996) and to visualize ADF-actin interactions. In cryofixed cells, ADF (Figure 2.5g) was seen dispersed throughout the cytoplasm, concentrated in the nucleus, and around the chloroplasts (Figure 2.5f). ADF co-localized with actin baskets (Figure 2.5h) surrounding the chloroplasts (Kandasamy and Meagher, 1999). Similar patterns of localization were observed in several cell types from leaf, root, and flower tissues (not shown). The co-localization of ADF with the actin baskets surrounding the chloroplasts suggested a weak decoration of actin filaments by ADF. The strong constitutive nuclear localization is in sharp contrast to mammalian cells where stress induces nuclear localization of ADF.

Subclass 2 ADF isovariants localize to polar growth regions of elongating cells

A second monoclonal antibody, mAbADF8a, was obtained from mice immunized with recombinant ADF8 protein (subclass IIb). Among the eleven recombinant ADF

proteins tested, mAbADF8a reacted strongly with subclass II isovariants (ADF 7, 8, 10, and 11) and very weakly with subclass IV isovariant ADF6 as shown in Figure 2.6a. These ADFs were expressed in root trichoblasts (ADF8, 11), pollen (ADF7, 10), and constitutively (ADF6), respectively. Equal amounts of total protein from various plant samples were seperated by SDS-PAGE. Western blots with mAbADF8a showed strong reactions with ADF protein in root, mature flower, and pollen (Figure 2.6b). The antibody did not detect ADF6 in vegetative shoot tissue samples where it is reasonably well expressed, perhaps because of the antibody's weak affinity for it. Thus, mAbADF8a appears to be subclass II specific.

In the tissues where they are expressed, the mAbADF8a localized ADF subclass II isovariants to the cytoplasm and weakly to the nucleus similar to the localization of subclass I ADFs seen with mAbADF4a. The strongest and most prevalent localization, however, was to the cytoplasmic elongating tip region of pollen tubes and emerging root hairs (Figure 2.6c, d, e, f, and g). As these tips emerged, there was a redistribution of ADF protein from the cytoplasm at the base of the cell to the growing tip. This is similar to the localization of a GFP-ADF fusion protein in *Nicotinana tobaccum* pollen tubes and ADF localized with ZmADF3 polyclonal antibody in *Zea mays* root hairs (Jiang *et al.*, 1997; Chen *et al.*, 2002). Significantly, we used the mAbADF8a to immunolocalize ADF protein in *Nicotiana tabacum* pollen tubes, and demonstrated the conservation of this polar tip localization pattern (Figure 2.6e, f, and g). There was also notable immunoflorescence of ADF surrounding the migrating nucleus in elongating *Nicotiana* pollen tubes (Figure 2.6g), but little staining of the nucleus itself. This indicates a

potential role for subclass II ADFs in the trafficking of organelles toward the pollen tube tip (Tiwari and Polito, 1988; Heslop-Harrison and Heslop-Harrison, 1989).

Conserved root and pollen localization of subclass II ADF members

Arabidopsis ADF Subclass II contains two clades of ADFs, IIa and IIb (Figure 2.1). Each clade is comprised of two pairs of genes that share distinct expression patterns, pollen specific *ADF7* and *ADF10* in subclass IIa and root trichoblast specific *ADF8* and *ADF11* in subclass IIb as shown in Figure 2.3. While these cell types are spatially and functionally distinct from each other, both exhibit polar tip growth, an actin cytoskeleton-driven process (Meagher and Williamson, 1994; Hepler *et al.*, 2001). To test whether the root/anther expression pattern of subclass II isovariants was conserved or unique to *Arabidopsis,* we used the mAbADF8 antibody to examine ADF protein in root and anther tissue from other plant species. The antibody reacted with 14 to 17 kDa ADF protein bands in root and anther tissue, but not in shoot tissue, from both *Brassica napus* (another member of Brassicaceae) and the monocot *O. sativa* as shown in Figure 2.7a. The completed genome sequence of *O. sativa* reveals that it encodes at least two subclass II ADFs, OsADF1 and OsADF6, and we wanted to examine whether these two genes, like Arabidopsis subclass II ADFs, exhibit differential root and anther expression patterns. Therefore, we used qRT-PCR to analyze the expression patterns of these two subclass II rice *ADF* genes (Figure 2.7b). In *O. sativa,* both *ADFs* were expressed in root and anther tissue, but not in shoot tissue. Further, neither gene was dominantly expressed in one organ over the other. Our results suggest that the

ancestral subclass II *ADFs* exhibited a tip-cell specific expression pattern consisting of expression in both pollen and root trichoblasts, and that the pollen and root trichoblast expression patterns of the two clades separated and became more specialized in duplicate gene copies in more recent ancestors of *Arabidopsis*.

DISCUSSION

Considering the extreme diversity within the plant *ADF* family (Maciver and Hussey, 2002; Feng *et al.*, 2006), we felt a cohesive study establishing the relationship of each ADF to one another was needed. Key to understanding the conservation and maintenance of this eleven-member gene family in *Arabidopsis* was a dissection of the regulation of each *ADF*. Although earlier studies describe the expression of a few ADF genes, this is the first comprehensive study describing the expression of the complete *Arabidopsis* gene family using multiple methods including qRT-PCR and reporter fusions that included the ADF promoter and enhancer element-containing intron sequences.

The *Arabidopsis* ADF gene family showed divergent expression patterns conserved among its phylogenetic subclasses in parallel to the actin gene family, which encodes eight functional actin genes that group into ancient vegetative and reproductive subclasses. Subclass I ADFs 1, 2, 3, and 4 are expressed strongly in all tissues and organs according to our qRT-PCR data and for example constitute 82.0% of the total *ADF* transcript in 10 day-old seedling tissue. The subclass I ADF GUS translational fusions are also expressed highly in all tissues and cell types except pollen throughout

development. Combined, we classify subclass I ADFs as the predominant vegetative group of ADF isovariants in the plant. In parallel to subclass I ADFs, actins ACT2 and ACT8 form an ancient clade in *Arabidopsis*, and are highly-expressed in vegetative tissues throughout development (An *et al.*, 1996). Given this overlap in strength of expression and localization between these subclasses of actins and ADFs, subclass I ADF isovariants are likely the major ADFs responsible for a majority of ADF-mediated actin cytoskeletal remodeling of filaments containing ACT2 and ACT8 isovariants. Additionally, the subclass I ADF pattern is quite similar to the vegetative/constitutive class of plant profilins, PRF1 and PRF2 (Kandasamy *et al.*, 2002a), further supporting the model of co-expressed components of the actin cytoskeleton interacting and co-evolving.

Subclass I ADF isovariants localized to both cytoplasmic and nuclear regions in leaf cells and co-localized with actin chloroplast-baskets. While ADF's function has been traditionally limited to remodeling actin filaments in the cytosol, solid experimental data suggests that ADF's have an important role in shuttling actin to the nucleus (Nebl *et al.*, 1996; Jiang *et al.*, 1997). Given that actin is a structural component of most chromatin remodeling complexes and interacts with all three classes of RNA polymerase (Jockusch *et al.,* 2006), ADFs could be responsible for shuttling actin to the nucleus and indirectly facilitate chromatin remodeling or gene expression. Future work in this area will aim to dissect the dual cytoplasmic and nuclear functions of ADF isovariants in relation to mutant phenotypes. It also suggests the intriguing possibility

that the phenotypes of actin and ADF mutants may not always be due to defects in the cytoplasmic cytoskeleton.

ADF subclass II members *ADF7* and *ADF10* (IIa), and *ADF8* and *ADF11* (IIb), exhibited pollen-specific and root trichoblast-specific expression patterns, respectively. This was the only example of extreme divergence of expression patterns within a subclass for the *Arabidopsis ADF* gene family. The *Arabidopsis* subclass IIa and IIb ADF clades are 88% identical at the amino acid level, and group together as one clade when compared with monocot subclass II ADF sequences (Figure 2.1), consistent with previously reported ADF phylogenies (Maciver and Hussey, 2002; Feng *et al.*, 2006). The entire subclass was originally reported to be reproductive-specific given evidence of pollen specific *Zea mays* ADF1 and ADF2 and *Lilium longiform* ADF1 (Lopez *et al.*, 1996; Allwood *et al.*, 2002; Maciver and Hussey, 2002). Beginning with the amplification of *Arabidopsis ADF8* from a root, but not a flower, cDNA library (unpublished data) and western blot analysis using the mAbADF8a showing root specific protein expression (Figure 2.6b), our data suggested that based on expression patterns there were different subtypes within this subclass in *Arabidopsis*. Furthermore, our expression and cellular localization data on subclass II ADFs provided evidence of a conserved functional role in polar tip growth as predicted for ADFs (Smertenko *et al.*, 2001; Chen *et al.*, 2002; Chen *et al.*, 2003). The late pollen actins and pollen specific profilins are expressed strongly and specifically in mature pollen grains and are required for normal fertility (Kandasamy *et al.*, 1999, 2002a; Pawloski *et al.*, 2006), but are not expressed in root trichoblasts. We propose that *Arabidopsis* Subclass IIa ADFs could

properly interact with and remodel this ancient subclass of late pollen actin isovariants. Having been specifically expressed in root trichoblasts, subclass IIb ADF isovariants have likely maintained interactions with the vegetative actin isovariants ACT2, ACT7, and ACT8, which are expressed in root hairs. Vegetative mis-expression of the late pollen actin ACT1 rescued the root hair defect of the vegetative actin *act2-1* mutant (Gilliland *et al.*, 2002), while still causing dominant aberrant phenotypes in shoot tissues (Kandasamy *et al.*, 2002b). These results can be reconciled given the endogenous expression of the subclass IIb ADFs in root hairs, which based on their homology to IIa ADFs might appropriately interact with pollen specific ACT1.

Because the pollen and root trichoblast expression patterns of *Arabidopsis* subclass II *ADFs* were so strikingly divergent, we assayed subclass II ADF protein in distantly related plant species using the mAbADF8a, and showed the dual pattern to be conserved (Figure 2.7a). To address the origin of the divergent expression patterns for subclass II ADFs within *Arabidopsis*, we hypothesized there had been a more recent subfunctionalization of expression patterns between paralogues in the *Arabidopsis* eudicot lineage. The ADF phylogeny contains at least two rice ADFs in subclass II, OsADF1 and OsADF6, which appear basal to the four *Arabidopsis* subclass II ADFs (Figure 2.1) and exhibit dual anther/root expression patterns, thus supporting this hypothesis (Figure 2.7b). The most parsimonious conclusion is that the ancestral expression pattern of subclass II *ADFs* was specific to cells that exhibit polar tip growth. We propose that within the eudicot lineage, gene duplication was followed by subfunctionalization to create two distinct expression clades, where one clade retained

expression in pollen and the other retained expression in root trichoblasts (Lynch, 2000). In contrast to *Arabidopsis*, the monocot species *O. sativa*'s *ADF* subclass II members have maintained their ancient dual pollen/root trichoblast specific expression patterns. It seems quite unlikely that a root trichoblast specific gene and a pollen specific gene could successfully fuse their regulatory elements to form the combined expression pattern seen in rice.

EXPERIMENTAL PROCEDURES

Plant strains and growth conditions

The Arabidopsis plants were of the Columbia ecotype and were grown on soil or agar in growth chambers at 22°C under fluorescent light for 16 h. Seeds were stratified prior to moving them into the growth chamber for germination. Transformations were performed with *Agrobacterium tumefaciens* strain C58C1 using the floral dip method (Clough, 2005). Transformants were selected by plating seeds on half-strength Murashige and Skoog (MS) media (Murashige and Skoog, 1962) containing 50 mg/L hygromycin and 300 mg/L tementin. Once germinated, the transformants were transferred to nonselective half-strength MS media, allowed to recover, and then transferred to soil.

GUS reporter gene constructs and histochemical analysis

A sense primer was designed approximately 1000nt upstream from the transcriptional start site and used in conjunction with a primer for the 3´ end of the first intron. Promoter-intron fragments were amplified from Arabidopsis genomic DNA using ex-taq

polymerase (Takara) under standard PCR reaction conditions. PCR products were purified and cloned into the pCAMBIA-HygR vector upstream of and in-frame with a previously cloned and sequenced *GUS* coding sequence and *nopthaline synthase* terminator using unique restriction sites (Hajdukiewicz *et al.*, 1994). Primer sequences for each promoter construct are listed in Supplemental Table 2.S1. GUS histochemical analysis of each reporter gene was performed on T2 generation seedlings of 10 independent T1 lines. Four and sixteen hour staining for GUS activity was performed on samples representing various stages plant development including emerging seedling, 7-10 day-old whole seedling, 20 day-old whole plant, and maturing buds and flowers using a GUS staining solution (Jefferson *et al.,* 1987).

qRT-PCR

RNA was isolated from the various plant tissues of *Arabidopsis* and *O. sativa (japonica cultivar group)* using the RNeasy plant mini kit (Qiagen). RNA was treated with RQ1 RNase-free DNase (Promega) before reverse transcription (RT). Three micrograms of treated RNA were added to RT reactions using the Invitrogen SuperscriptIII first strand synthesis kit with random hexamer primers to make cDNA. qRT-PCR was used to analyze cDNA populations using 18s plant-universal primers as the endogenous control. Real-time PCR was performed on an Applied Biosystems 7500 real-time PCR system using SYBR Green detection chemistry (Applied Biosystems). The 2^-(dCT)*10000 method of relative quantification was used in all experiments Primer sequences for each real-time reaction are listed in Supplemental Table 2.S2.

Production of monoclonal antibodies

Monoclonal antibodies against 6-his tagged ADF4 and ADF8 recombinant protein were produced as described in Kandasamy et al. 1999.

Protein Blot Analysis

Protein from *Arabidopsis* and *O. sativa (japonica cultivar group)* was prepared for immunoblotting as described in Kandasamy *et al.,* 1999 and Kandasamy *et al.,* 2001.

Immunocytochemistry

Leaf tissue was chemically fixed using the method described previously (Kandasamy *et al.,* 2001). A modified procedure using 2% formaldehyde and 1% glutaraldehyde during fixation, and 0.3% Cellulase, 0.3% Pectinase, 0.05% Pectolyase (Gold Biotechnology), and 0.4 M Manitol was used on root hairs and pollen tubes during enzymatic permeablization. Cryofixed samples were prepared as described previously (Kandasamy and Meagher, 1999).

Sequence Comparisons and Phylograms

Sequences were aligned with ClustalW 1.82 (Higgins and Sharp, 1988) using default settings and phylogenies were constructed with PAUP 4.0 (Rogers and Swofford, 1999) using the neighbor-joining method. Ties were broken randomly using the initial seed function. Bootstrap support values were based on 1000 replicates using a full heuristic

search. Sequence comparisons were made using BL2SEQ (Altschul *et al.*, 1997). *Chlamydomonas reinhardtii* ADF1 sequence was obtained from the US Department of Energy Joint Genome Institute (http://www.jgi.doe.gov/Chlre3).

ACKNOWLEDGEMENTS

We would like to thank Roger Deal and Yolanda Lay for helping with various parts of the experiments described in this manuscript, Sue Wessler for providing rice plants, and Judith Mank for her help and guidance with the phylogenetic analysis. This research was supported by funding from the National Institutes of Health (GM 36397-21) to R.B.M. ; an NIH training grant (GM 07103-31) to D.R.R.; and an NIH supplement (20S1/C103JD) to B.B..

REFERENCES

Allwood, E.G., Anthony, R.G., Smertenko, A.P., Reichelt, S., Drobak, B.K., Doonan, J.H., Weeds, A.G. and Hussey, P.J. (2002) Regulation of the pollen-specific actin-depolymerizing factor LlADF1. *Plant Cell*, **14**, 2915-2927.

Altschul, S.F., Madden, T.L., Schaffer, A.A., Zhang, J., Zhang, Z., Miller, W. and Lipman, D.J. (1997) Gapped BLAST and PSI-BLAST: a new generation of protein database search programs. *Nucleic Acids Res*, **25**, 3389-3402.

An, Y.Q., McDowell, J.M., Huang, S., McKinney, E.C., Chambliss, S. and Meagher, R.B. (1996) Strong, constitutive expression of the *Arabidopsis ACT2/ACT8* actin subclass in vegetative tissues. *Plant J*, **10**, 107-121.

Bamburg, J.R. (1999) Proteins of the ADF/cofilin family: essential regulators of actin dynamics. *Annu Rev Cell Dev Biol*, **15**, 185-230.

Baskin, T.I., Miller, D.D., Vos, J.W., Wilson, J.E. and Hepler, P.K. (1996) Cryofixing single cells and multicellular specimens enhances structure and immunocytochemistry for light microscopy. *J Microsc*, **182**, 149-161.

Blair Hedges, S. and Kumar, S. (2003) Genomic clocks and evolutionary timescales. *Trends Genet*, **19**, 200-206.

Borisy, G.G. and Svitkina, T.M. (2000) Actin machinery: pushing the envelope. *Curr Opin Cell Biol*, **12**, 104-112.

Chan, A.Y., Bailly, M., Zebda, N., Segall, J.E. and Condeelis, J.S. (2000) Role of cofilin in epidermal growth factor-stimulated actin polymerization and lamellipod protrusion. *J Cell Biol*, **148**, 531-542.

Chaw, S.M., Chang, C.C., Chen, H.L. and Li, W.H. (2004) Dating the monocot-dicot divergence and the origin of core eudicots using whole chloroplast genomes. *J Mol Evol*, **58**, 424-441.

Chen, C.Y., Wong, E.I., Vidali, L., Estavillo, A., Hepler, P.K., Wu, H.M. and Cheung, A.Y. (2002) The regulation of actin organization by actin-depolymerizing factor in elongating pollen tubes. *Plant Cell*, **14**, 2175-2190.

Chen, C.Y., Cheung, A.Y. and Wu, H.M. (2003) Actin-depolymerizing factor mediates Rac/Rop GTPase-regulated pollen tube growth. *Plant Cell*, **15**, 237-249.

Clough, S.J. (2005) Floral dip: agrobacterium-mediated germ line transformation. *Methods Mol Biol*, **286**, 91-102.

Cvrckova, F., Novotny, M., Pickova, D. and Zarsky, V. (2004) Formin homology 2 domains occur in multiple contexts in angiosperms. *BMC Genomics*, **5**, 44.

Deeks, M.J., Hussey, P.J. and Davies, B. (2002) Formins: intermediates in signal-transduction cascades that affect cytoskeletal reorganization. *Trends Plant Sci*, **7**, 492-498.

Dong, C.H., Kost, B., Xia, G. and Chua, N.H. (2001) Molecular identification and characterization of the *Arabidopsis AtADF1*, *AtADFS* and *AtADF6* genes. *Plant Mol Biol*, **45**, 517-527.

Feng, Y., Liu, Q. and Xue, Q. (2006) Comparative study of rice and Arabidopsis actin-depolymerizing factors gene families. *J Plant Physiol*, **163**, 69-79.

Ghosh, M., Song, X., Mouneimne, G., Sidani, M., Lawrence, D.S. and Condeelis, J.S. (2004) Cofilin promotes actin polymerization and defines the direction of cell motility. *Science*, **304**, 743-746.

Gilliland, L.U., Kandasamy, M.K., Pawloski, L.C. and Meagher, R.B. (2002) Both vegetative and reproductive actin isovariants complement the stunted root hair phenotype of the *Arabidopsis act2-1* mutation. *Plant Physiol.*, **130**, 2199-2209.

Hajdukiewicz, P., Svab, Z. and Maliga, P. (1994) The small, versatile pPZP family of *Agrobacterium* binary vectors for plant transformation. *Plant Mol Biol*, **25**, 989-994.

Hepler, P.K., Vidali, L. and Cheung, A.Y. (2001) Polarized cell growth in higher plants. *Annu Rev Cell Dev Biol*, **17**, 159-187.

Heslop-Harrison, J. and Heslop-Harrison, Y. (1989) Conformation and movement of the vegetative nucleus of the angiosperm pollen tube: association with the actin cytoskeleton. *J. Cell Sci.*, **93**, 299-308.

Higgins, D.G. and Sharp, P.M. (1988) CLUSTAL: a package for performing multiple sequence alignment on a microcomputer. *Gene*, **73**, 237-244.

Hussey, P.J., Allwood, E.G. and Smertenko, A.P. (2002) Actin-binding proteins in the Arabidopsis genome database: properties of functionally distinct plant actin-depolymerizing factors/cofilins. *Philos Trans R Soc Lond B Biol Sci*, **357**, 791-798.

Jefferson, R.A., Kavanagh, T.A. and Bevan, M.W. (1987) GUS fusions: beta-glucuronidase as a sensitive and versatile gene fusion marker in higher plants. *Embo J*, **6**, 3901-3907.

Jeong, Y.M., Mun, J.H., Kim, H., Lee, S.Y. and Kim, S.G. (2007) An upstream region in the first intron of petunia actin-depolymerizing factor 1 affects tissue-specific expression in transgenic Arabidopsis (*Arabidopsis thaliana*). *Plant J.*, **50 (2)**, 230-239.

Jiang, C.J., Weeds, A.G. and Hussey, P.J. (1997) The maize actin-depolymerizing factor, ZmADF3, redistributes to the growing tip of elongating root hairs and can be induced to translocate into the nucleus with actin. *Plant J.*, **12**, 1035-1043.

Jockusch, B.M., Schoenenberger, C.A., Stetefeld, J. and Aebi, U. (2006) Tracking down the different forms of nuclear actin. *Trends Cell Biol*.

Kandasamy, M.K., McKinney, E.C. and Meagher, R.B. (1999) The late pollen-specific actins in angiosperms. *Plant J*, **18**, 681-691.

Kandasamy, M.K. and Meagher, R.B. (1999) Actin-organelle interaction: association with chloroplast in *Arabidopsis* leaf mesophyll cells. *Cell Motil Cytoskeleton*, **44**, 110-118.

Kandasamy, M.K., McKinney, E.C. and Meagher, R.B. (2002a) Plant profilin isovariants are distinctly regulated in vegetative and reproductive tissues. *Cell Motil. Cytoskeleton*, **52**, 22-32.

Kandasamy, M.K., McKinney, E.C. and Meagher, R.B. (2002b) Functional nonequivalency of actin isovariants in Arabidopsis. *Mol Biol Cell*, **13**, 251-261.

Kim, S.R., Kim, Y. and An, G. (1993) Molecular cloning and characterization of anther-preferential cDNA encoding a putative actin-depolymerizing factor. *Plant Mol Biol*, **21**, 39-45.

Klahre, U., Friederich, E., Kost, B., Louvard, D. and Chua, N.H. (2000) Villin-like actin-binding proteins are expressed ubiquitously in *Arabidopsis*. *Plant Physiol*, **122**, 35-48.

Kovar, D.R., Drobak, B.K. and Staiger, C.J. (2000) Maize profilin isoforms are functionally distinct. *Plant Cell*, **12**, 583-598.

Livak, K.J. and Schmittgen, T.D. (2001) Analysis of relative gene expression data using real-time quantitative PCR and the 2(-Delta Delta C(T)) Method. *Methods*, **25**, 402-408.

Lopez, I., Anthony, R.G., Maciver, S.K., Jiang, C.J., Khan, S., Weeds, A.G. and Hussey, P.J. (1996) Pollen specific expression of maize genes encoding actin depolymerizing factor-like proteins. *Proc. Natl. Acad. Sci., U.S.A.*, **93**, 7415-7420.

Lynch (2000) The evolutionary fate and concequences of duplicate genes. *Science*, **290**, 1151-1155.

Maciver, S.K. and Hussey, P.J. (2002) The ADF/cofilin family: actin-remodeling proteins. *Genome Biol*, **3**, reviews3007.

McDowell, J.M., Huang, S., McKinney, E.C., An, Y.Q. and Meagher, R.B. (1996) Structure and evolution of the actin gene family in *Arabidopsis thaliana*. *Genetics*, **142**, 587-602.

Meagher, R.B. and Williamson, R.E. (1994) The Plant Cytoskeleton. In *Arabidopsis*, Vol. 38 (Meyerowitz, E. and Somerville, C., eds). Cold Spring Harbor: Cold Spring Harbor Laboratory Press, pp. 1049-1084.

Meagher, R.B., McKinney, E.C. and Kandasamy, M.K. (1999a) Isovariant dynamics expand and buffer the responses of complex systems: the diverse plant actin gene family. *Plant Cell*, **11**, 995-1006.

Meagher, R.B., McKinney, E.C. and Vitale, A.V. (1999b) The evolution of new structures: clues from plant cytoskeletal genes. *Trends Genet*, **15**, 278-284.

Meagher, R.B. and Fechheimer, M. (2003) The Cytoskeletal Proteome of *Arabidopsis*. In *Arabidopsis*, Vol. www.aspb.org/publications/arabidopsis/toc.cfm (Meyerowitz, E. and Somerville, C., eds). Cold Spring Harbor, NY: Cold Spring Harbor Laboratory Press.

Mun, J.H., Yu, H.J., Lee, H.S., Kwon, Y.M., Lee, J.S., Lee, I. and Kim, S.G. (2000) Two closely related cDNAs encoding actin-depolymerizing factors of petunia are mainly expressed in vegetative tissues. *Gene*, **257**, 167-176.

Mun, J.H., Lee, S.Y., Yu, H.J., Jeong, Y.M., Shin, M.Y., Kim, H., Lee, I. and Kim, S.G. (2002) Petunia actin-depolymerizing factor is mainly accumulated in vascular tissue and its gene expression is enhanced by the first intron. *Gene*, **292**, 233-243.

Murashige, T. and Skoog, F. (1962) A revised medium for rapid growth and bioassays with tobacco tissue culture. *Plant Physiol.*, **15**, 473-497.

Nebl, G., Meuer, S.C. and Samstag, Y. (1996) Dephosphorylation of serine 3 regulates nuclear translocation of cofilin. *J Biol Chem*, **271**, 26276-26280.

Ouyang, S., Zhu, W., Hamilton, J., *et al.,* (2007) The TIGR Rice Genome Annotation Resource: improvements and new features. *Nucleic Acids Res*, **35**, D883-887.

Paavilainen, V.O., Bertling, E., Falck, S. and Lappalainen, P. (2004) Regulation of cytoskeletal dynamics by actin-monomer-binding proteins. *Trends Cell Biol*, **14**, 386-394.

Pawloski, L.C., Kandasamy, M.K. and Meagher, R.B. (2006) The late pollen actins are essential for normal male and female development in Arabidopsis. *Plant Mol Biol*, **62**, 881-896.

Pollard, T.D., Blanchoin, L. and Mullins, R.D. (2000) Molecular mechanisms controlling actin filament dynamics in nonmuscle cells. *Annu Rev Biophys Biomol Struct*, **29**, 545-576.

Rhee, S.Y., Beavis, W., Berardini, T.Z., *et al.,* (2003) The Arabidopsis Information Resource (TAIR): a model organism database providing a centralized, curated gateway to Arabidopsis biology, research materials and community. *Nucleic Acids Res*, **31**, 224-228.

Rogers, J.S. and Swofford, D.L. (1999) Multiple local maxima for likelihoods of phylogenetic trees: a simulation study. *Mol Biol Evol*, **16**, 1079-1085.

Smertenko, A.P., Allwood, E.G., Khan, S., Jiang, C.J., Maciver, S.K., Weeds, A.G. and Hussey, P.J. (2001) Interaction of pollen-specific actin-depolymerizing factor with actin. *Plant J*, **25**, 203-212.

Staiger, C.J. (2000) Signaling to the actin cytoskeleton in plants. *Annu. Rev. Plant Physiol. Plant Mol. Biol.*, **51**.

Theriot, J.A. (1997) Accelerating on a treadmill: ADF/cofilin promotes rapid actin filament turnover in the dynamic cytoskeleton. *J Cell Biol*, **136**, 1165-1168.

Tiwari, S.C. and Polito, V.S. (1988) Organization of the cytoskeleton in pollen tubes of *Pyrus communis*: a study employing conventional and freeze substitution electron microscopy, immunofluorescence, and rhodamine-phalloidin. *Protoplasma*, **147**, 100-112.

Tuskan, G.A., Difazio, S., Jansson, S., *et al.,* (2006) The genome of black cottonwood, Populus trichocarpa (Torr. & Gray). *Science*, **313**, 1596-1604.

Wasteneys, G.O. and Galway, M.E. (2003) Remodeling the cytoskeleton for growth and form: an overview with some new views. *Annu Rev Plant Biol*, **54**, 691-722.

Zimmermann, P., Hirsch-Hoffmann, M., Hennig, L. and Gruissem, W. (2004) GENEVESTIGATOR. *Arabidopsis* microarray database and analysis toolbox. *Plant Physiol*, **136**, 2621-2632.

Table 2.1: Relative Quantity[a] of *ADF* Expression Detected by qRT-PCR in Various Tissues

	ADF1	ADF2	ADF3	ADF4	ADF5	ADF6	ADF7	ADF8	ADF9	ADF10	ADF11
Callus	371	483	1526	473	506	282	0	60	2617	19	146
Root	598	641	2535	373	639	156	0	329	79	10	1297
36h Seedling	403	437	652	368	228	128	0	77	16	9	124
10d Seedling	934	726	1614	740	400	374	0	3	12	32	19
Leaf	1171	949	3255	1374	600	600	0	11	8	52	29
Immature Flower	669	646	1433	646	812	296	168	5	74	254	84
Mature Flower	2017	2183	4212	2400	1478	1088	512	16	226	386	87

[a]Relative quantity calculated as described in Experimental Procedures

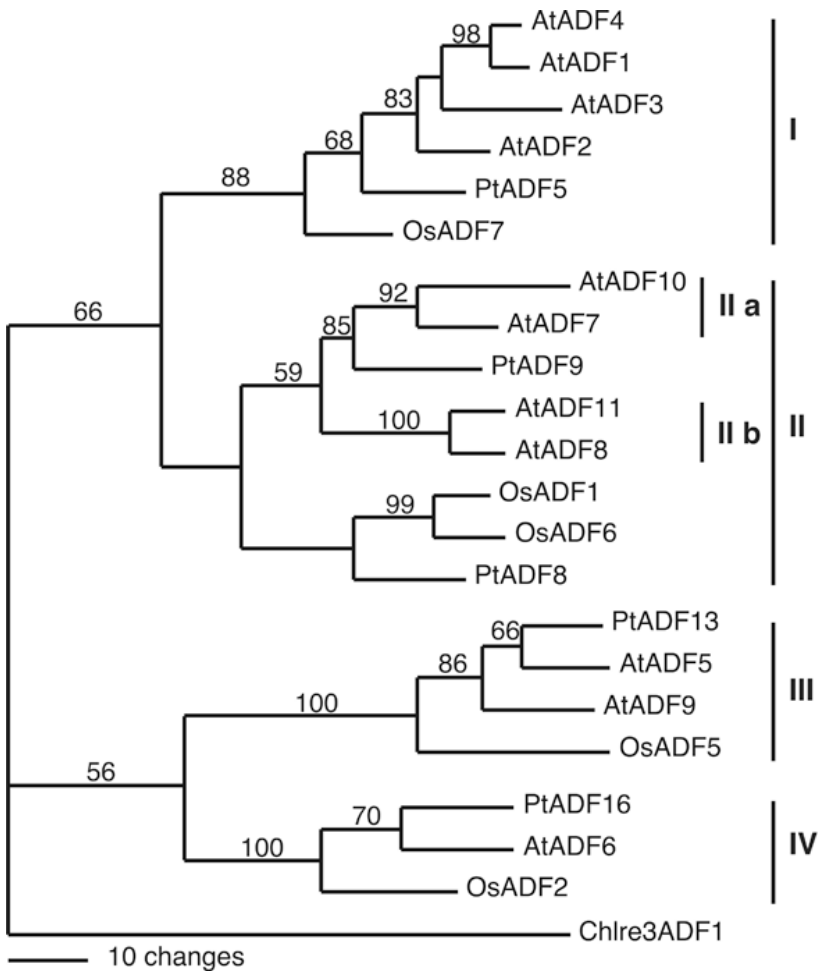

Figure 2.1 Neighbor-joining protein sequence phylogeny showing all eleven ADF proteins from *Arabidopsis* (At), and representatives from rice (Os) and poplar (Pt). Bootstrap values are shown on the branch points of the tree. Subclasses I to IV indicated by vertical bars at right. Subclass II was further separated into subclasses IIa and IIb. Analysis was rooted using the *Chlamydomonas reinhardtii* Chlre3ADF1 sequence. *Arabidopsis* ADF protein sequences and gene designations: ADF1 (At3g46010), ADF2 (At3g46000), ADF3 (At5g59880), ADF4 (At5g59890), ADF5 (At2g16700), ADF6 (At2g31200), ADF7 (At4g25590), ADF8 (At4g00680), ADF9

(At4g34970), ADF10 (At5g52360), and ADF11 (At1g01750); *Oryza sativa* ADF protein sequences and gene designations: ADF7 (Os05g02250), ADF1 (Os02g44470), ADF6 (Os04g46910), ADF5 (Os03g13950), ADF2 (Os03g56790); *Populus trichocarpa* ADF protein sequences and desginations: ADF5 (ID number Pt720178), ADF10 (Pt570479), ADF9 (Pt88969), ADF8 (Pt554345), ADF13 (Pt648773), ADF16 (Pt685386); and *Chlamydomonas reinhardtii* ADF1 Protein ID 26103.

Figure 2.2 Analysis of *Arabidopsis* Subclass I ADF Expression Patterns.

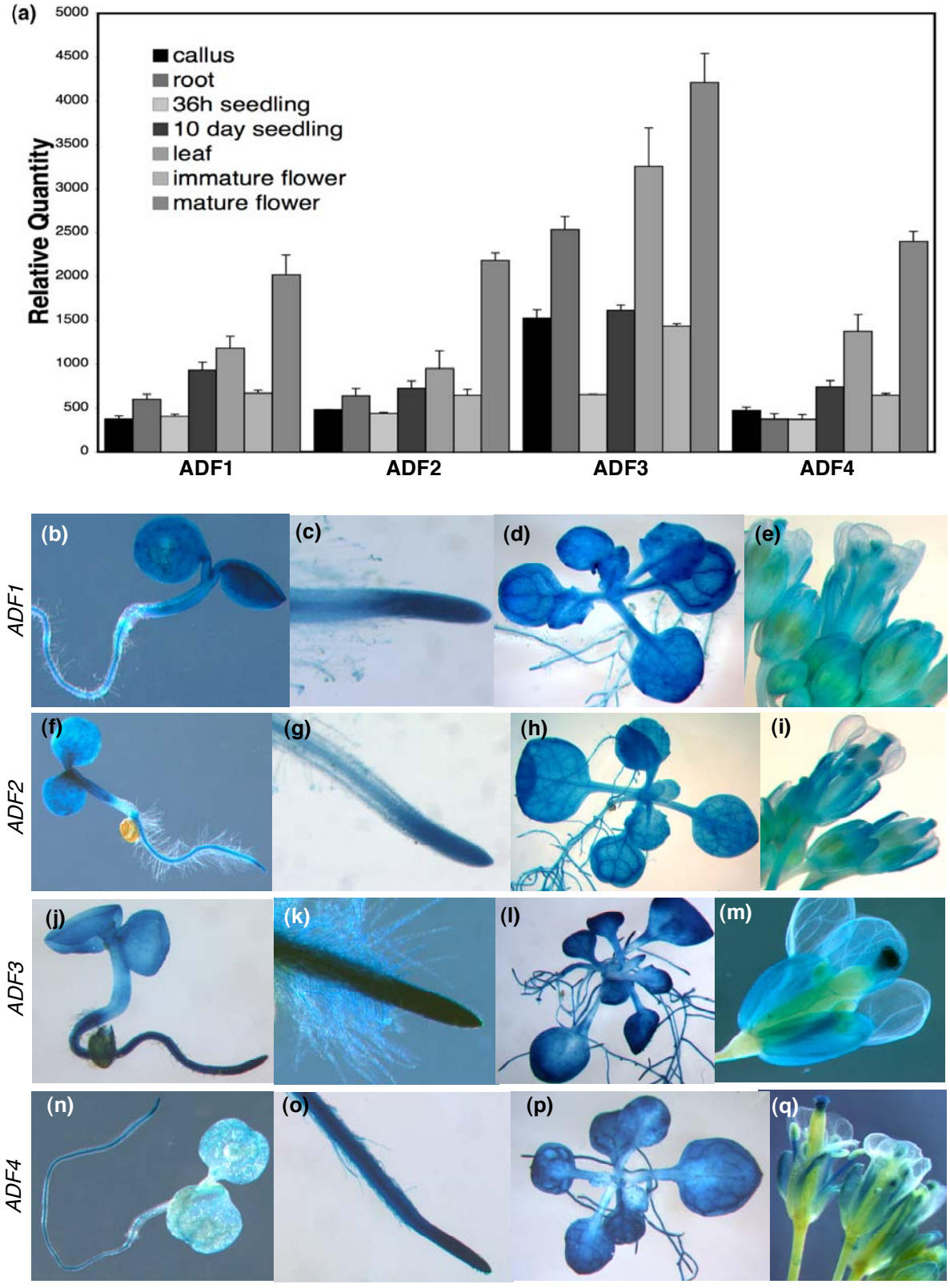

Figure 2.2 Analysis of *Arabidopsis* Subclass I ADF Expression Patterns.

(a) Relative quantity of transcripts encoding the four subclass I ADFs, *ADF1*, *ADF2*, *ADF3*, and *ADF4*, as detected by qRT-PCR of RNA samples from callus, root, 36 hour-old seedling, 10 day-old seedling, leaf, immature flower, and mature flower.

(b-q) Translational fusions of the subclass I *ADF* regulatory sequences with the *GUS* reporter gene were examined in transgenic *Arabidopsis* plants. Histochemical staining was performed on 2 day-old seedlings, roots, 20 day-old plants, and floral organs.

(b-e) *ADF1p::GUS* expression;

(f-i) *ADF2p::GUS* expression;

(j-m) *ADF3p::GUS* expression;

(n-q) *ADF4p::GUS* expression.

Figure 2.3 Analysis of *Arabidopsis* Subclass II ADF Expression Patterns.

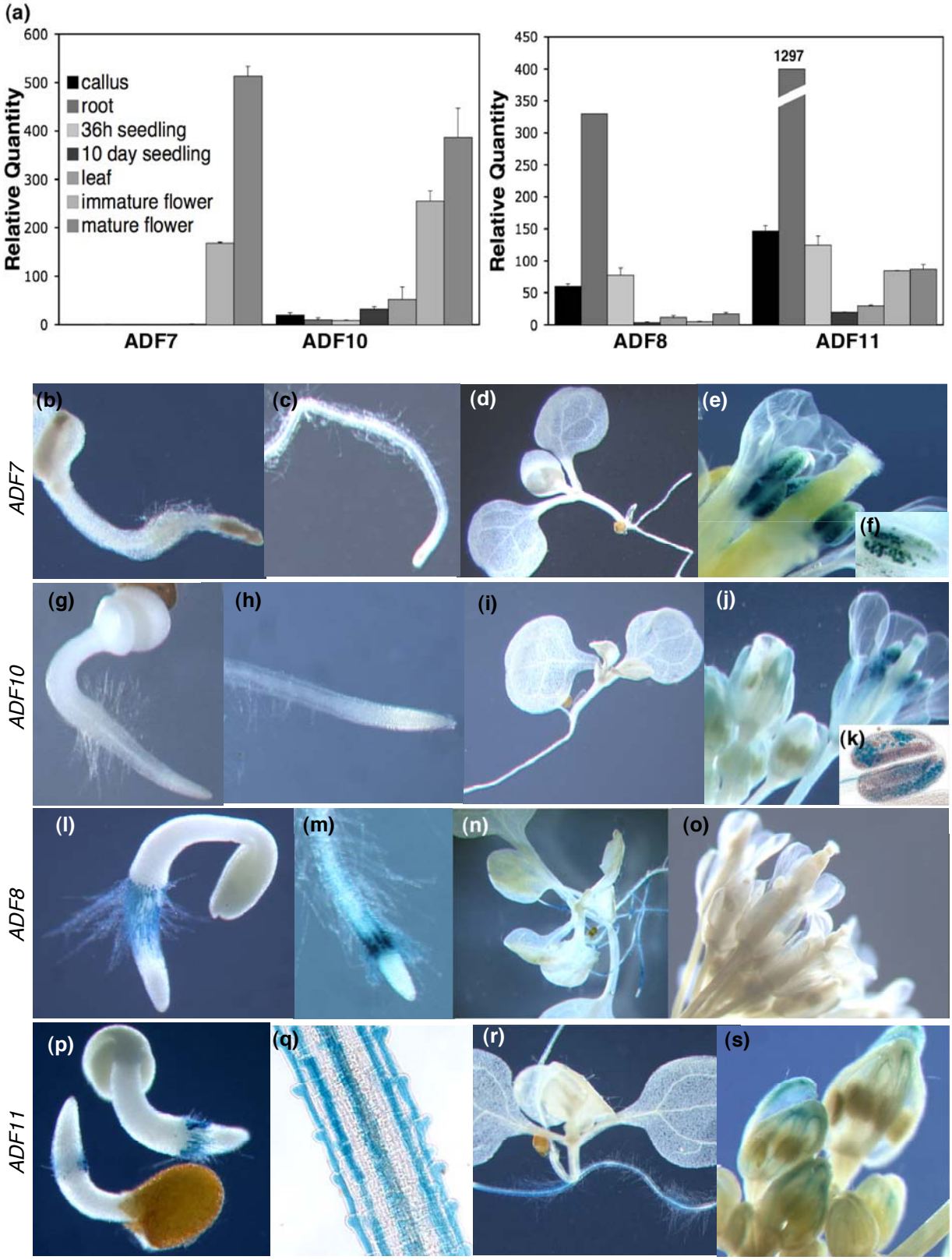

Figure 2.3 Analysis of *Arabidopsis* Subclass II ADF Expression Patterns.

(a) Relative quantity of transcripts encoding the four subclass II ADFs, *ADF7*, *ADF10*, *ADF8*, and *ADF11*, as detected by qRT-PCR of RNA samples from callus, root, 36 hour-old seedling, 10 day-old seedling, leaf, immature flower, and mature flower.

(b-s) Translational fusions of the subclass II *ADF* regulatory sequences with the *GUS* reporter gene were examined in transgenic *Arabidopsis* plants. Histochemical staining was performed on emerging seedling, roots, 7 to 20 day-old plants, and floral organs.

(b-f) *ADF7p::GUS* expression;

(g-k) *ADF10p::GUS* expression;

(l-o) *ADF8p::GUS* expression;

(p-s) *ADF11p::GUS* expression.

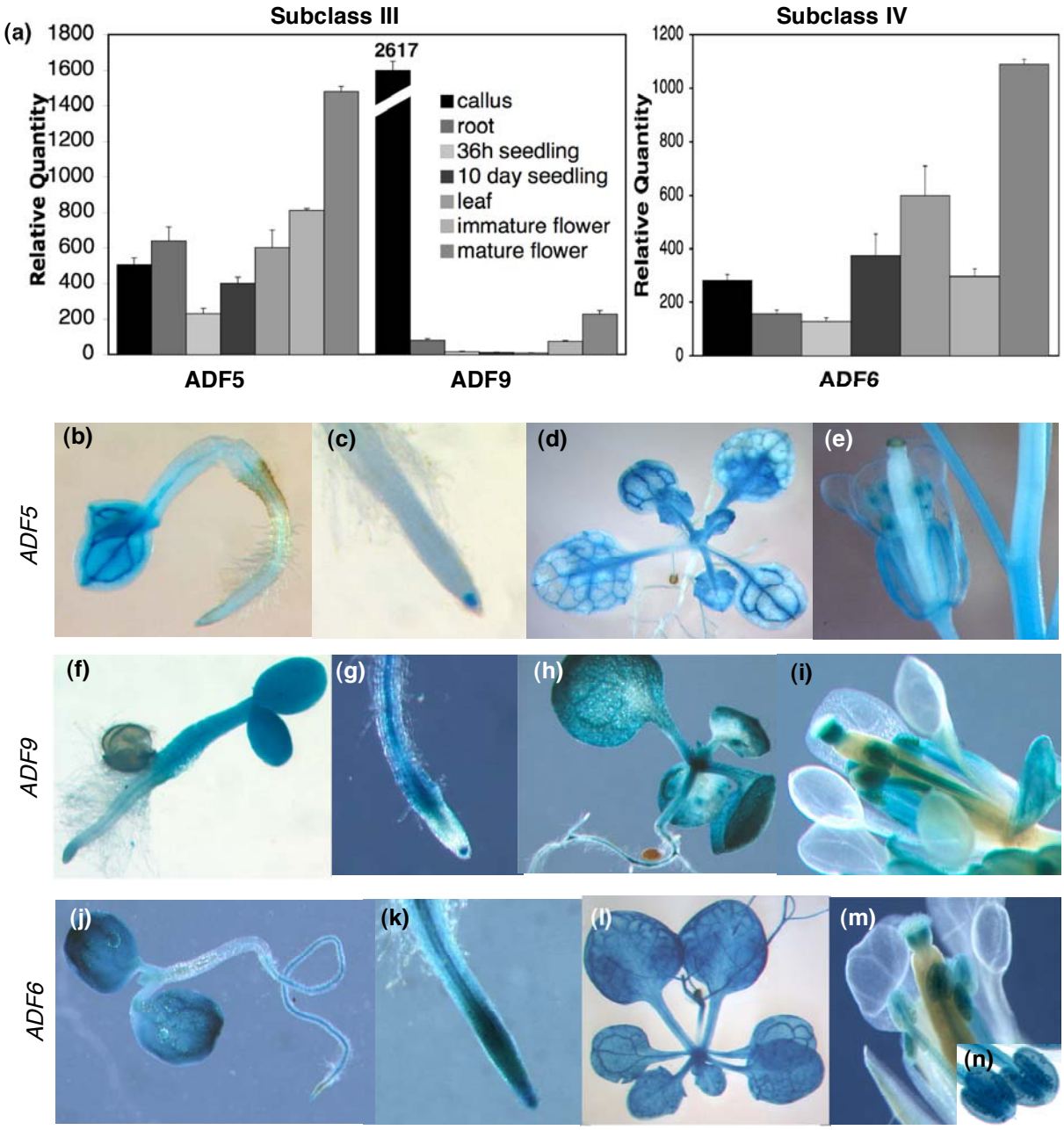

Figure 2.4 Analysis of *Arabidopsis* Subclass III and IV ADF Expression Patterns.

(a) Relative quantity of transcripts encoding the two subclass III ADFs, *ADF5* and *ADF9*, and the single subclass IV ADF, *ADF6*, as detected by qRT-PCR of RNA

samples from callus, root, 36 hour-old seedling, 10 day-old seedling, leaf, immature flower, and mature flower.

(b-i) Translational fusions of the subclass III and IV *ADF* regulatory sequences with the *GUS* reporter gene were examined in transgenic *Arabidopsis* plants. Histochemical staining was performed seedlings, roots, 12 to 20 day-old plants, and floral organs.

(b-e) *ADF5p::GUS* expression;

(f-i) *ADF9p::GUS* expression;

(j-n) *ADF6p::GUS* expression.

Figure 2.5 Characterization of mAbADF4a and ADF Subclass I Immunolocalization.

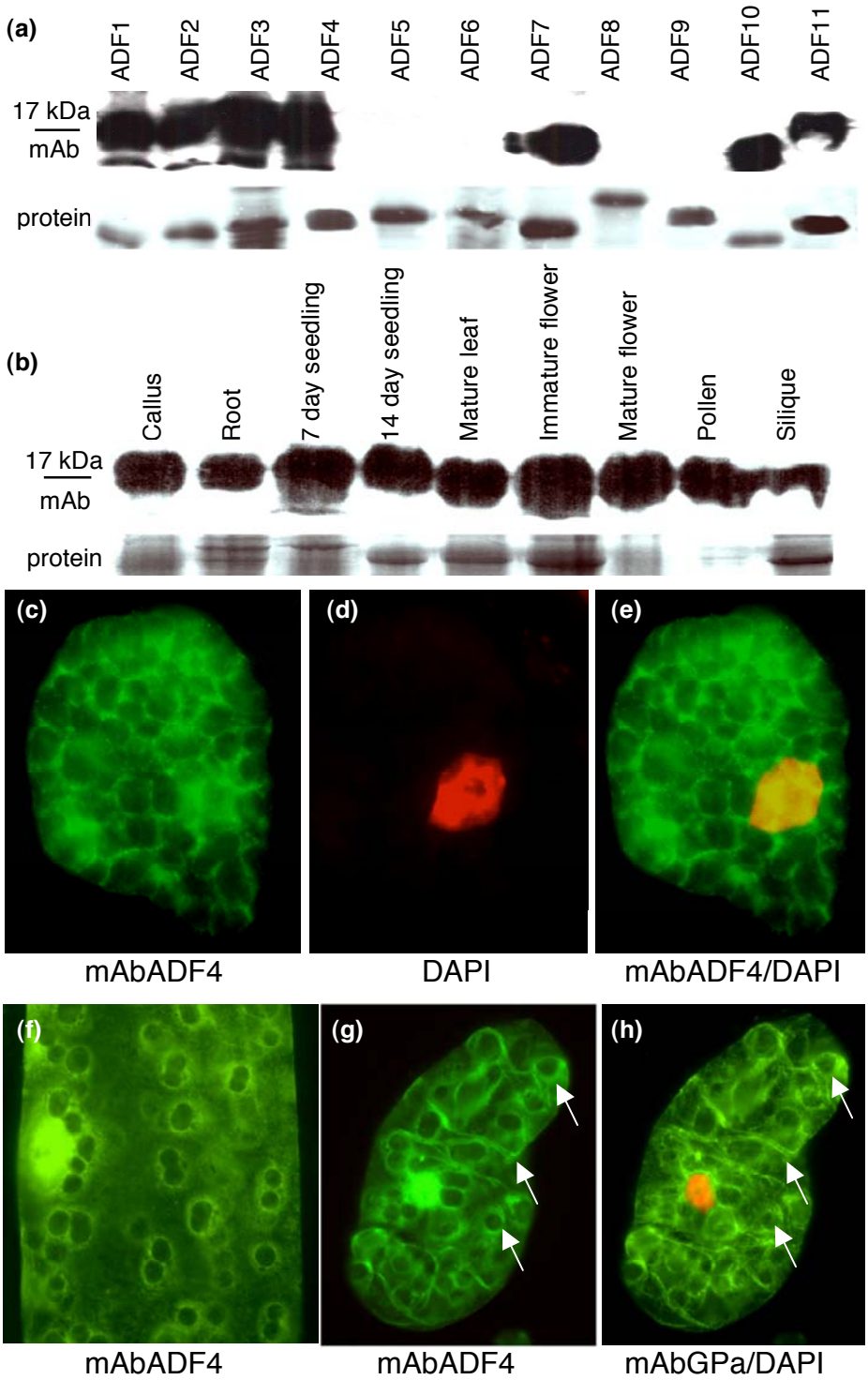

Figure 2.5 Characterization of mAbADF4a and ADF Subclass I Immunolocalization.

(a, b) Western blot analysis with monoclonal antibody mAbADF4a

(a) Specificity of mAbADF4a with the eleven recombinant ADF protein isovariants (top panel, see Experimental Procedures) and by Coomassie stained protein (bottom panel)

(b) Specificity of mAbADF4a with callus, root, 7 day-old seedling, 14 day-old seedling, mature leaf, immature flower, pollen, and silique plant samples (top panel) and

Coomasie stained protein (52-50 kDa) (bottom panel).

(c-h) Immunocytochemical localization of subclass I ADF isovariants with mAbADF4a.

(c) Isolated leaf cell prepared by chemical fixation-method probed with mAbADF4a;

(d) DAPI (4´,6-diamidino-2-phenylindole) image of DNA in (c);

(e) Merge of images shown in (c) and (d).

(f, g) Isolated leaf cells prepared by the cryofixation-method probed with mAbADF4a showing localization of ADF protein around chloroplasts and filaments (arrows).

(h) Cryofixation-method isolated leaf cell probed with mAbGPa and DAPI showing co-localization of actin (arrows) with mAbADF4a localization in (g).

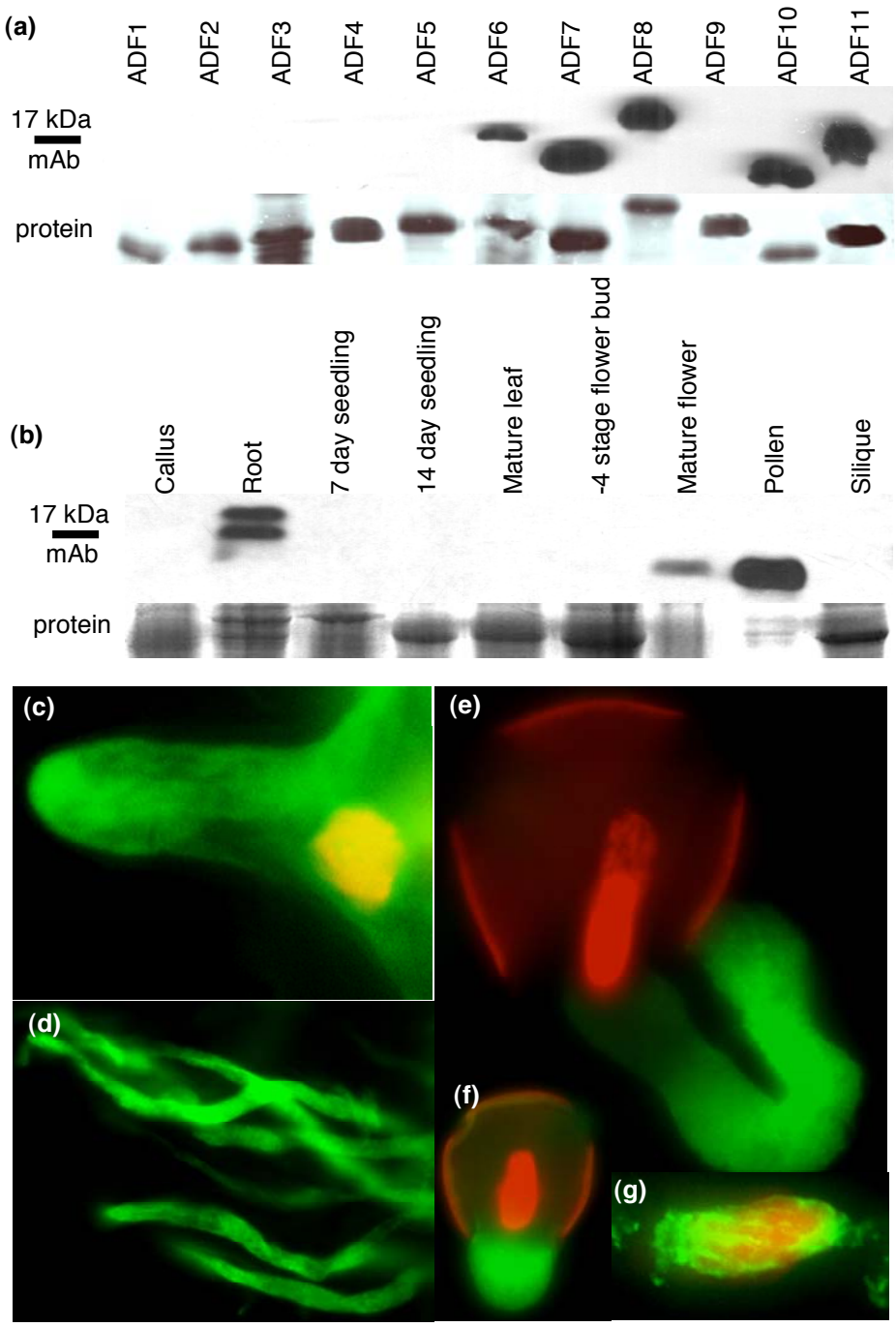

Figure 2.6 Characterization of mAbADF8a and ADF subclass II immunolocalization.

(a, b) Western blot analysis with monoclonal antibody mAbADF8a

(a) Specificity of mAbADF8a with the eleven recombinant ADF protein isovariants (top panel) and by Coomassie stained protein (bottom panel)

(b) Specificity of mAbADF8a with callus, root, 7 day-old seedling, 14 day-old seedling, mature leaf, immature flower, pollen, and silique plant samples (top panel) and Coomassie stained protein (52-60 kDa) (bottom panel).

(c-f) Immnohistochemical localization of subclass IIa and IIb isovariants with mAbADF8a using the chemical fixation method.

(c) Isolated emerging root hair probed with mAbADF8a (green) and DAPI (red) showing ADF localization throughout the cell and concentrated at the tip.

(d) Isolated elongating pollen probed with mAbADF8a showing pollen tube and tip localization.

(e-g) Germinated *N. tobaccum* pollen probed with mAbADF8a (green) and DAPI (red) showing localization to the emerging pollen tube (e and f) and surrounding the migrating vegetal nucleus (g).

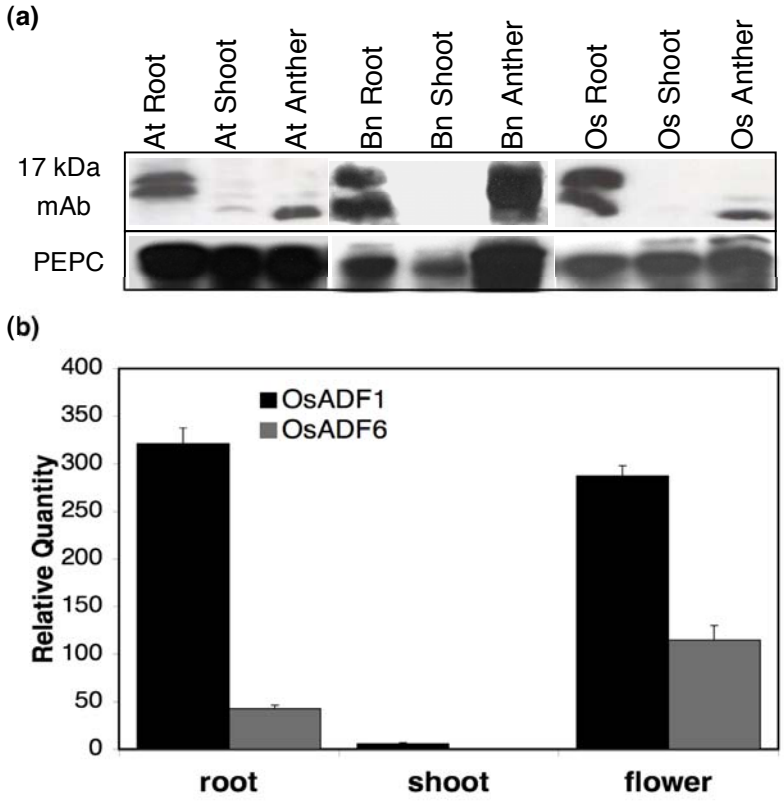

Figure 2.7 Ancient conservation of the subclass II expression pattern indicates subfunctionalization in the *Arabidopsis* lineage.

(a) Protein gel blot of root, shoot, and anther tissue from *Arabidopsis*, *Brassica napus*, and *Oryza sativa* probed with mAbADF8a (top) and PEPC (bottom).

(b) Relative quantity of *O. sativa* subclass II ADFs *ADF1* and *ADF6* detected by qRT-PCR.

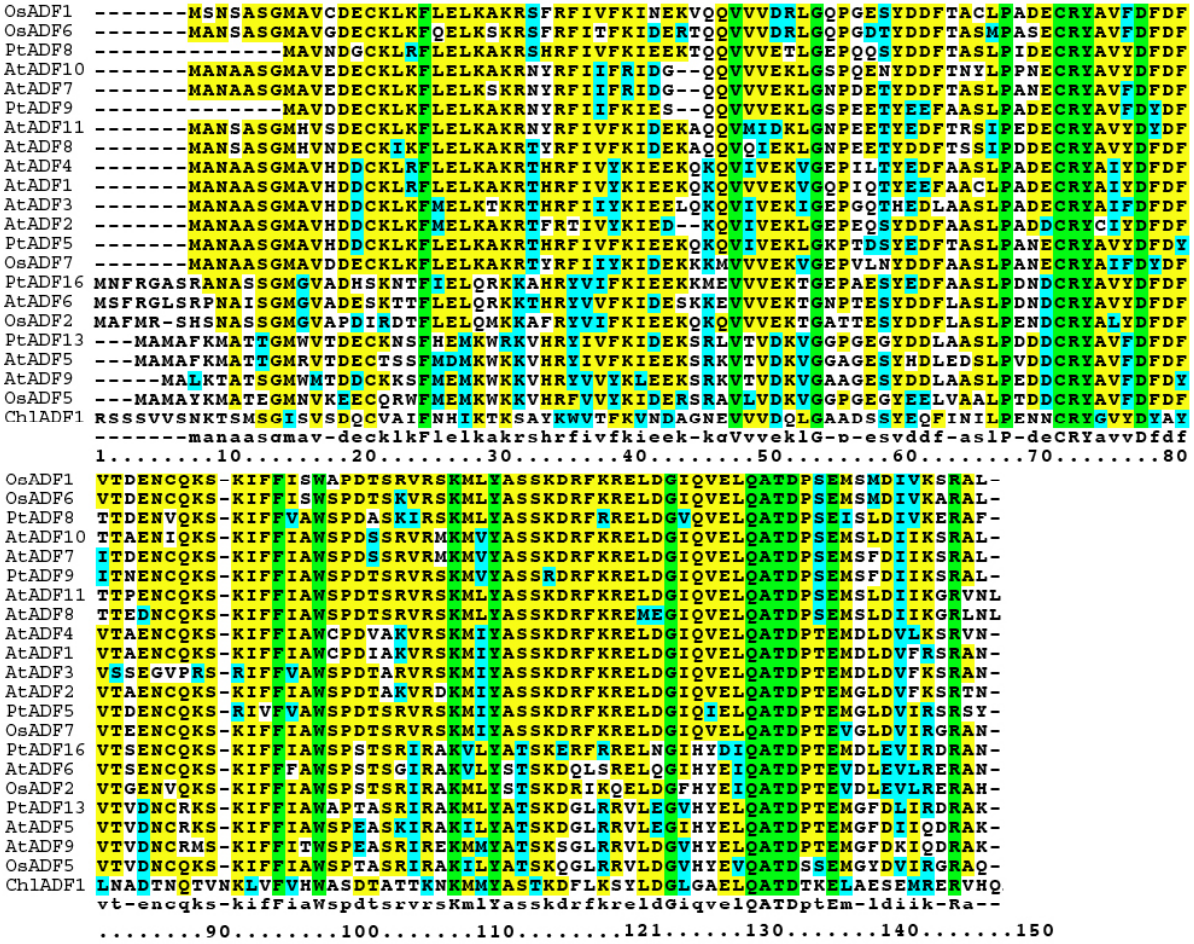

Supplemental Figure 2.S1: Boxshade diagram of ADF sequences aligned from Figure 2.1 phylogeny using ClustalW.

Table 2.S1 Primer sequences used to make the ADFp::GUS reporter cassettes

GUS S- TAG TGA GCC ATG GCT ATG TTA CGT CCT GTA GAA ACC CCA

A- TAA CGC TAA GGG CCC TCA TTG TTT GCC TCC CTG CTG CGG

NOS S- TAG TGA GGT ACC GCC ATG GCT CCC GGG ACA GGG CCC ATC GTT CAA ACA TTT GGC AAT AAA

A- TAA CGC TAA GAA TTC CCG ATG TAG TAA CAT AGA TGA CAC

ADF1 S-TAG GTC GAC TGC AAT TTG TAG TCT AGT GAC TAG

A-TAG CCA TGG CTG TTA AAC CAA ACA ACA CTC ATA

ADF2 S- TAG TCT AGA GTC CGG ATA TTG CTA AGG TGA GAA

A-TAG CCA TGG CTG TTA TCA TAT CAA TAC ACA TAA

ADF3 S- TAG TCT AGA TTA CTA CAA AAT TAC AAA ATA TTT

A-TAA TAA AGC CAT GGC CTG TTA CCA ACA AAA CAT AGA ACA T

ADF4 S-TAG TGA TCT AGA TGC GAC TAT TTC AGG TTC AAA

A- TAA TAA AGC CAT GGC CTG ATT TCA ATA AAA CAA CAG

ADF5 S-TAA GCA TGC TCG ATG AAA TAA AAG TGA AAA ATT

A-TAA TCT AGA AAC AAT AAT AGT CTA ATA GTT

ADF6 S- TAG TAG TCT AGA TAT AGA GAA GAA GTA AAG AAA GAA ACT T

A- TAA TAA AGC CAT GGC CTA CAG ATA TAA AAC CAA AAC ACA T

ADF7 S- TAG TGA TCT AGA CGC CAA ATT TTC AAA ACT ACC CCA AAA

A-TAA CGC TAA AGC CAT GGC CTT TTC ATT CAC ATA AAT TAG GAG GA

ADF8 S- TAG TGA TCT AGA AAC CAA CAA TTT GAA CCT GAG AAA TCG

A-TAA CGC TAA AGC ATG GCC TGC ACA ACA CAC ACA CAC ACA CAC G

ADF9 S- TAG TGA TCT AGA AAT AAA ATA AAT TCA ATA TTA

A- TAA TAA AGC CAT GGC CTA TTC CAA TAA CAA CCA

ADF10 S- TAG GAA TCC ACA TAT TAG TTT TTA TGC TCC TTG ATC TCA

A- TAA TAA AGC CAT GGC CTT TTC AGT TCA TAT ATC AGT CAA

ADF11 S- TAG TGA TCT AGA TTC TCG CAC TAG CTA GTAGCT AAA

A- TAA CGC TAA AGC CAT GGC CTG CAC AGT CAA ACA CAT GCA TAG TCA

Table 2.S2 Primer sequences used in qRT-PCR amplification of the 11 ADF gene transcripts

18s rRNA S- GGG GGC ATT CGT ATT TCA TA

A- TTC GCA GTT GTT CGT CTT TC

ADF1 S- GGG AAC TAG ATG GGA TTC AAG TAG AG

A- GGC TCC TGA AAA CAT CGA GAT C

ADF2 S- GCC AAA GTG AGA GAC AAG ATG ATT T

A- GAA TTC CAT CTA GTT CTC TCT TGA ACC T

ADF3 S- TCG GTT GAA TCA AAC TTT TTC GT

A- GGT ACC GTC ACA GCA AAC TTT AGG

ADF4 S- TGT TTT CTA TTC TCT TAC AGT CTC TTG TGA

A- CAG AGA ACA GAC CAG ACA GAT AGA ATG

ADF5 S- CGT TTG TGT TTT GAT TGT GTT GTT AA

A- CCG TTA CTC GTA GGA CAA ATT CG

ADF6 S- AGC TAC TGA TCC TAC TGA GGT TGA TCT

A- GCA ATC TTG CTT GCT CTC AGT TC

ADF7 S- AGC GAG ATG AGC TTC GAC ATT AT

A- TCG ATG ATA GAG ATA TAG ATC GTT GAA AA

ADF8 S- CAT TTT GTG TGG ATT CAA TGT CTT TA

A- GCC AAA GCA TTC CAT ACC AAG T

ADF9 S- CTC AAA ATA TAA CGA AAG AAC AAG AAG ACA

A- CAC TCG TCG CCG TCT TCA A

ADF10 S- GAC CCG AGC GAG ATG AGT CT

A- GGA TAT ATA ATT AGA AAA GCA AGG AGA TCT AGA

ADF11 S- GGT ACG CAA TAA TCA TCC CAA TAG A

A- GTT GCT TGA AAT TGC CAG CTT

OsADF1 S- TCA TCT CCT GGG CTC CTG AT

A- CCT TGG AGC TAG CAT ACA GCA TCT

OsADF6 S- CGC CGG ACA CGT CGA A

A- TCC CTC TTG AAC CGG TCC TT

CHAPTER 3

ARABIDOPSIS ACTIN DEPOLYMERIZING FACTOR5 FUNCTIONS IN MULTICELLULAR DEVELOPMENT AND IS A REPRESSOR OF THE *CBF* COLD RESPONSE TRANSCRIPTION FACTORS[1]

[1] Daniel R. Ruzicka, Libby C. McKinney, Muthugapatti K Kandasamy, and Richard B. Meagher To Be Submitted to Plant Physiology

ABSTRACT

The actin cytoskeleton is a critical component for multiple cell functions including signaling cascades and stress responses. Actin Depolymerizing Factor (ADF) is a key facilitator of this dynamic response by translating a cellular signal into physical actin cytoskeleton remodeling. Here we analyze the function of Arabidopsis *ADF5* as an important regulator of organ and cell development and as an essential and specific repressor of the CBF cold response transcription factors. The *adf5-1* null allele exhibited an increased number of cauline and rosette leaves, an increased number of trichome and stomata cells, delayed flowering time, and a stabilized F-actin cytoskeleton. *ADF5* was induced 20-fold during cold stress conditions, and yet *adf5-1* was freeze-tolerant compared to wild-type. Cold-response transcription factors *CBF1*, *2*, and *3* were de-repressed in the mutant in the absence of cold stress. Furthermore, micrococcal nuclease protection and chromatin immunoprecipitation assays demonstrated that the loss of ADF5 altered nucleosome structure within the *CBF1* promoter. Lastly, *ADF5* expression was less-efficiently induced in response to cold stress in a *cbf2* mutant background, placing ADF5 in a feedback loop both upstream and downstream of the CBF transcription factors as a novel modulator of freeze tolerance.

INTRODUCTION

The actin-based cytoskeleton plays an essential role in plant and animal development (Meagher and Williamson, 1994; Pollard *et al.*, 2000; Staiger, 2000; Wasteneys and Galway, 2003). Actin filaments and bundles dynamically contribute to the programming of organ, tissue, and cell development by facilitating the assembly of various cellular structures. Actin's role in cell polarity and division plane determination is particularly important in plants, where cells do not migrate during multicellular organ development. Destabilization of the plant actin cytoskeleton is required for membrane rigidification, which subsequently induces a cytosolic calcium influx and freeze tolerance (Orvar, 2000). Actin also controls gene expression via nuclear roles in chromatin remodeling and transcription, and via additional cytoplasmic roles controlling the localization and activity of various transcription factors (Bettinger *et al.*, 2004; Ruegg *et al.*, 2004; Visa, 2005; Miralles and Visa, 2006). Control of actin function is modulated by the activity of hundreds of actin-binding proteins (ABPs) (Meagher and Fechheimer, 2003; Cvrckova *et al.*, 2004), some of which contribute to actin's nuclear activities (Bettinger *et al.*, 2004).

Actin depolymerizing factor (ADF) and closely related vertebrate cofilin form a class of proteins that binds F-actin and promotes depolymerization and severing in response to diverse stimuli, resulting in enhanced actin cytoskeleton remodeling (Theriot, 1997; Bamburg, 1999; Chan *et al.*, 2000; Ghosh *et al.*, 2004). ADFs exhibit cytoplasmic and nuclear localization and have been shown to be required for the

nuclear import of actin, thus potentially indirectly modulating actin's nuclear activities (Nebl *et al.*, 1996; Bamburg, 1999; Pendleton *et al.*, 2003; Ruzicka *et al.*, 2007).

ADFs are encoded by an ancient gene family in both plants and animals (Maciver and Hussey, 2002). The Arabidopsis ADF family is comprised of 11 gene members in several divergent classes (Ruzicka *et al.*, 2007). Previous reports identified a cold-induced actin depolymerizing factor (TaADF) protein in a cold-hardy wheat cultivar (Danyluk *et al.*, 1996; Ouellet *et al.*, 2001). Based on amino acid sequence, this wheat ADF is most similar to *Arabidopsis* Subclass III ADFs including ADF5 (Supplemental Figure 3.S1). Expression analysis of Arabidopsis *ADF5* found it to be responsive to cold temperatures as well, arguing for a conserved functional role between the wheat and Arabidopsis orthologues. Herein, we characterize the function of *Arabidopsis* ADF5 as a strong pleiotropic regulator of organ and cell development. ADF5 is a specific negative regulator of the *CBF1, 2,* and *3* transcription factors affecting freeze tolerance via a novel mechanism that appears to involve alterations to the chromatin of the *CBF1* promoter.

RESULTS

The *adf5-1* defective allele

An *ADF5* T-DNA insertion allele, *adf5-1*, was isolated in the Arabidopsis Columbia ecotype and obtained from ABRC (Salk_018325). The insertion was located 69 base pairs into the third exon of the *ADF5* gene and deleted a total of 36 bases starting at bp 350 as shown in Figure 3.1A. *ADF5* mRNA levels in the *adf5-1* mutant were assayed

relative to *ubiquitin* mRNA levels and normalized to wild-type tissue using qRT-PCR. *ADF5* mRNA levels were reduced 99.7% in *adf5-1* compared to wild-type (Figure 3.1B), and, combined with the exon location of the T-DNA insertion, *adf5-1* was classified as a null allele.

Developmental phenotypes of *adf5-1*

Adf5-1 plants displayed several developmental phenotypes including an increase in rosette and cauline leaf numbers and an increase in flowering time as shown in Figure 3.1C through J. Wild-type plants had 13 leaves when the inflorescence first emerged (24 days), while *adf5-1 plants* already had 22 leaves at 24 days, and flowered 5 days later (Figure 3.1C-E, and M). Because *adf5-1* plants had more leaves than wild-type plants at 24 days, the *adf5* mutant initiated leaves faster in addition to exhibiting a delay in flowering. The *adf5-1* mutant also exhibited an increase in cauline leaf number at inflorescence stem junctions (Figure 3.1F and G). Normal *Arabidopsis* primary inflorescence stems have single cauline leaves at secondary branch junctions, while 67% of the primary inflorescences of *adf5-1* plants had two or three cauline leaves at secondary branch junctions. Thus, the *adf5-1* mutant exhibits an organ-number and organ initiation phenotype.

In addition to an increase in leaf number, there was also an increase in trichome and stomata cell numbers relative to puzzle epidermal cells on *adf5-1* leaves. To correct for potential differences in leaf-surface cell density caused by differences in leaf growth rates, trichome and stomata cell counts were performed on mature leaves. Fully

mature wild-type leaves had an average of 30.3 +/- 0.9 trichomes per 1cm^2 compared to *adf5-1* leaves that had an average of 67.0 +/- 5.0 trichomes per 1cm^2 (Figure 3.1H and O). Wild-type leaves also had an average of 17.8 +/- 0.7 stomata per 0.22 mm^2, whereas *adf5-1* leaves had an average of 26.5 +/- 1.3 stomata per 0.22 mm^2 (Figure 3.1I, J, and N). Scanning electron-microscope images were taken of wild-type and *adf5-1* leaf surfaces to determine if the trichome and stomata phenotypes also signaled changes in leaf epidermal cell size, shape, or number. Epidermal pavement cells were not different in size, architecture, or number in *adf5-1* (Figure 3.1I and J). All rosette and leaf phenotypes are summarized in Table 3.1.

Genetic complementation and overexpression

A construct expressing *ADF5* from the strong and constitutive Actin2 promoter-terminator expression cassette (*A2pt:ADF5*) was introduced into *adf5-1* and wild-type plants to genetically complement the *adf5-1* defects and to test the effect of *ADF5* over-expression. The *A2pt:ADF5* transgene produced extremely high levels of *ADF5* transcript ranging from 35- to 90-fold above wild-type (Figure 3.1B). The *A2pt:ADF5* transgene quantitatively complemented all *adf5-1* morphological phenotypes as shown in Figures 3.1 and 3.2, and Table 3.1. Rosette and cauline leaf number were indistinguishable from wild-type in the *adf5-1*/*A2pt:ADF5* complemented lines, and trichome and stomata numbers were restored to wild-type levels. Of note, the over-expression of *ADF5* mRNA did not produce dominant morphological phenotypes in relation to leaf number or any other obvious morphological phenotype.

ADF5 affects the organization and morphology of the F-actin cytoskeleton

Classically, ADFs bind the barbed end of actin filaments, change the filament's helical twist, and promote actin monomer depolymerization and small polymer severing. To assay the organization of the actin cytoskeleton in the *adf5-1* mutant, we transformed wild-type and *adf5-1* plants with the Green Fluorescent Protein/fimbrin actin binding domain 2 fusion (GFP:fABD2) F-actin reporter construct (Wang *et al.*, 2005). The actin cytoskeleton morphology was observed using confocal microscopy in multiple independently transformed wild-type and *adf5-1*/*GFP:fABD2* lines. F-Actin morphology was examined in root cells and leaf trichomes, where *ADF5* is expressed and GFP-labeled actin filaments are easily visualized. In wild-type leaf trichome cells, the actin cytoskeleton is organized into a network of fine filaments and bundles primarily arrayed longitudinally along the axis of cell growth (Figure 3.1K). In *adf5-1* leaf trichome cells, the general organization of filaments was similar to wild-type, but the thickness of bundles was increased and the number of fine filaments decreased compared to wild-type (Figure 3.1L). The organization of the F-actin cytoskeleton was not grossly affected in root cells in *adf5-1*, correlating with the absence of a root morphological phenotype (data not shown). The altered F-actin cytoskeleton in *adf5-1* leaf trichomes argues that ADF5 affects F-actin cytoskeleton remodeling and organization, and that the loss of ADF5 results in an increase in F-actin stability.

ADF5 is weakly and constitutively expressed, but is highly induced during cold stress

Previous examination of an *ADF5* promoter-reporter fusion established that *ADF5* was expressed constitutively, but was more strongly expressed in the root-tip meristem and in emerging leaves (Ruzicka *et al.*, 2007). Because the ADF5-orthologue in wheat was induced during cold stress, *ADF5* mRNA levels were assayed using qRT-PCR in 14 day-old wild-type seedlings at various time points of 4°C cold stress. Figure 3.2A details a time course of *ADF5* mRNA levels normalized to time zero (23°C). After 6 and 8 hours of 4°C temperatures, *ADF5* levels were 20-fold higher than at time zero. Interestingly, *ADF5* levels decreased to within 4-fold higher than time zero after 24 hours of 4°C exposure. These data suggest *ADF5's* cold induction profile is comprised of a burst of transcription with maximum mRNA accumulation approximately 6-8 hours after the initiation of cold-stress.

adf5-1 mutant plants are freeze-tolerant

The winter annual Arabidopsis weakly tolerates sub-zero temperatures, however, when a period of 4.0°C cold acclimation precedes freezing, the freeze tolerance of Arabidopsis increases dramatically (Thomashow, 1999). After 24 hours of cold acclimation, Arabidopsis is able to withstand sub-zero temperatures down to -12.0°C, primarily because of the induction of multiple freeze tolerance factors in the plant cells during this acclimation period (Van Buskirk and Thomashow, 2006). Because *ADF5* is induced during cold stress, we hypothesized that the *adf5-1* mutant might exhibit a cold-

sensitivity phenotype. Under this model, the absence of ADF5 would lead to a plant that is hypersensitive to cold and may have a lower tolerance for freeze conditions. To test this, adult plants were transferred for 12 minutes to a freeze chamber at -15°C. Freeze tolerance was quantified by assaying the percentage of individual leaves that died within 24 hours of the freeze treatment. In this experiment, 46.8% of wild-type leaves versus 18.5% of *adf5-1* leaves were chlorotic and significantly damaged as shown in Figures 3.2B, C, and D. Thus, ADF5-defiency has the unexpected property of being freeze tolerant. Additionally, *adf5-1* plants expressing the *A2pt:ADF5* complementation transgene restored freeze resistance to wild-type levels (40.4% leaf death, Figure 3.2D and Table 3.1). In order to better quantify the ***increase*** in freeze tolerance in *adf5-1*, we measured electrolyte leakage in wild-type and *adf5-1* plants after freeze exposure (Sukumara.Np and Weiser, 1972; Gilmour *et al.*, 1988). Electrolyte leakage was calculated as the percentage of electroconductivity of a solution containing plant material frozen at –15°C for 12 minutes as compared to the sample's electroconductivity after an 8 hour –80°C-mediated total cell lysis. Wild-type tissue exhibited 25.2% electrolyte leakage compared to *adf5-1* tissue's 11.7% electrolyte leakage after the 12 minute –15°C freeze (Figure 3.2E and Table 3.1), consistent with the results of the leaf damage assay.

Cold temperature stress results in significant changes to the plant transcriptome and ultimately freeze tolerance (Kreps *et al.*; Chinnusamy *et al.*, 2003). Arabidopsis cold tolerance is known to operate via multiple mechanisms including a signal transduction pathway through the CBF transcription factors as shown in Figure 3.3A.

The CBFs bind to CRT-domains in the promoters of a suite of cold responsive (COR) genes including KIN1, ERD10, and COR15, resulting in their induction during cold-stress (Gilmour *et al.*, 1998; Steponkus *et al.*, 1998; Thomashow, 1998). The expression of these COR genes ultimately results in increased freeze tolerance at the cellular and organismal levels (Jaglo-Ottosen *et al.*, 1998). Previous studies have indicated that the CBF-mediated cold-stress signaling pathway undergoes feedback-regulation after long periods of cold temperatures (As reviewed in (Chinnusamy *et al.*, 2006)), thus providing a possible model for ADF5 function given the contradicting observations of *ADF5* cold-induced expression and *adf5-1* freeze tolerance. To test whether the freeze tolerance phenotype seen in the *adf5-1* mutant was due to altered transcriptional regulation of the CBF-mediated cold-stress signaling pathway, we analyzed the expression of a suite of known cold-signaling pathway factors in the *adf5-1* mutant using qRT-PCR as summarized in Figures 3.3A and B. Significantly, the cold response genes *COR15a, KIN1, ERD10, and COR78* were up-regulated 3.5-, 61.4-, 1.7-, and 2.1-fold, respectively, in *adf5-1* during normal growth conditions at 22°C (Figure 3.3A). Previous studies have characterized these genes as direct targets of the CBF/DREB family of transcription factors (Jaglo-Ottosen *et al.*, 1998; Fowler and Thomashow, 2002). qRT-PCR analysis of *CBF1, 2, 3*, and *DDF1* message levels demonstrated dramatic increases of 10-, 2.5-, 7.5-, and 14.1-fold, respectively, in *adf5-1* (Figure 3.3B). Because the CBFs are repressed during normal temperature conditions, we classify these changes in CBF expression in *adf5-1* as de-repression. In the cold-signaling pathway, the transcription factor ICE1 is an upstream activator of the *CBFs*,

and qRT-PCR confirmed no change in the expression of *ICE1* or homologous bHLH proteins (At1g12860, At5g10570, At5g65640) (Supplemental Figure 3.S2) (Chinnusamy *et al.*, 2003; Zarka *et al.*, 2003). These results indicate that the *adf5-1* freeze tolerance phenotype is likely due to changes in expression of the *CBFs*. However, ICE1 activity is modulated by post-translational regulation. Therefore, we cannot conclusively state that ADF5 only acts in this CBF cold signaling pathway at the level of *CBF* expression, and not also on the post-translational modification of ICE1. To rule out changes in alternative pathways that affect freeze tolerance, we also tested the expression levels of *ATHVA22B* (At5g62490) and *HSI2* (At2g30470), known abscisic acid (ABA) and Ca^{2+} responsive genes that are not cold-induced (Chen *et al.*, 2002; Nakashima *et al.*, 2006). We did not observe a significant change in expression of these genes in *adf5-1* (Supplemental Figure 3.2S). These results suggest that the de-repression of the CBF genes in *adf5-1* was not the result of a defect in tangential ABA- or Ca^{2+}- signaling pathways.

Over-expression of *ADF5* does not affect *CBF* expression

Given that ADF5 is **necessary** for the repression of the *CBFs* during normal growth conditions, we asked whether ADF5 is also **sufficient** to repress *CBF* expression. *CBF* levels were assayed in *ADF5* over-expression plants using qRT-PCR. The over-expression of *ADF5* did not have a dominant effect on the expression of the *CBFs* in either normal or cold-stress conditions (Figure 3.3C). In the *adf5-1* mutant, the *A2pt:ADF5* transgene fully complemented *CBF1, 2, and 3* expression, restoring each

back to wild-type levels (Figure 3.3B). While this confirms that *CBF* de-repression in *adf5-1* is due to the loss of ADF5, the lack of a dominant *A2pt:ADF5* suppression phenotype argues that an unidentified co-factor is rate limiting for the ADF5-mediated repression of the *CBFs*.

ADF5 significantly alters the chromatin of the *CBF1* promoter

Actin has been shown to participate directly in various chromatin remodeling complexes and also to affect the nuclear localization of transcription factors and other actin-bound signaling molecules (Rando *et al.*, 2002; Miralles *et al.*, 2003; Miralles and Visa, 2006). ADF5 might regulate actin's participation in these complexes directly by transporting actin into the nucleus or altering the dynamic remodeling capacity of the actin cytoskeleton and thus regulate the localization of transcription factors (Pendleton *et al.*, 2003; Ruegg *et al.*, 2004). Following from these models, the de-repression of the CBF genes may result from changes to the structure of chromatin at the *CBF* locus in the *adf5-1* mutant. To test this hypothesis, we performed micrococcal nuclease (MNase) protection assays and Chromatin Immuno-Precipitation (ChIP) assays comparing wild-type and *adf5-1* chromatin structure within the promoter region of *CBF1*.

First we assayed nucleosome occupancy in this region using qPCR analysis of DNA fragments protected by nucleosomes from nuclease digestion as detailed in Appendix 1. We isolated nuclei, digested chromatin with MNase, and purified the protected, undigested DNA. This DNA was then assayed with qPCR using primers specific to small (70-90 base pair) overlapping regions of the *CBF1* promoter as

mapped in Figure 3.4A. When DNA is stably wrapped around a nucleosome, it will be well protected from digestion, and thus exhibit high levels of qPCR amplification. Figure 3.4B shows the qPCR amplification difference between wild-type and *adf5-1* at the various regions mapped in figure 3.4A. The –678, -562, and –538 primer-pair regions all showed significant increases in qPCR amplification, and thus increases in MNase protection, in the *adf5-1* mutant under normal growth conditions (22°C). Therefore, we conclude that the chromatin structure at the *CBF1* promoter region is more compact in the *adf5-1* mutant, resulting in this increase in nuclease protection.

Three ChIP assays were performed to assay the chromatin state of the CBF1 promoter more directly because the changes in nuclease protection could result from a variety of changes to the chromatin including altered nucleosome stability and/or position, and altered histone methylation and/or acetylation (He *et al.*, 2003; Gendrel *et al.*, 2005). Antibodies detecting the core histone H2B, the H3Lys4Lys9 Acetylation (H3k4k9Ac) histone modification, and the H3Lys9 trimethylation (H3k9Me) histone modification were used to assay changes in nucleosome structure. Immunoprecipitated DNA was analyzed at four locations along the *CBF1* promoter (-736, -562, -415, and -135 upstream of the transcriptional start site) as shown in the diagram of Figure 3.4A. Core histone H2B-bound chromatin DNA was enriched in *adf5-1* across the CBF1 promoter to levels ranging from 1.5- to 3-fold (Figure 3.4C). The vast majority of nucleosomes contain the core H2B histone, thus the H2B ChIP provided an independent assay for general nucleosome occupancy reaffirming the nuclease protection experiment results. In contrast to the H2B result, chromatin

immunoprecipitated using the anti-H3k4k9Ac antibody was significantly depleted across the *CBF1* promoter in the *adf5-1* mutant (Figure 3.4D). Furthermore, ChIP assays using a H3k9Me antibody were enriched over 5-fold in *adf5-1* at the -736 and –567 regions of the *CBF1* promoter and over 2-fold at the -415 region indicating a significant increase in H3k9Me-containing nucleosomes in the upstream regions of the *CBF1* promoter (Figure 3.4E). However, the H3k9Me ChIP at the -135 region detected an over 3-fold depletion in *adf5-1*. Altogether, these results indicate that the chromatin organization and structure at the *CBF1* promoter is significantly altered in the *adf5* mutant, and more specifically, is significantly compacted.

ADF5 functions at the *CBF1* promoter independently of cold-stress mechanisms

The de-repression of the *CBF* transcription factors in *adf5-1* appears to result in increased freeze-tolerance similar to the effect of cold acclimation. To test whether the *adf5-1* nuclease protection phenotype at the *CBF1* promoter is phenocopied in wild-type plants that have been cold-stressed for 2 hours (thus causing the induction of *CBF1*), the MNase protection assay was repeated comparing wild-type plants harvested at 22°C to wild-type plants harvested after being cold stressed at 4°C for 2 hours. Figure 3.5 shows that in the cold-stressed wild-type plant sample, the nuclease protection is decreased across most of the *CBF1* promoter region, a significantly different result from the *adf5-1* mutant at 22°C (see figure 3.4B). Significantly, the nuclease protection of the –678 and -538 *CBF1* promoter regions decreased 2- and 10- fold, respectively, in the cold-stressed wild-type: a result nearly opposite to the *adf5-1* mutant at 22°C.

Therefore, we conclude that the loss of ADF5 function does not cause cold-mediated *CBF* induction, but instead ADF5 is a component of a novel *CBF* repression mechanism that may function during normal temperature conditions.

ADF5 is downstream of the CBFs in the cold-stress signaling pathway

Given the induction of *ADF5* expression after 8 hours of 4ºC cold stress, and given the *adf5-1* phenotype of de-repressed CBF expression levels, we propose a testable model whereby ADF5 is involved in the auto-regulated repression of the CBFs. The *CBF* transcription factors are known to peak in expression approximately 3 hours after transfer to 4°C, while target genes downstream of CBF, including *COR15a,* peak 8-24 hours after transfer (Gilmour *et al.*, 1998). Thus, the induction of *ADF5,* which peaked in the T_{4°=6-8 time range, was similar to that of many other COR genes (Figure 3.2A). Analysis of the ADF5 promoter revealed 2 TGCCGACGAGAA motifs in the first 500bp (Supplemental Figure 3.3S), which contain the C-repeat (CRT) CCGAC common to COR gene promoters and the binding site for CBFs (Yamaguchi-Shinozaki and Shinozaki, 1994).

To directly test the hypothesis that *ADF5* is regulated by the CBFs, we analyzed *ADF5* levels in a *cbf2* mutant characterized by Thomashow and Doherty (Salk_009689). Previous reports indicated that COR genes were up-regulated in a *cbf2* mutant, likely because *CBF1* and *CBF3* were constitutively expressed (Novillo *et al.*, 2004). In this *cbf2* allele, *ADF5* expression levels were down 1.5-fold under normal 22ºC temperature conditions, and *ADF5* expression levels were down 6.3-fold in the *cbf2* mutant after 8

hours of 4ºC cold stress as shown in Figure 3.6. The simplest conclusion drawn from these data is that *ADF5* is in fact regulated by CBF2, and is therefore involved in a feedback loop that is part of the auto-regulation of the CBF transcription factors.

Other Arabidopsis ADFs cannot fully complement the loss of ADF5

To test whether the over-expression of other Arabidopsis ADFs could complement the loss of ADF5 and restore the proper regulation of the cold-stress signaling pathway, we transformed the *adf5-1* mutant with transgenes expressing *ADF7* or *ADF9* under the control of the strong and ubiquitous *ACT2* promoter/terminator. For each complementation, multiple independent *adf5/A2pt:ADF* lines were characterized for morphological and cold-stress signaling phenotypes. We quantified the expression level of CBF1 in these complementation lines, and compared them to wild-type and *adf5-1* levels. Significantly no complementation was observed in multiple independent lines of each the *adf5/A2pt:ADF7* or *adf5/A2pt:ADF9* complementation alleles as shown in Supplemental Figure 3.S4. Therefore, we conclude that ADF5 is specifically required for the proper regulation of the cold-stress signaling pathway, and this function cannot be rescued by the over-expression of subclass II *ADF7* or the more closely related subclass III *ADF9*.

DISCUSSION

The loss of ADF5 causes mild actin cytoskeleton defects

The actin cytoskeleton is required for a wide range of cellular functions including organ initiation, cell specification, cell proliferation and division, and membrane fluidity (Orvar, 2000; Barrero *et al.*, 2002; Dhonukshe *et al.*, 2005). Thus, the *adf5-1* mutant phenotypes of altered leaf, stomata, and trichome numbers, and of an increase in freeze tolerance may result from alterations to the cytoplasmic actin cytoskeleton. However, ADF5 is one of seven ADF isovariants expressed in leaf tissue and *ADF5* is not highly expressed compared to these other *ADFs.* Therefore, *adf5-1* is less likely to cause gross actin cytoskeletal defects because of the likely redundancy among these seven ADFs. Supporting this redundancy hypothesis, *adf5-1* trichome cells exhibited only a moderate increase in filament bundling and F-actin polymerization, indicating that ADF5 is required for proper remodeling and organization of the F-actin cytoskeleton, but plays a relatively minor role. Simply put, it is hard to reconcile the mild actin cytoskeleton phenotype described here as the cause of the highly specific and severe developmental and cold-stress phenotypes of the *adf5-1* mutant.

The *adf5-1* freeze tolerance phenotype does not agree with the conventional actin-cytoskeleton membrane fluidity model

Furthermore, while the actin cytoskeleton does effect cold-stress signaling, it is a **destabilization** of the actin cytoskeleton that increases membrane rigidity, resulting in

the constitutive expression of freeze tolerance genes (Orvar, 2000). The *adf5-1* mutant exhibits a stabilized actin cytoskeleton phenotype indicating that the *adf5-1* freeze tolerance phenotype does not result from an increase in membrane rigidity. In conclusion, we argue that ADF5 exhibits highly specific functions outside of a general actin binding and cytoskeletal remodeling activity.

ADF5's role in gene regulation

The diverse developmental and freeze-tolerance *adf5-1* phenotypes could be the result of a more direct mis-regulation of the *CBFs* and other shoot meristem transcription factors (Takada *et al.*, 2001; Cole *et al.*, 2006). One model to account for a gene regulation phenotype in an ADF is through its role in the nuclear localization of actin. Studies have shown ADF/cofilin to be required for the nuclear localization of actin, and it is now widely accepted that actin is required for multiple nuclear functions including chromatin remodeling, general transcription, and mRNA processing(Pendleton *et al.*, 2003). Therefore, a defect in an ADF could result in a nuclear actin defect, thereby affecting gene regulation as shown in model 1 of Figure 3.7. If an Arabidopsis actin-containing complex were required for the repression of the CBFs, a defect in ADF5-mediated nuclear localization of actin may specifically affect that complex's activity, and thus CBF expression.

There is a second model that could account for the *adf5-1* mutant phenotypes given our current knowledge of the function of the actin cytoskeleton. Cytosolic actin dynamics have been shown to regulate stress-signaling pathways through a diverse

range of mechanisms. For example, the modulation of the G-actin monomer pool is required for the translocation and ultimately the activity of the transcription factor MAL in its stimulation of serum response factor (SRF) (Miralles *et al.*, 2003; Ruegg *et al.*, 2004; Miralles and Visa, 2006). Cytosolic actin dynamics control the nuclear localization of MAL, and nuclear G-actin modulates MAL's promotion of SRF expression in response to cellular stress. In another example, cytosolic actin cytoskeletal dynamics have been shown to be required for the proper nucleo-cytoplasmic localization of glucocorticoid receptor (GR), thus affecting the regulation of multiple GR-dependent pathways (Ruegg *et al.*, 2004). Perhaps most relavent to the Arabidopsis ADF5 work, recent studies have shown that Arabidopsis HEXOKINASE1 (HXK1) binds to the F-actin cytoskeleton, and actin cytoskeleton dynamics regulate the nuclear localization and function of HXK1 (Balasubramanian *et al.*, 2007). HXK1 is a glucose-signaling molecule whose localization is required for proper gene regulation of metabolic pathways, making it an interesting candidate for ADF developmental and stress phenotypes (Harrington and Bush, 2003; Cho *et al.*, 2006). Given this model, ADF5 may specifically remodel the actin cytoskeleton in response to diverse stimuli including cold stress, resulting in the translocation of specific transcription factors. These factors could act directly to repress the *CBFs* and alter the expression of other high-level master regulators of development, thereby accounting for the *adf5-1* chromatin and gene regulation phenotypes. Importantly, this highly regulated and stimulus-specific ADF5 remodeling activity may not result in gross actin cytoskeleton phenotypes visible with the F-actin GFP reporter, in agreement with our observations of only minor changes to the organization and

structure of the actin cytoskeleton in the *adf5-1* mutant. Further work is necessary to characterize the level at which ADF5 affects gene regulation, and whether ADF's functions from the cytoplasm or nucleus.

ADF5 represses freeze tolerance during normal temperature conditions

Freeze tolerance has been extensively studied in Arabidopsis and is modulated by the CBF signaling pathway, therefore making it an excellent candidate pathway to further characterize ADF5 function. Our data suggest that de-repression of *CBF1* in the *adf5-1* mutant results from changes to the structure of chromatin at the *CBF1* promoter. These changes could have resulted from alterations in the activity of chromatin remodeling complexes or repressor or activator binding to the DNA sequence. Our assays of chromatin structure at CBF1 revealed significant changes in specific regions of the *CBF1* promoter, and specifically, an increase in nucleosome density. One possible mechanism could be an ADF5-dependant repressor complex no longer binding to the CBF1 promoter, thus allowing nucleosomes to shift into the space. Assuming that ADF5 does not act directly on the CBF1 promoter, we plan to purify ADF5-containing protein complexes to identify the downstream factors that link ADF5 to the CBF1 promoter.

Of note, many of the chromatin changes seen in *adf5-1* were outside of the previously defined minimal CBF1 promoter required to confer freeze tolerance and were significantly different than chromatin changes induced by cold stress (Van Buskirk and Thomashow, 2006). It is likely that the function of this upstream region and its affect on

CBF1 expression is part of a novel mechanism of *CBF* regulation. Cold stress of wild-type plants resulted in more open *CBF1* promoter chromatin structure, significantly different from the *adf5-1* chromatin structure during normal temperature conditions. In summary, ADF5 and cold stress affect the *CBF1* promoter chromatin structure and thus *CBF1* expression through independent mechanisms. Importantly, our results summarizing the effect of cold stress on the chromatin structure of the *CBF1* locus highlight a significant development in the understanding of the chromatin remodeling control of stress-response signaling pathways.

In conclusion, Arabidopsis ADF5 is an important regulator of organ and cell proliferation and is required for a novel mechanism of repression of the *CBF* transcription factors during normal temperatures. Previous studies have proposed multiple models that could account for nuclear phenotypes in an actin binding protein mutant. First, ADF5 could be required for classical actin cytoskeleton remodeling resulting in proper cell proliferation and membrane fluidity. Second, ADF5 may be required for the nuclear localization of actin, which may subsequently be required for *CBF* repression via one of actin's nuclear functions in chromatin remodeling complexes or transcriptional machinery. Lastly, specific ADF5/actin dynamics in the cytoplasm may release an unidentified transcriptional repressor, facilitating its translocation into the nucleus and subsequent repression the *CBFs*. Future studies on ADF5's role in gene regulation would likely focus on both the downstream mechanisms of action as detailed in the above models, and also the upstream factors regulating ADF5 activity including Ca^{2+}, pH, PIP_2, and Serine/Threonine kinases (Bamburg, 1999).

MATERIALS AND METHODS

Phylogenetic Sequence Analysis

The eleven Arabidopsis ADF and the wheat ADF1 amino sequences were aligned using ClustalW. The phylogenetic tree in supplemental figure 3.S1 was built using PAUP 4.0 with the branch and bound method (Higgins and Sharp, 1988; Rogers and Swofford, 1999).

Plant materials and growth conditions

The T-DNA insertion mutant *adf5-1* (SALK_056064) in the *ADF5* gene (At2g16700) was in an *Arabidopsis thaliana* Columbia ecotype genetic background and was obtained from TAIR (www.arabidopsis.org). The mutant was backcrossed twice with wild-type Columbia and examined for a single insertion before phenotypic analysis. Seeds from wild-type and *adf5-1* plants were sown directly into soil (Fafard 2B) for all experiments. Leaf numbers were quantified on 24 day old plants (n=15). Epidermal, trichome and stomata cell numbers were assayed on fully mature leaves (n=4) with 6 areas assayed per leaf.

Determination of genotypes by PCR

Allele and gene specific primers were designed to amplify identifying fragments from the wild-type *ADF5* and *adf5-1* alleles. A 820 bp fragment for the ADF5 allele was amplified using the sense primer ADF5-5´utrS (5´-ATGGCGATGGCTTTCAAGATGGTA) and antisense primer ADF5-3´utrA (5´-AAACATTAACCGATGACCTAATTA). A 900-bp

fragment of the *adf5-1* mutant allele was amplified with a left border T-DNA primer LBaI (5´-GGTTCACGTAGTGGGCCATCG) and the sense primer ADF5-5´utrS, and a 400-bp fragment of the *adf5-1* mutant allele was amplified with a left border T-DNA primer LBaI (5´-GGTTCACGTAGTGGGCCATCG) and the antisense primer ADF5-3´utrA. The PCR products of the mutant allele were sequenced to confirm the exact insertion site. The DNA used as a template for genotype and sequence determination was prepared using the Sigma Plant DNA extraction kit.

Freeze tolerance and Electrolyte leakage experiments

Twenty day-old plants of each genotype were placed in a -15°C freezer at 2.5 hours after dawn for 12 minutes, quickly moved to 4°C for 1 hour, and moved back into the 22°C growth chamber for recovery. Freeze tolerance was assayed by counting the number of leaves that exhibited significant freeze damage (eventual chlorosis and death) compared to the total number of leaves. Each experimental replicate included 15 plants of each genotype.

To assay electrolyte leakage, the exact same experiment as outlined for freeze tolerance was performed and whole rosettes from three plants (~1.5 grams) were excised and placed in a beaker with 50 mL dH_20 immediately after freezing with three biological replicates (total of nine plants). The tissue was incubated at room temperature for 20 hours under moderate shaking. A conductivity probe (Hanna Instruments) was placed into the solution and EC measured in μS/cm (EC_{freeze}). In order to account for slight differences in tissue weight or total electrolytes, the samples were

then moved to a -80°C freezer overnight for complete cell lysis. After 18 hours, the samples were removed and thawed to room temperature and EC measured again (EC_{total}). EC_{freeze}/EC_{total} *100 = % electrolyte leakage.

Mutant Complementation and ADF5 overexpression

For complementation, the *adf5* mutant plants were transformed with Agrobacterium carrying the pCAMBIA binary vector containing ADF5 cDNA under the control of the Actin2 promoter and terminator. Positive transformants were selected using BASTA and moved to individual pots. Paralogous complementation experiments were conducted in the *adf5* mutant with ADF4, ADF7, ADF8, or ADF9 cDNAs expressed under the Actin2 promoter system. Positive transformants were selected with hygromycin on plates (1/2 MS with 1% sucrose and 0.8% agar) and moved to soil. All complementation experiments were performed on drug-selected T2 generation plants.

Real-time PCR analysis

RNA was isolated from 20-day-old plants using the RNeasy Plant Mini Kit (Qiagen, Valencia, CA, USA), and 1.5 µg of total RNA from each sample was transcribed into cDNA with the Super Script III kit (Invitrogen, Carlsbad, CA, USA) following the manufacturer's instructions except that incubations were performed for only 30 min and at 55°C using oligo (dT) primer. Aliquots of the cDNA were used as template for the qRT-PCR analysis of triplicate reactions for each of the biological replicates on an Applied Biosystems 7500 Real Time PCR Instrument. Real time PCR reactions

consisted of 2X SYBR GREEN PCR Master Mix (Applied Biosystems, Foster City, CA, USA), 0.4 µM of each primer, and 5 µl of 1:30 diluted cDNA in a 25 µl reaction volume. Primer sets used for qRT-PCR assays of transcript levels are listed in supplemental table 3.1S for the following genes: ADF5, COR15, CBF1, CBF2, CBF3, ICE, ICElike-1, ICElike-2, ICElike-3, UBQ10, ACT2. We used the 2^{-ddCt} method (Livak and Schmittgen, 2001) of relative quantification in all qRT-PCR calculations.

Chromatin structure assays at *CBF1*

ChIP assays on the *CBF1* locus were performed on sheared chromatin from 14-day-old shoots grown at 22ºC using primers starting at -736, -538, -415, and -135 upstream from the transcriptional start site as described previously. ChIP assays for histone H3 trimethylation at lysine 4, H3 acetylation at lysine 9 and 14, and histone H2B were performed identically except that the H3K4Me3 (#07-473), H3K9K14Ac (#06-599), and H2B antibodies (Upstate (Lake Placid, NY)) were used in the respective precipitation assays. The H3K4Me3 ChIP assay was normalized to a region in the *ACT2* 3´UTR, the H3K9K14Ac assay was normalized to a LINE2 element, and the H2B assay was normalized to a region in the *ACT2* 3´UTR.

Nucleosome occupancy was assayed in the promoter region of *CBF1* by a modification of the method described for yeast genes by Sekinger et al. (2005) starting with 1 g of 14-day-old whole seedlings kept at 22C or moved for 2 hours to 4C (Sekinger *et al.*, 2005). Nucleosomes were prepared by a modification of Vega-Palas and Ferl, 1995 (Vega-Palas and Ferl, 1995). The qPCR assays on nucleosomal DNA were

performed using the primer pairs listed in Supplemental Table 3.S1. Relative quantity (RQ) data were normalized to input DNA concentration by subtracting the raw Cycle Threshold (CT) value for *actin 2* (*ACT2*) from the Target CT value. qPCR was performed as above for qRT-PCR. The nucleosome preparation, qPCR assays, and calculations are detailed in Appendix 1.

ADF5 repression in the *cbf2* mutant

A *cbf2* mutant allele was obtained from Mark Thomashow (Salk_009689). Shoot tissue was harvested from *cbf2* and wild-type seedlings grown at 22°C and from seedlings moved to 4°C for 8 hours. *ADF5* expression levels were obtained using qRT-PCR as outlined above.

ACKNOWLEDGEMENTS

We would like to acknowledge Roger Deal, Yolanda Lay, Lori King-Reid, and Aaron Smith for their contributions in the design and execution of the research, and Mark Thomashow and Colleen Doherty at Michigan State University for the *cbf2* allele.

REFERENCES

Balasubramanian, R., Karve, A., Kandasamy, M., Meagher, R.B. and Moore, B. (2007) A role for F-actin in hexokinase-mediated glucose signaling. *Plant Physiol*, **145**, 1423-1434.

Bamburg, J.R. (1999) Proteins of the ADF/cofilin family: essential regulators of actin dynamics. *Annu Rev Cell Dev Biol*, **15**, 185-230.

Barrero, R.A., Umeda, M., Yamamura, S. and Uchimiya, H. (2002) Arabidopsis CAP regulates the actin cytoskeleton necessary for plant cell elongation and division. *Plant Cell*, **14**, 149-163.

Bettinger, B.T., Gilbert, D.M. and Amberg, D.C. (2004) Actin up in the nucleus. *Nat Rev Mol Cell Biol*, **5**, 410-415.

Chan, A.Y., Bailly, M., Zebda, N., Segall, J.E. and Condeelis, J.S. (2000) Role of cofilin in epidermal growth factor-stimulated actin polymerization and lamellipod protrusion. *J Cell Biol*, **148**, 531-542.

Chen, C.N., Chu, C.C., Zentella, R., Pan, S.M. and Ho, T.H.D. (2002) AtHVA22 gene family in Arabidopsis: phylogenetic relationship, ABA and stress regulation, and tissue-specific expression. *Plant Molecular Biology*, **49**, 633-644.

Chinnusamy, V., Ohta, M., Kanrar, S., Lee, B.H., Hong, X., Agarwal, M. and Zhu, J.K. (2003) ICE1: a regulator of cold-induced transcriptome and freezing tolerance in Arabidopsis. *Genes Dev*, **17**, 1043-1054.

Chinnusamy, V., Zhu, J. and Zhu, J.K. (2006) Gene regulation during cold acclimation in plants. *Physiologia Plantarum*, **126**, 52-61.

Cho, Y.H., Yoo, S.D. and Sheen, J. (2006) Regulatory functions of nuclear hexokinase1 complex in glucose signaling. *Cell*, **127**, 579-589.

Cole, M., Nolte, C. and Werr, W. (2006) Nuclear import of the transcription factor SHOOT MERISTEMLESS depends on heterodimerization with BLH proteins expressed in discrete sub-domains of the shoot apical meristem of Arabidopsis thaliana. *Nucleic Acids Res*, **34**, 1281-1292.

Cvrckova, F., Novotny, M., Pickova, D. and Zarsky, V. (2004) Formin homology 2 domains occur in multiple contexts in angiosperms. *BMC Genomics*, **5**, 44.

Danyluk, J., Carpentier, E. and Sarhan, F. (1996) Identification and characterization of a low temperature regulated gene encoding an actin-binding protein from wheat. *FEBS Lett*, **389**, 324-327.

Dhonukshe, P., Kleine-Vehn, J. and Friml, J. (2005) Cell polarity, auxin transport, and cytoskeleton-mediated division planes: who comes first? *Protoplasma*, **226**, 67-73.

Dong, C.H., Kost, B., Xia, G. and Chua, N.H. (2001) Molecular identification and characterization of the Arabidopsis AtADF1, AtADFS and AtADF6 genes. *Plant Mol Biol*, **45**, 517-527.

Fowler, S. and Thomashow, M.F. (2002) Arabidopsis transcriptome profiling indicates that multiple regulatory pathways are activated during cold acclimation in addition to the CBF cold response pathway. *Plant Cell*, **14**, 1675-1690.

Gendrel, A.V., Lippman, Z., Martienssen, R. and Colot, V. (2005) Profiling histone modification patterns in plants using genomic tiling microarrays. *Nat Methods*, **2**, 213-218.

Ghosh, M., Song, X., Mouneimne, G., Sidani, M., Lawrence, D.S. and Condeelis, J.S. (2004) Cofilin promotes actin polymerization and defines the direction of cell motility. *Science*, **304**, 743-746.

Gilmour, S.J., Hajela, R.K. and Tomashow, M.F. (1988) Cold acclimation in *Arabidopsis thaliana*. *Plant Physiol.*, **87**, 745-750.

Gilmour, S.J., Zarka, D.G., Stockinger, E.J., Salazar, M.P., Houghton, J.M. and Thomashow, M.F. (1998) Low temperature regulation of the Arabidopsis CBF family of AP2 transcriptional activators as an early step in cold-induced COR gene expression. *Plant J*, **16**, 433-442.

Harrington, G.N. and Bush, D.R. (2003) The bifunctional role of hexokinase in metabolism and glucose signaling. *Plant Cell*, **15**, 2493-2496.

He, Y., Michaels, S.D. and Amasino, R.M. (2003) Regulation of flowering time by histone acetylation in *Arabidopsis*. *Science*, **302**, 1751-1754.

Higgins, D.G. and Sharp, P.M. (1988) CLUSTAL: a package for performing multiple sequence alignment on a microcomputer. *Gene*, **73**, 237-244.

Jaglo-Ottosen, K.R., Gilmour, S.J., Zarka, D.G., Schabenberger, O. and Thomashow, M.F. (1998) Arabidopsis CBF1 overexpression induces COR genes and enhances freezing tolerance. *Science*, **280**, 104-106.

Jefferson, R.A., Kavanagh, T.A. and Bevan, M.W. (1987) GUS fusions: beta-glucuronidase as a sensitive and versatile gene fusion marker in higher plants. *Embo J*, **6**, 3901-3907.

Kreps, J.A., Wu, Y., Chang, H.S., Zhu, T., Wang, X. and Harper, J.F. (2002) Transcriptome changes for Arabidopsis in response to salt, osmotic, and cold stress. *Plant Physiol*, **130**, 2129-2141.

Maciver, S.K. and Hussey, P.J. (2002) The ADF/cofilin family: actin-remodeling proteins. *Genome Biol*, **3**, reviews3007.

Meagher, R.B. and Williamson, R.E. (1994) The Plant Cytoskeleton. In *Arabidopsis*, Vol. 38 (Meyerowitz, E. and Somerville, C., eds). Cold Spring Harbor: Cold Spring Harbor Laboratory Press, pp. 1049-1084.

Meagher, R.B. and Fechheimer, M. (2003) The Cytoskeletal Proteome of *Arabidopsis*. In *Arabidopsis*, Vol. www.aspb.org/publications/arabidopsis/toc.cfm (Meyerowitz, E. and Somerville, C., eds). Cold Spring Harbor, NY: Cold Spring Harbor Laboratory Press.

Miralles, F., Posern, G., Zaromytidou, A.I. and Treisman, R. (2003) Actin dynamics control SRF activity by regulation of its coactivator MAL. *Cell*, **113**, 329-342.

Miralles, F. and Visa, N. (2006) Actin in transcription and transcription regulation. *Curr Opin Cell Biol*, **18**, 261-266.

Nakashima, K., Fujita, Y., Katsura, K., Maruyama, K., Narusaka, Y., Seki, M., Shinozaki, K. and Yamaguchi-Shinozaki, K. (2006) Transcriptional regulation of ABI3- and ABA-responsive genes including RD29B and RD29A in seeds, germinating embryos, and seedlings of Arabidopsis. *Plant Molecular Biology*, **60**, 51-68.

Nebl, G., Meuer, S.C. and Samstag, Y. (1996) Dephosphorylation of serine 3 regulates nuclear translocation of cofilin. *J Biol Chem*, **271**, 26276-26280.

Novillo, F., Alonso, J.M., Ecker, J.R. and Salinas, J. (2004) CBF2/DREB1C is a negative regulator of CBF1/DREB1B and CBF3/DREB1A expression and plays a central role in stress tolerance in Arabidopsis. *Proc Natl Acad Sci U S A*, **101**, 3985-3990.

Orvar, S., Omann, Dhindsa (2000) Early steps in cold sensing by plant cells: the role of actin cytoskeleton and membrane fluidity. *PLANT JOURNAL*, **23**, 785-794.

Ouellet, F., Carpentier, E., Cope, M.J., Monroy, A.F. and Sarhan, F. (2001) Regulation of a wheat actin-depolymerizing factor during cold acclimation. *Plant Physiol*, **125**, 360-368.

Pendleton, A., Pope, B., Weeds, A. and Koffer, A. (2003) Latrunculin B or ATP depletion induces cofilin-dependent translocation of actin into nuclei of mast cells. *J Biol Chem*, **278**, 14394-14400.

Pollard, T.D., Blanchoin, L. and Mullins, R.D. (2000) Molecular mechanisms controlling actin filament dynamics in nonmuscle cells. *Annu Rev Biophys Biomol Struct*, **29**, 545-576.

Rando, O.J., Zhao, K., Janmey, P. and Crabtree, G.R. (2002) Phosphatidylinositol-dependent actin filament binding by the SWI/SNF-like BAF chromatin remodeling complex. *Proc Natl Acad Sci U S A*, **99**, 2824-2829.

Rogers, J.S. and Swofford, D.L. (1999) Multiple local maxima for likelihoods of phylogenetic trees: a simulation study. *Mol Biol Evol*, **16**, 1079-1085.

Ruegg, J., Holsboer, F., Turck, C. and Rein, T. (2004) Cofilin 1 is revealed as an inhibitor of glucocorticoid receptor by analysis of hormone-resistant cells. *Mol Cell Biol*, **24**, 9371-9382.

Ruzicka, D.R., Kandasamy, M.K., McKinney, E.C., Burgos-Rivera, B. and Meagher, R.B. (2007) The ancient subclasses of Arabidopsis Actin Depolymerizing Factor genes exhibit novel and differential expression. *Plant J*, **52**, 460-472.

Sekinger, E.A., Moqtaderi, Z. and Struhl, K. (2005) Intrinsic histone-DNA interactions and low nucleosome density are important for preferential accessibility of promoter regions in yeast. *Mol Cell*, **18**, 735-748.

Staiger, C.J. (2000) Signaling to the actin cytoskeleton in plants. *Annu. Rev. Plant Physiol. Plant Mol. Biol.*, **51**.

Steponkus, P.L., Uemura, M., Joseph, R.A., Gilmour, S.J. and Thomashow, M.F. (1998) Mode of action of the COR15a gene on the freezing tolerance of Arabidopsis thaliana. *Proc Natl Acad Sci U S A*, **95**, 14570-14575.

Sukumara.Np and Weiser, C.J. (1972) Freezing Injury in Potato Leaves. *Plant Physiology*, **50**, 564-&.

Takada, S., Hibara, K., Ishida, T. and Tasaka, M. (2001) The CUP-SHAPED COTYLEDON1 gene of Arabidopsis regulates shoot apical meristem formation. *Development*, **128**, 1127-1135.

Theriot, J.A. (1997) Accelerating on a treadmill: ADF/cofilin promotes rapid actin filament turnover in the dynamic cytoskeleton [comment]. *J Cell Biol*, **136**, 1165-1168.

Thomashow, M.F. (1998) Role of cold-responsive genes in plant freezing tolerance. *Plant Physiol*, **118**, 1-8.

Thomashow, M.F. (1999) PLANT COLD ACCLIMATION: Freezing Tolerance Genes and Regulatory Mechanisms. *Annu Rev Plant Physiol Plant Mol Biol*, **50**, 571-599.

Van Buskirk, H.A. and Thomashow, M.F. (2006) Arabidopsis transcription factors regulating cold acclimation. *Physiologia Plantarum*, **126**, 72-80.

Vega-Palas, M.A. and Ferl, R.J. (1995) The Arabidopsis Adh gene exhibits diverse nucleosome arrangements within a small DNase I-sensitive domain. *Plant Cell*, **7**, 1923-1932.

Visa, N. (2005) Actin in transcription. Actin is required for transcription by all three RNA polymerases in the eukaryotic cell nucleus. *EMBO Rep*, **6**, 218-219.

von Arnim, A.G. and Deng, X.W. (1994) Light inactivation of Arabidopsis photomorphogenic repressor COP1 involves a cell-specific regulation of its nucleocytoplasmic partitioning. *Cell*, **79**, 1035-1045.

Wang, L., Liu, Y.M. and Li, Y. (2005) Comparison of F-actin fluorescent labeling methods in pollen tubes of *Lilium davidii*. *Plant Cell Rep*, **24**, 266-270.

Wasteneys, G.O. and Galway, M.E. (2003) Remodeling the cytoskeleton for growth and form: an overview with some new views. *Annu Rev Plant Biol*, **54**, 691-722.

Yamaguchi-Shinozaki, K. and Shinozaki, K. (1994) A novel cis-acting element in an Arabidopsis gene is involved in responsiveness to drought, low-temperature, or high-salt stress. *Plant Cell*, **6**, 251-264.

Zarka, D.G., Vogel, J.T., Cook, D. and Thomashow, M.F. (2003) Cold induction of Arabidopsis CBF genes involves multiple ICE (Inducer of CBF expression) promoter elements and a cold-regulatory circuit that is desensitized by low temperature. *Plant Physiology*, **133**, 910-918.

Table 3.1: Quantification of the *adf5-1* developmental and freeze tolerance phenotypes.

	Leaf number at 24 days	Trichome number per 1cm^2	Stomata number per 0.22 mm^2	Epidermal cell size (μM^2)	Percent leaf freeze	Percent electrolyte leakage
Wild-type	12.9 +/- 1.1	30.3 +/- 0.9	17.8 +/- 0.7	4975 +/- 299	46.8 +/- 5.61	25.2 +/- 1.8
adf5-1	19.9 +/- 1.5	67.0 +/- 5.0	26.5 +/- 1.3	5412 +/- 1060	18.5 +/- 1.32	11.7 +/- 0.9
adf5-1 /A2pt:ADF5	14.7 +/- 1.1	40.3 +/- 3.0	18.5 +/- 0.4	ND	40.4 +/- 0.43	ND

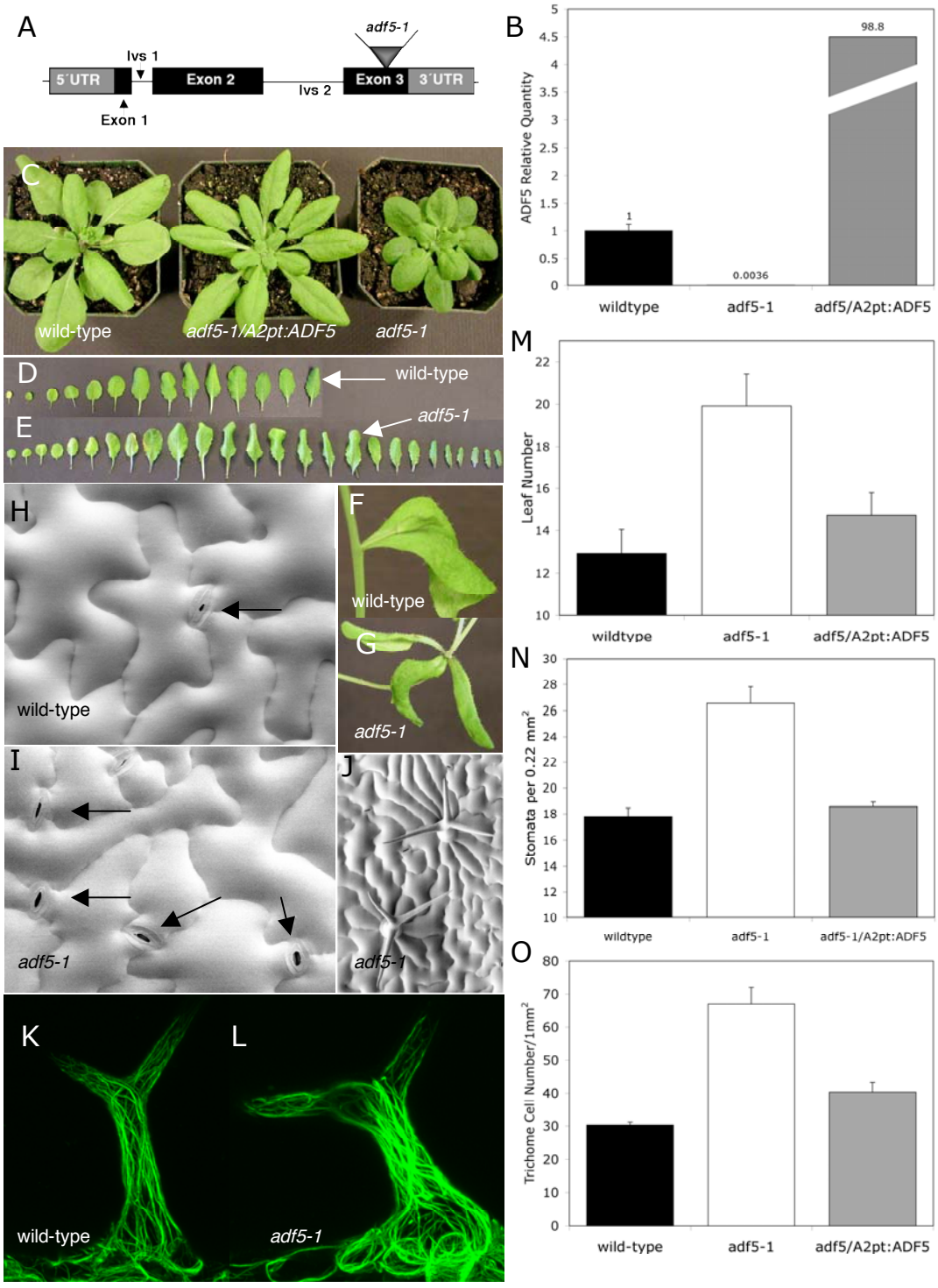

Figure 3.1: The *adf5-1* mutant allele exhibits multiple developmental phenotypes.

The *adf5-1* mutant allele contains an insertion in the 3rd exon (A). *ADF5* expression levels in wild-type, *adf5-1* mutant, and *A2pt:ADF5* over-expression lines were quantified

by qRT-PCR (B). Leaf number and rosette morphology are significantly altered in the *adf5-1* mutant (C-G). The *adf5-1* mutant also exhibits an increase in cauline leaf number (F, G). SEM images of the leaf surface show an increase in the number of stomata and trichomes, but not a change in the number or size of epidermal pavement cells (H-J). The GFP/fABD2 F-actin reporter decorates actin filaments and bundles. Confocal microscopy images of mutant and wild-type trichome cells show the adf5-1 cytoskeleton exhibits thicker bundles and fewer fine filaments indicating a more stabilized, less dynamically remodeled actin cytoskeleton phenotype (K, L). Leaf and cell phenotypes are quantified in M-O and table 3.1.

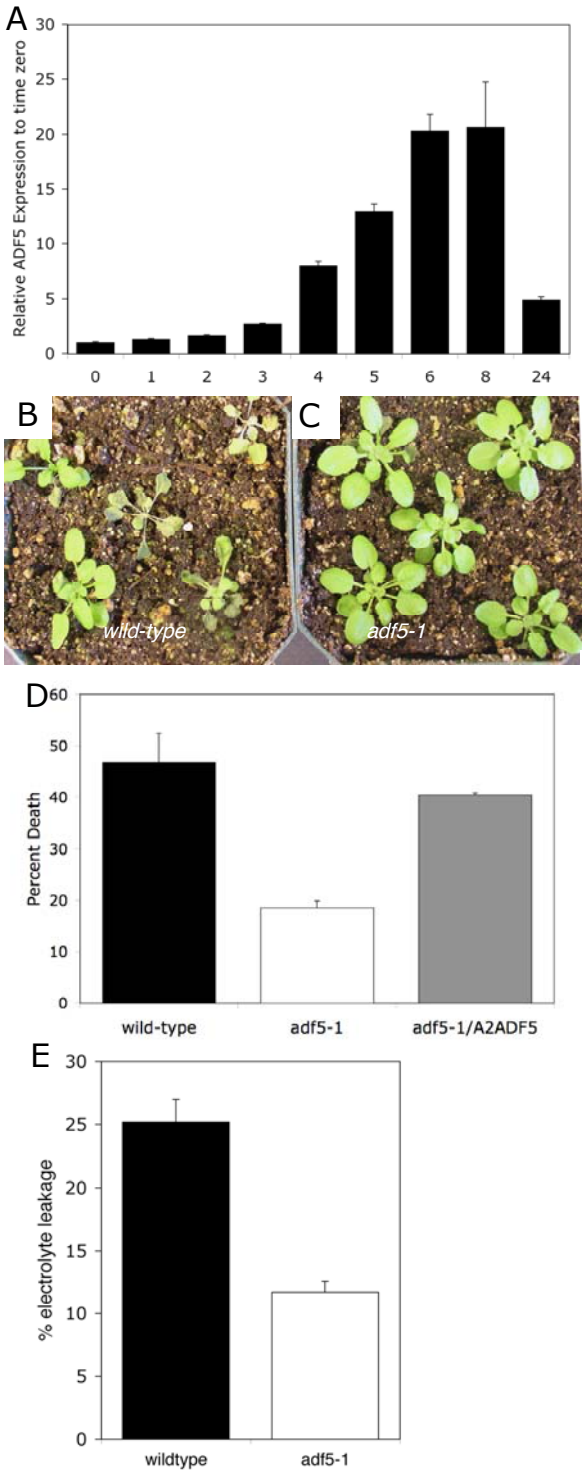

Figure 3.2 ***ADF5*** **is induced by cold temperatures, but the** ***adf5-1*** **mutant is freeze tolerant compared to wild-type.** Wild-type plants were placed in 4° C and tissue collected at hourly intervals. RNA was extracted and analyzed for

ADF5 expression levels at each time point using qRT-PCR (A). Wild-type (B) and *adf5-1* mutant (C) plants were moved directly from 22° C growth chambers to -15° freezer for 12 minutes, allowed to thaw at 4°, and assayed for freeze tolerance. The *adf5-1* mutant exhibited lower levels of leaf death (D) and electrolyte leakage (E) under these freeze conditions.

Figure 3.3 The CBF cold-stress signaling pathway is de-repressed in the *adf5-1* mutant

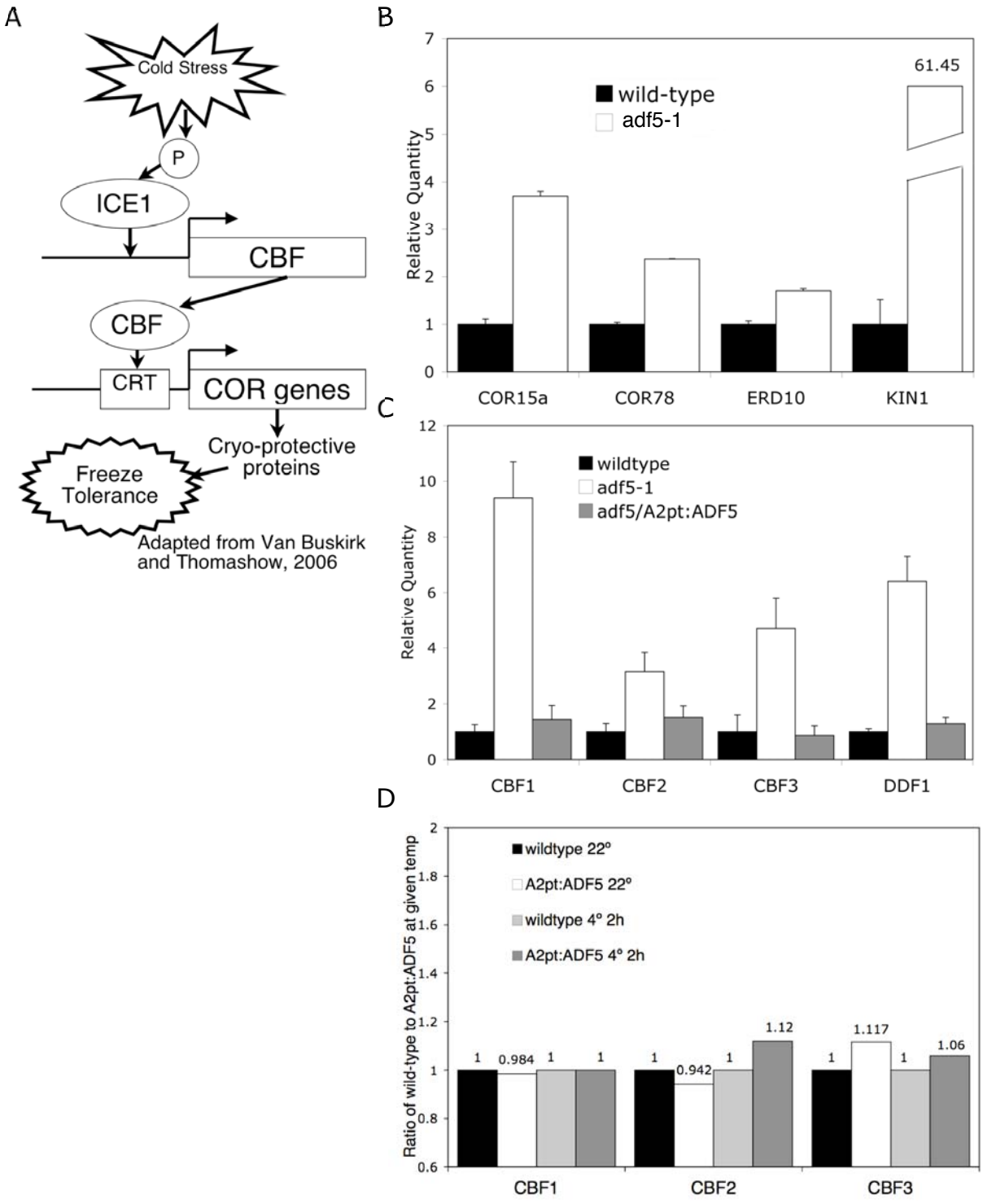

Figure 3.3 The CBF cold-stress signaling pathway is de-repressed in the *adf5-1* mutant. The cold-stress signaling pathway translates cold temperature stress into an up-regulation of a host of *COR* genes, ultimately resulting in freeze tolerance (A). Cold-response genes including *COR15* and *78* are significantly induced in the *adf5-1* mutant as assayed by qRT-PCR (B), possibly accounting for *adf5-1's* increase in freeze tolerance. The *CBF* transcription factor family members are de-repressed in the *adf5-1* mutant under normal temperature conditions (C), likely accounting for the induction of *COR* genes. While ADF5 is necessary for the proper regulation of the *CBF* TFs, it is not sufficient. The over-expression of *ADF5* does not affect *CBF* expression levels with or without cold stress (D).

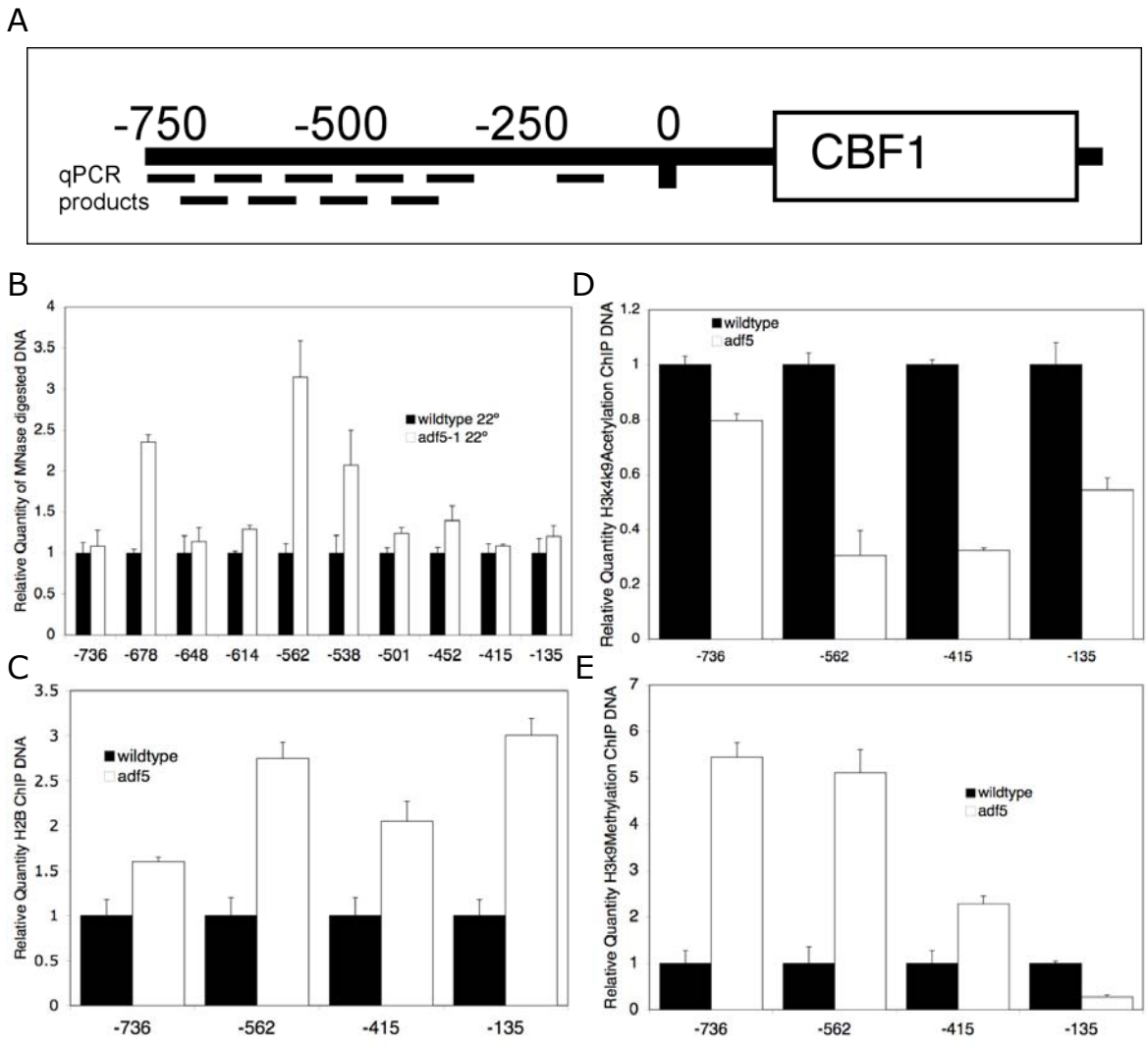

Figure 3.4 ADF5 is required for proper chromatin structure at the *CBF1* promoter. (A) Map of the *CBF1* locus with numbers indicating position from the transcriptional start site and dashes the locations of qPCR amplification products. Wild-type and *adf5-1* chromatin DNA was digested with micrococcal nuclease, purified, and amplified using qPCR (B). The graph displays relative quantity of DNA, indicating the fold-change in nuclease digest protection. Chromatin immunoprecipitation assays utilizing antibodies against H2B (C), H3Ac (D), and H3triMe (E) histone components indicate significant changes to the *CBF1* locus' chromatin structure in the *adf5-1* mutant.

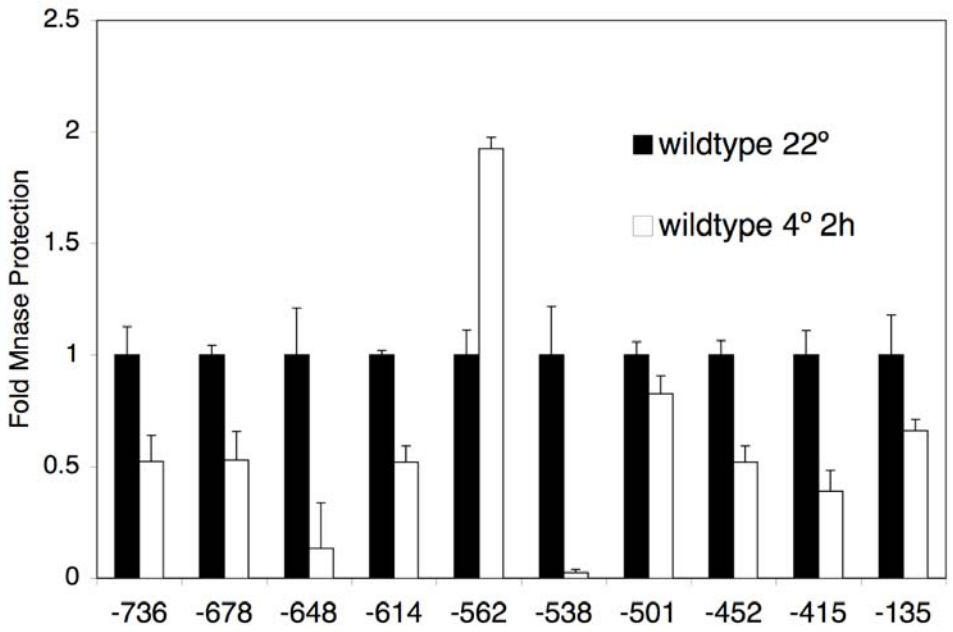

Figure 3.5 Cold-stress induced changes to the *CBF1* promoter's chromatin structure do not overlap with changes caused by the loss of ADF5. Wild-type plants were cold-stressed for 2 hours at 4°C to determine whether the *adf5-1* chromatin phenotype overlaps with that of cold stress. Cold-stress induced significantly different changes to the *CBF1* promoter chromatin structure compared to the effects of the *adf5-1* mutant (See Figure 3.4B). Overall, cold stress opened the chromatin structure of the CBF1 promoter, causing significantly less MNase protection compared to wild-type or *adf5-1* at 22° C.

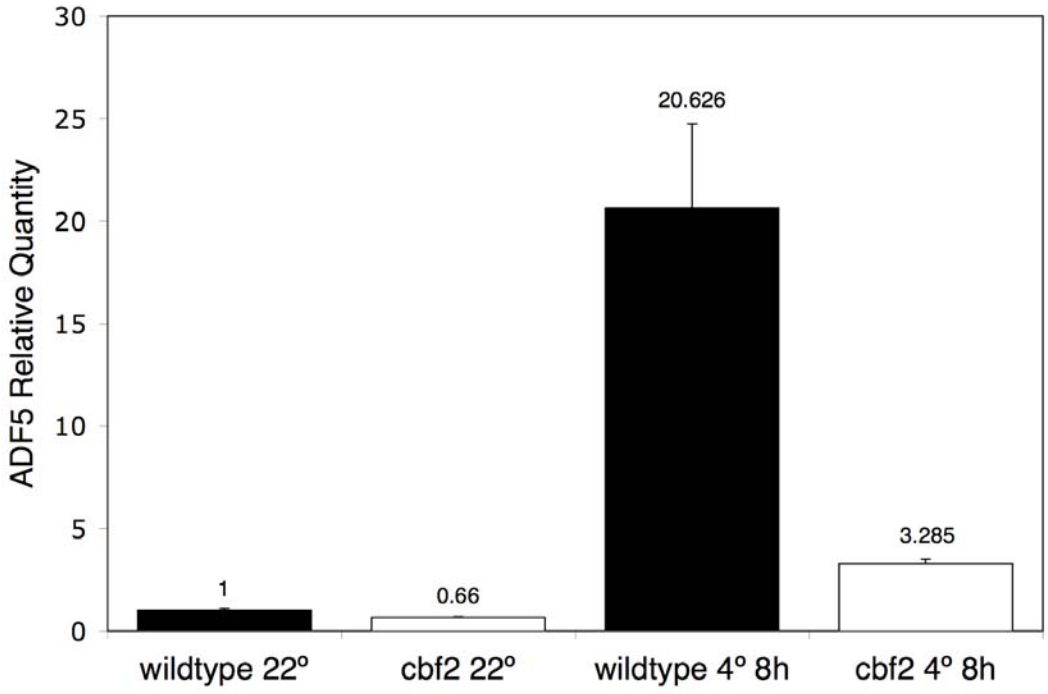

Figure 3.6 *ADF5* is regulated by CBF2, placing it in a cold-stress feedback loop. Graph of *ADF5* expression in *cbf2* under normal and 8h cold temperatures, showing *ADF5* is less induced during cold-stress conditions in the *cbf2* mutant. Summarizing this result with that of Figure 3.3, ADF5 is induced by CBF2 during cold stress, and is required for CBF repression under normal temperature conditions placing it both upstream and downstream of the CBFs.

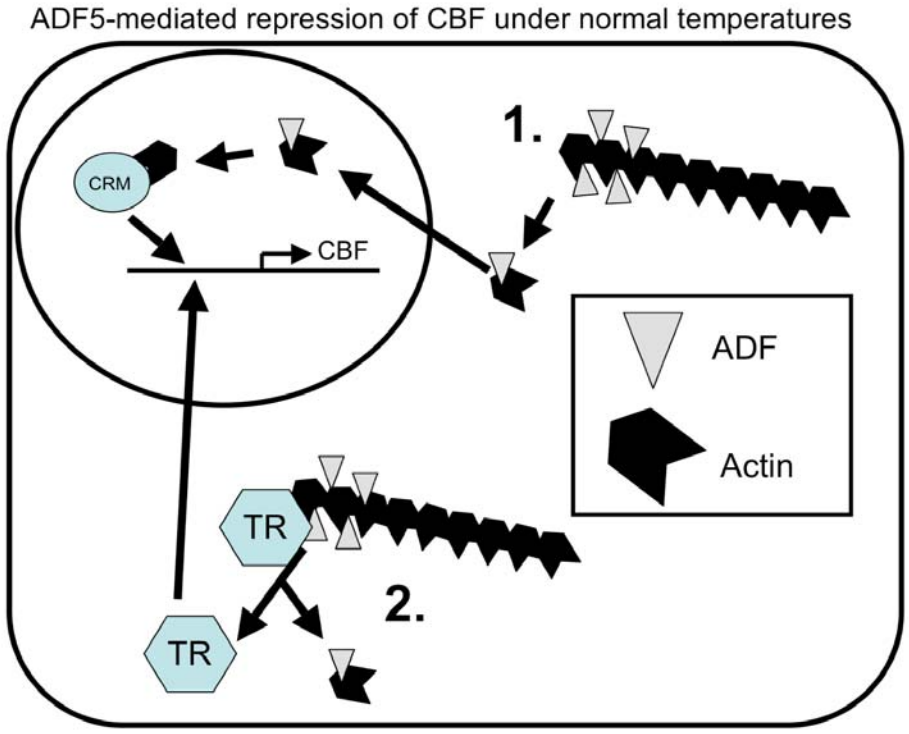

Figure 3.7 A model for the gene regulation activity of ADF5. ADF5 may be required to transport actin into the nucleus and effect actin's participation in nuclear activities including chromatin remodeling (CRM) (model 1). Alternatively, ADF5 may modulate the activity of a transcriptional repressor (TR) via cytoskeletal dynamics (model 2). With either model, ADF5's specific, and likely highly regulated, role in actin cytoskeleton remodeling may not cause gross changes to F-actin organization observable with the GFP reporter.

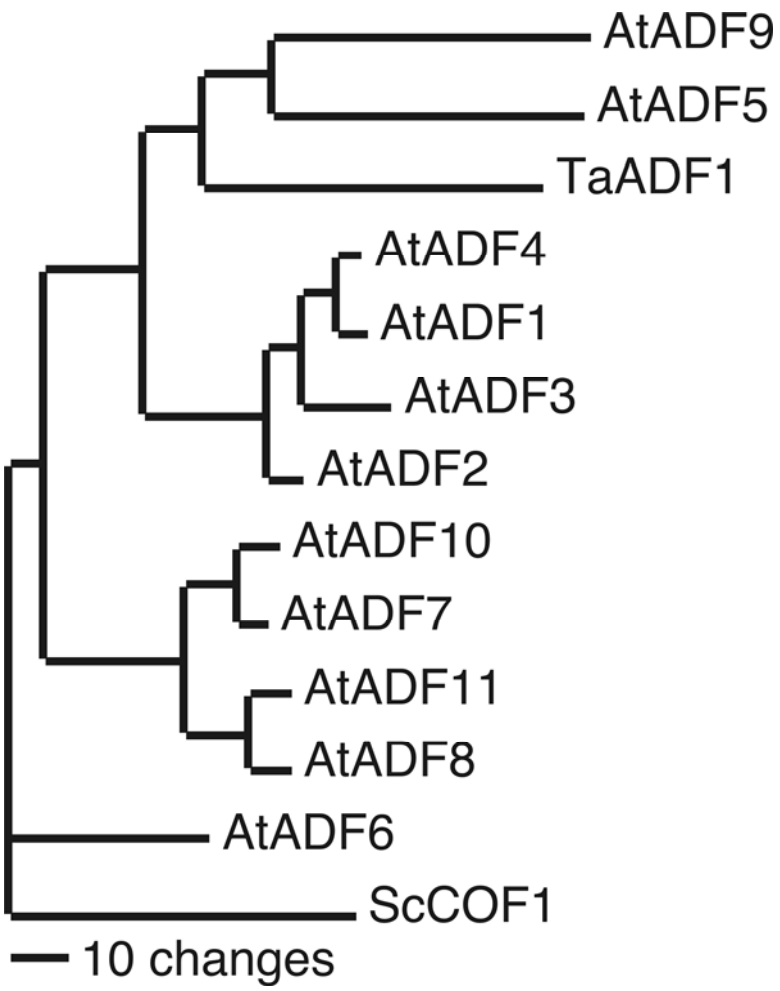

Supplemental Figure 3.S1 The *Triticum aestivum* TaADF1 is most similar to subclass III ADF5 and ADF9 A CLUSTALW alignment of the 11 Arabidopsis ADF and the wheat TaADF1 amino acid sequences was constructed to build a phylogenetic tree using the branch and bound-method in PAUP4.0 (Higgins and Sharp, 1998; Rogers and Swofford, 1999). *Saccharomyces cerevisiae* Cofilin1 was used as the outgroup sequence.

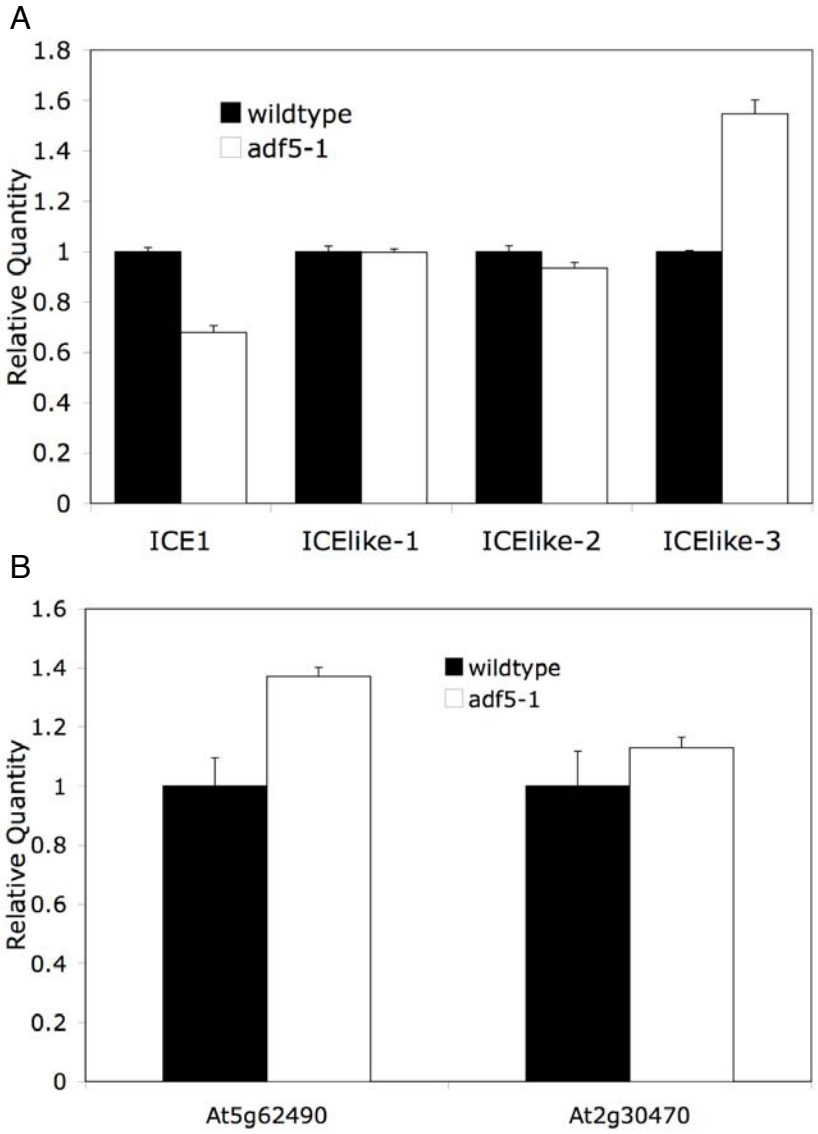

Supplemental Figure 3.S2 *ICE1*, *ICE-like*, ABA-responsive, and Calcium-responsive genes are not significantly mis-regulated in the *adf5-1* mutant. The ICE1 transcription factor regulates the expression of the *CBF* TFs. To test whether *ICE1* expression is modulated in the *adf5-1* mutant, qRT-PCR was used to analyze *ICE1* and *ICE-like* mRNA levels in wild-type and mutant samples (A). ABA and Calcium signaling also effect freeze tolerance and *CBF* expression. We determined that

At5g62490 and Atg30470, known ABA- and Ca- responsive genes, were not significantly mis-regulated in the *adf5-1* mutant (B).

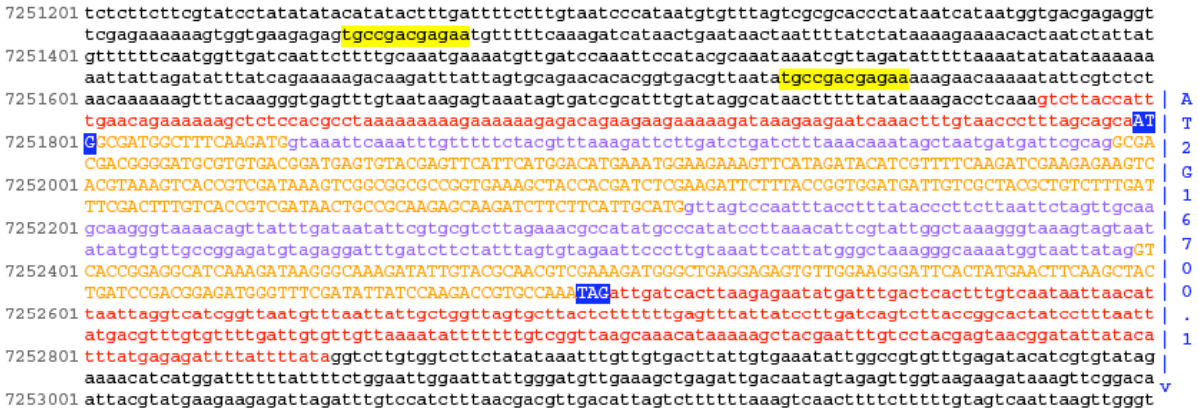

Supplemental Figure 3.S3 The *ADF5* promoter contains two CRT CCGAC motifs

The ADF5 promoter contains a TGCCGACGAGAA sequence motif twice in the 500 base pairs upstream of the transcriptional start site. Within this large motif is the CCGAC sequence where CBF transcription factors could bind and subsequently induce the *ADF5* during cold stress.

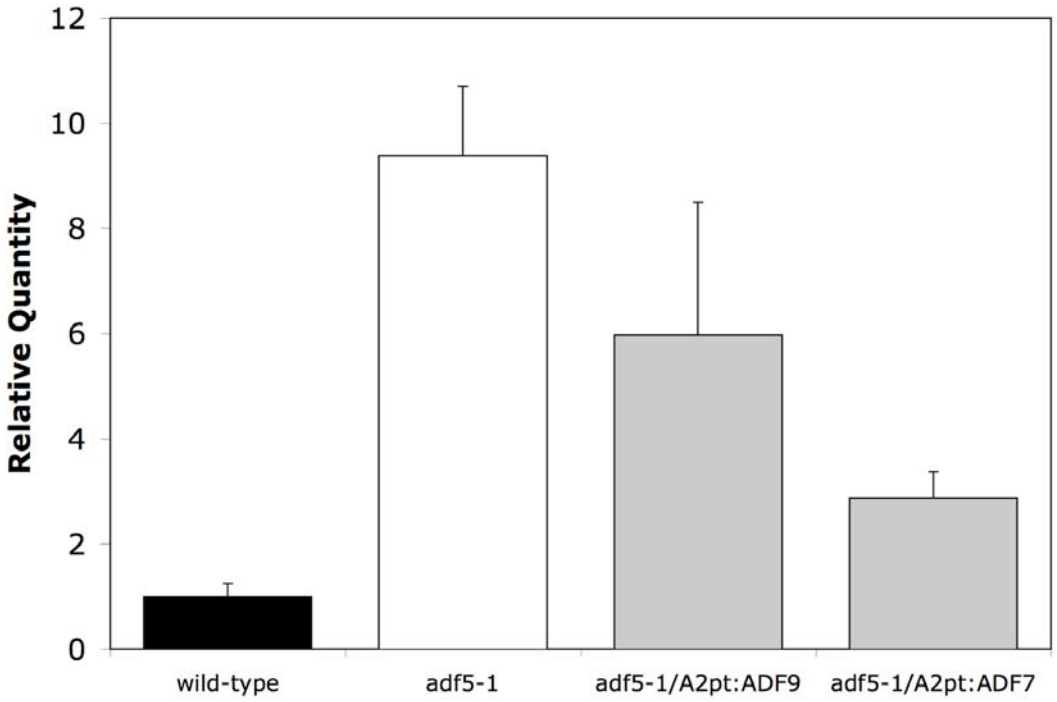

Supplemental Figure 3.S4 Over-expression of *ADF7* or *ADF9* cannot fully complement the de-repression of *CBF1* caused by the loss of ADF5. *CBF1* expression levels were examined in *adf5-1* plants over-expressing subclass II *ADF7* or subclass III *ADF9* from the *ACT2* promoter/terminator transgene using qRT-PCR. While the level of *CBF1* expression was decreased slightly, it was not restored to wild-type levels in either case. Because over-expression of *ADF5* under the same promoter was able to restore wild-type *CBF1* expression levels (see Figure 3.3B), we conclude that these other ADFs cannot fully complement the *adf5-1* defect because of functional differences between the various ADF isovariants.

CHAPTER 4

ARABIDOPSIS ACTIN DEPOLYMERIZING FACTOR11 IS REQUIRED FOR ROOT HAIR DEVELOPMENT[1]

[1] Daniel Ruzicka, M.K. Kandasamy, E.C. McKinney, and R.B. Meagher

To be submitted to New Phytologist

ABSTRACT

The Arabidopsis Actin Depolymerizing Factor (ADF) gene family contains eleven expressed members that group into four ancient subclasses. Subclass 2 *ADFs'* expression patterns split into two subgroups, root hair specific and mature pollen specific, cell types that require polar tip elongation. RNA interference (RNAi) was used to specifically silence *ADF11* (*ADF11Ri*) in order to study the function of one root hair specific ADF. *ADF11Ri* epiallele plants exhibited shortened root hairs and frequent root hair branching. Defects in the organization and architecture of the F-actin cytoskeleton in *ADF11Ri* root hair cells include an accumulation of transversely oriented filaments at the base of the root hair. The *ADF11Ri* phenotypes were complemented by the over-expression of subclass II *ADF* (*ADF8*, *ADF10*, *ADF11)* cDNAs, but not subclass I *ADF4* or subclass III *ADF9* cDNAs, indicating functional differences exist among the more distant Arabidopsis ADF isovariants. We propose a model where the *ADF11Ri* root hair phenotypes are the result of a change in the stoichimetric balance between actin and subclass II ADF isovariants in root hairs.

INTRODUCTION

The actin cytoskeleton is required for a wide range of cellular processes including cytoplasmic streaming, organelle movement and positioning, vesicle transport, establishment of cell polarity, and polar tip growth (Meagher and Williamson, 1994; Staiger, 2000; Wasteneys and Galway, 2003). Specifically, in elongating root hair cells the actin cytoskeleton facilitates the cytoplasmic streaming necessary for vesicle transport to deliver cell wall precursors to the growing tip of the cell (Emons, 1987; Valster *et al.*, 1997). Actin filaments are dynamically organized and remodeled by a suite of actin binding proteins (ABPs) whose activity depends on multiple cellular signals including pH, Calcium gradients, and post-translational modifications (Borisy and Svitkina, 2000; Pollard *et al.*, 2000; Paavilainen *et al.*, 2004). One such ABP, actin depolymerizing factor (ADF), binds actin filaments, alters the filament's helical twist, and promotes depolymerization and severing of actin monomers and small polymers, respectively (Bamburg, 1999). These filament degradation products can re-supply the G-actin pool or initiate new filament products (Ghosh *et al.*, 2004). Broadly, ADF functions to enhance the dynamic turnover ability of actin cytoskeleton remodeling. This turnover process, termed actin treadmilling, creates a cytoplasmic flow of cellular products to the growing tip of the cell.

In the Arabidopsis root, surface epidermal cells are arranged in an alternating root hair (trichoblast) and non-root hair (atrichoblast) pattern. Trichoblast development requires multiple cellular cues for both cell identity and hair development. After cell specification of the trichoblast, root hair development is marked by four distinct

developmental stages including hair initiation, bulge formation, tip growth, and growth duration (elongation and maintenance) (Schiefelbein and Somerville, 1990; Dolan *et al.*, 1993; Dolan and Roberts, 1995; Schiefelbein, 2000). This developmental process requires the coordination of multiple pathways and factors, as indicated by the large number of mutants isolated that exhibit root hair development phenotypes (Swarbreck *et al.*, 2008).

The actin cytoskeleton is central to root hair development at each of these distinct stages. Mutants in multiple actin cytoskeleton genes including actin and the ABPs profilin, ADF, and AIP1 have resulted in a wide range of root hair phenotypes including cell specification, hair initiation, bulge formation, tip growth, and growth duration stage defects (Ramachandran *et al.*, 2000; Dong *et al.*, 2001; Ketelaar *et al.*, 2007). Importantly, mutants in the three vegetative actins show distinct root hair phenotypes including defects in root hair cell specification (*act7*), defects in root hair initiation (*act2* and *act8*), and short, stunted root hairs (*act2* and *act8*) (Kandasamy *et al.*, 2001; Gilliland *et al.*, 2002; Ringli *et al.*, 2002; Gilliland *et al.*, 2003; Diet *et al.*, 2004). Additionally, various actin cytoskeleton altering drugs effect root hair development and cause short root hair phenotypes similar to genetic defects in the actin cytoskeleton (Miller *et al.*, 1999; Baluska *et al.*, 2000).

The *Arabidopsis ADF* gene family is encoded by eleven genes exhibiting diverse vegetative, stress-responsive, pollen-specific, and root hair-specific expression patterns (Ruzicka *et al.*, 2007). The Arabidopsis subclass II ADFs are split into pollen specific and root hair specific subgroups, but each of the *Oryza sativa* subclass II ADF genes

has maintained these two expression patterns. Despite this subfunctionalization of expression patterns within the Arabidopsis lineage, we have argued that the Arabidopsis subclass II ADFs may have maintained their complement of isovariant functions because root hairs and pollen tubes require similarly regulated polar tip growth (Ruzicka *et al.*, 2007).

Arabidopsis *ADF11* is specifically expressed in root hair cells, and most strongly in the root hair cells nearest the elongation zone of the growing root tip as shown in Figure 4.1A. To test the hypothesis that subclass II ADFs are required for proper tip cell development, this study reports on the morphological and actin cytoskeletal phenotypes of multiple *ADF11* RNAi knockdown epiallele (*ADF11Ri*) lines. We present complementation experiments where various Arabidopsis *ADF* cDNAs were expressed in root tissue rescuing the *ADF11Ri* phenotypes. Lastly, we propose a model and future experiments to test whether the ratio of ADF11 to actin isovariants is responsible for the *ADF11Ri* root hair phenotypes and the various *actin* root hair phenotypes as well.

RESULTS AND DISCUSSION

ADF11 RNAi silencing results in shorter root hairs that exhibit occasional branching

Because T-DNA insertion alleles in the *ADF11* gene were unavailable among the various public Arabidopsis mutant collections, we constructed an RNA interference construct to knockdown *ADF11* mRNA expression (Materials and Methods). Transgenes encoding double stranded RNA stem-loops have been shown to specifically

silence endogenous gene expression (Hannon, 2002; McGinnis *et al.*, 2005). To avoid silencing the other *ADF* mRNAs, the stem of the RNAi was constructed from the distinct *ADF11* 3'UTR sequence as shown in Figure 4.1B. Multiple independently transformed epiallele plant lines (*ADF11Ri* 1-20) were isolated and propagated for further characterization. Quantitative real-time PCR was used to screen these epialleles for *ADF11* mRNA silencing (Figure 4.1C). A western blot of root tissue proteins using an ADF subclass II-specific monoclonal antibody confirmed that the knockdown of *ADF11* mRNA also resulted in the reduction of ADF11 protein (Figure 1D). This antibody detects both ADF8 and ADF11 protein in root tissue, but the isovariants run as two distinct bands on an SDS-PAGE gel (Ruzicka *et al.*, 2007). In the *ADF11Ri* epiallele lines, the top band (ADF8) is unchanged in intensity compared to wild-type, while the lower band (ADF11) is reduced 40 to 90% compared to equally loaded wild-type. In summary, *ADF11* mRNA was significantly silenced in multiple epiallele lines, and this silencing resulted in a proportional decrease in protein levels.

The *ADF11Ri* epiallele lines were grown vertically to assay potential root and root hair phenotypes. The overall root length of the *ADF11Ri* lines was not significantly different than wild-type, but there was a significant root hair phenotype. *ADF11Ri* lines produced root hairs that were shorter and fewer in number than wild-type as shown in Figure 4.2A, B, C, and D compared to Figure 4.2E, F, and G and quantified in 4.2M. In addition to having shorter root hairs, the *ADF11Ri* root hairs were also frequently branched (Figure 4.2B). The branching occurred on the side of the root hair, not at the base or tip, indicating that the defect is in stage 3 or 4 of root hair development, and not

due to a defect in hair initiation or bulge formation (Schiefelbein *et al.*, 1993; Grierson *et al.*, 1997; Ryan *et al.*, 1998; Jones *et al.*, 2002). During stage 3 and 4 of root hair elongation, the active treadmilling of the actin cytoskeleton is required to facilitate the transport of secretory vesicles to the tip and to establish a polarized cytoplasm via a calcium gradient (Foissner and Wasteneys, 1997; Vidali and Hepler, 2001; Vidali *et al.*, 2001). The *ADF11Ri* root hair phenotype fits a model where a defect in active treadmilling could result in shortened root hairs. However, the *ADF11Ri* branching phenotype indicates that the shortened root hair may still experience tip growth, just in a depolarized manner. In conclusion, our observations indicate that root hair initiation remained unaffected in the *ADF11Ri* plants, but root hair elongation and possibly the maintenance of cell polarity were defective.

ADF11Ri knockdown phenotypes are complemented by *ADF11* and Subclass II *ADF8* and *ADF10* cDNAs, but not Subclass I *ADF4* or Subclass III *ADF9* cDNA

Previous work characterized the phylogenetic relationships and expression patterns of the Arabidopsis subclass II ADFs and determined that there are in fact two subgroups within subclass II, IIA and IIB, that have pollen-specific and root hair specific expression patterns. However, in distantly related Oryza sativa, these two expression patterns were maintained in each subclass II gene member. This result argued that the ancient subclass II ADF functioned in both pollen and root hairs, and these functions may have subdivided between the root hair specific and pollen specific ADFs in Arabidopsis. However, the functional need for cytoskeletal remodeling in root hairs and pollen tubes

appears conserved given the ability of mis-expressed reproductive ACTIN1 to suppress vegetative *actin2* root hair phenotypes (Kandasamy *et al*., 2007). From this, we propose a hypothesis that the subclass II ADFs have overlapping functions and would thus be able to complement an ADF11 loss of function phenotype when sufficiently expressed in root hairs.

The subclass II cDNAs *(ADF11*, *ADF8*, and *ADF10)* were cloned into the *Actin2* promoter-terminator construct with a linked hygromycin resistance gene in order to sufficiently express these genes in root hair cells. Homozygous *ADF11Ri -4* knockdown plants were transformed with these transgenes and selected on hygromycin. Plants co-expressing an homologous (*ADF11*) or paralogous (*ADF8* and *ADF10*) complementation transgene and the *ADF11Ri* silencing transgene were characterized for the phenotypic rescue of the *ADF11Ri* shortened root hair phenotype. First, the majority (~70%) of the *ADF11Ri-4/A2pt:ADF11* lines demonstrated full complementation of the *ADF11Ri* root hair defects (Figure 4.2H). For the subclass II *ADF8* and *ADF10* paralogous complementation transgenes, individuals showing a rescued root hair phenotype were isolated as well (Figure 4.2I and J). Of note however, only a few morphologically normal (paralogue complemented) *ADF11Ri-4*/*A2pt:ADF8* and *ADF11Ri-4*/*A2pt:ADF10* lines were identified out of more than 40 drug resistant independent transformants characterized. For the subclass I *ADF4* and subclass III *ADF9* paralogous complementation transgenes, no plants exhibited a wild-type root hair phenotype (Figure 4.2K and L). While the expression levels of the *A2pt:ADF4* and *A2pt:ADF9* transgenes are not yet quantified, other studies using wild-type plants

transformed with these same transgenes showed increased levels of *ADF4* and *ADF9* transcripts, respectively (data not shown). In the very near future, experiments will be conducted to confirm the expression of the paralogous complementation transgenes and the silencing of endogenous *ADF11* in all of these lines.

The actin cytoskeleton fails to properly organize in the elongating root hair in *ADF11Ri*

The classic cytoskeletal-remodeling role of ADF is the depolymerization and severing of actin monomers and small polymers from the older, pointed end of actin filaments. These degradation products serve to re-supply the G-actin pool and act as sites of new filament initiation, increasing F-actin dynamics. Given the strong root hair phenotypes of the *ADF11Ri* plants, we sought to characterize the organization of the actin cytoskeleton in root hair cells. The *ADF11Ri* transgene was transformed into wild-type plants stably expressing a GFP F-actin reporter (GFP:fABD2) (see Materials and Methods) (Sheahan *et al.*, 2004). The GFP:fABD2 reporter/*ADF11Ri* lines were analyzed using confocal microscopy to examine multiple stages of root hair development as shown in Figure 4.3. Interestingly, the organization and architecture of the actin cytoskeleton in newly emerging root hair cells was not significantly different from wild-type (figure 4.3A and F). However, as the root hair began to exhibit tip growth (stage 3), two significant aberrant cytoskeleton phenotypes emerged. First, thick accumulations of transversely-oriented actin rings appeared in the base of root hair cells (Figure 4.3B). These structures were rarely seen in wild-type roots (less than 0.1% of

root hairs) compared to 75-80% of all stage 3 root hair cells in *ADF11Ri* roots. Second, in partially elongated *ADF11Ri* root hairs (stage 3 and 4), transverse actin ring structures also appeared in the elongated root hair (Figure 4.3C, D, and E). This phenotype was not found in any root hairs of wild-type plants, but was present in ~80% of *ADF11Ri* elongated root hairs. In wild-type root hairs, the actin cytoskeleton is organized in a predominantly longitudinal orientation with long actin filaments and bundles extending in the same direction as root hair elongation (Figure 4.3E-J). These long longitudinal filaments were largely absent in the *ADF11Ri* root hairs and were instead replaced by the transverse actin rings and large regions devoid of any actin filaments.

Transversely arrayed actin bundling phenotypes have previously been reported in a wide range of actin cytoskeleton mutants (Kobayashi *et al.*, 1987; Kandasamy *et al.*, 2002; Ketelaar *et al.*, 2007). Interestingly, the over-expression of Arabidopsis *Rop1* resulted in a stunted root hair phenotype with abnormal accumulations of transverse-oriented actin rings (Kost *et al.*, 1999; Fu *et al.*, 2001). Rop1 is a member of the Plant-RhoGTPase family, and RhoGTPases are high-level regulators of ADF activity via their activation of the kinases that phosphorylate ADF (Mackay and Hall, 1998; Chen *et al.*, 2003). It is interesting to postulate that the reason the loss of *ADF11* and the over-expression of *Rop1* result in similar root hair morphology and actin cytoskeleton phenotypes is because they function through the same signaling pathway. If Rop1 functions to phosphorylate ADF11, thus inactivating it, then *Rop1* over-expression would likely result in an *ADF11* hypomorphic phenotype, similar to an *ADF11Ri* knockdown

allele. Similarly, over-expressing *ADF11* or expressing a mutated, constitutively active *ADF11* might suppress the *Rop1* over-expression phenotype. Although beyond the scope of this study, it would be interesting to test the Rop1 – ADF11 relationship by combining the *ADF11Ri* transgene with the *Rop1* over-expression line.

Testing the effect of *ADF11* knockdown and over-expression on the *act2* and *act7* mutant phenotypes

The *ADF11Ri* knockdown phenotypes are symptomatic of a decrease in the remodeling capacity of the actin cytoskeleton. A mutation in the vegetative actin *ACT2* gene also shows a stunted root hair phenotype, indicating that changes to the stoichastic balance between actin and actin binding proteins result in root hair phenotypes. To test the epistatic relationship between ADF11 and ACT2 or ACT7, we transformed *act2* and *act7* null mutant plants with the *ADF11Ri* and *ADF11* over-expression (*A2pt:ADF11*) transgenes. Our expectation is that if the ratio of ADF11 to ACT2 or ACT7 affects root hair growth, these *ADF11Ri* knockdown and *A2pt:ADF11* over-expression transgenes should have an additive or suppressive effect on the actin mutant phenotypes. For example, while the *act2* mutant and the *ADF11Ri* knockdown plants both exhibit stunted root hair phenotypes, the *ADF11Ri* transgene may suppress the *act2* phenotype by restoring a stoichiometric balance to the actin/ADF ratio in the root hair cell cytoskeleton. Alternatively, while the over-expression of *ADF11* does not cause a dominant root hair phenotype, *ADF11* over-expression in the *act2* mutant may result in a more severe root hair defect, because the actin/ADF ratio is shifted more severely

towards excess ADF. In terms of this stoichiometric balance, the *act2/A2pt:ADF11* plants may exhibit similar phenotypes to the bald root *act2/act8* double mutant which has normal ADF11 levels, but much less actin (Kandasamy *et al.*, In Preparation). Figure 5 summarizes the model of actin/ADF ratios and their possible effect on root hair phenotypes.

MATERIALS AND METHODS

Plant Strains and Growth Conditions

Except for experiments using *act2* and *act7* mutant plants, all experiments utilized *Arabidopsis thaliana* ecotype Columbia plants containing the GFP:fABD2 transgene. Plants were grown in Petri plates containing 1/2 Murashige Skoog Salts (Caison) media supplemented with 1% sucrose and solidified with 0.8% agar (Caison) or in soil (Fafard 2B) under standard 23ºC 16h-light conditions (Murashige and Skoog, 1962). All root analysis was performed on plates with plants grown vertically, and excluded any individual plants whose roots either entered the agar media or grew aerially because of the effects of these growth habits on root hairs.

ADF11 RNAi transgene construction

The *ADF11Ri* transgene was produced using the pFGC5941 binary vector (Kerschen *et al.*, 2004). The first 150bp of the annotated ADF11 3´UTR was cloned in the sense and antisense orientation into the vector using inner and outer sets of restriction enzyme recognition sites added in the PCR amplification step. The pFGC5941 vector uses the

35S tobacco mosaic virus promoter and *ocs* terminator to drive the expression of the stem-loop transgene, and the *Chs* intron sequence as the stem-loop spacer.

After confirming the proper sequence of the sense and antisense *ADF11* 3´UTR sequences, the plasmid was transformed into Agrobacterium and subsequently wild-type Arabidopsis plants containing a stable fABD:GFP cytoskeletal marker transgene. Positive transformants were selected with BASTA herbicide and seeds collected. These seeds were germinated on plates containing BASTA (30μM) and lines showing resistance were moved to drug free plates to grow root tissue and analyze *ADF11* transcript levels using qRT-PCR. Four strong knockdown lines were moved to soil and seeds collected. T3 plants were sprayed with BASTA to isolate homozygous insertion lines in order to characterize root phenotypes without side effects from germination on drugs. These T3 lines were subsequently used for all characterization including final gene expression analysis, root hair morphological phenotypes, and actin cytoskeleton phenotypes.

qRT-PCR

RNA was isolated from root tissue using the RNeasy plant mini kit (Qiagen). RNA was treated with RQ1 RNase-free DNase (Promega) before reverse transcription (RT). 1.5 micrograms of treated RNA were added to RT reactions using the Invitrogen SuperscriptIII first strand synthesis kit with oligo dT primers to make cDNA. qRT-PCR was used to analyze cDNA populations using target primers with ubiquitin primers as the endogenous control (For primer sequences see Ruzicka et al., 2007). Real-time

PCR was performed on an Applied Biosystems 7500 real-time PCR system using SYBR Green detection chemistry (Applied Biosystems).

Protein Blot Analysis

Protein from *Arabidopsis* root tissue was prepared for immunoblotting as described in (Kandasamy *et al.*, 1999; Kandasamy *et al.*, 2001) using the anti-ADF8 monoclonal antibody described in Ruzicka *et al.*, 2007.

ACKNOWLEDGEMENTS

We would like to thank Steve McCurdy for sharing the GFP:fABD2 reporter plant line that was used in this study. Thanks also to Roger Deal, Lori King-Reid, and Yolanda Lay for their contributions to experimental design and execution.

REFERENCES

Baluska, F., Salaj, J., Mathur, J., Braun, M., Jasper, F., Samaj, J., Chua, N.H., Barlow, P.W. and Volkmann, D. (2000) Root hair formation: F-actin-dependent tip growth is initiated by local assembly of profilin-supported F-actin meshworks accumulated within expansin-enriched bulges. *Dev Biol*, **227**, 618-632.

Bamburg, J.R. (1999) Proteins of the ADF/cofilin family: essential regulators of actin dynamics. *Annu Rev Cell Dev Biol*, **15**, 185-230.

Borisy, G.G. and Svitkina, T.M. (2000) Actin machinery: pushing the envelope. *Curr Opin Cell Biol*, **12**, 104-112.

Chen, C.Y., Cheung, A.Y. and Wu, H.M. (2003) Actin-depolymerizing factor mediates Rac/Rop GTPase-regulated pollen tube growth. *Plant Cell*, **15**, 237-249.

Diet, A., Brunner, S. and Ringli, C. (2004) The enl mutants enhance the lrx1 root hair mutant phenotype of Arabidopsis thaliana. *Plant Cell Physiol*, **45**, 734-741.

Dolan, L., Janmaat, K., Willemsen, V., Linstead, P., Poethig, S., Roberts, K. and Scheres, B. (1993) Cellular organization of the *Arabidopsis thaliana* root. *Development*, **119**, 71-84.

Dolan, L. and Roberts, K. (1995) The development of cell pattern in the root epidermis. *Phil Trans. R. Soc. Lond.*, **350**.

Dong, C.H., Xia, G.X., Hong, Y., Ramachandran, S., Kost, B. and Chua, N.H. (2001) ADF proteins are involved in the control of flowering and regulate F- actin organization, cell expansion, and organ growth in *Arabidopsis*. *Plant Cell*, **13**, 1333-1346.

Emons, A.M.C. (1987) The cytoskeleton and secretory vesicles in root hairs of *Equisetum* and *Limnobium* and cytoplasmic streaming in root hairs of *Equisetum*. *Ann. Bot.*, **60**, 625-632.

Foissner, I. and Wasteneys, G.O. (1997) A cytochalasin-sensitive actin filament meshwork is a prerequiste for local wound wall deposition in *Nitella* internodal cells. *Protoplasma*, **200**, 17-30.

Fu, Y., Wu, G. and Yang, Z. (2001) Rop GTPase-dependent dynamics of tip-localized F-actin controls tip growth in pollen tubes. *J Cell Biol*, **152**, 1019-1032.

Ghosh, M., Song, X., Mouneimne, G., Sidani, M., Lawrence, D.S. and Condeelis, J.S. (2004) Cofilin promotes actin polymerization and defines the direction of cell motility. *Science*, **304**, 743-746.

Gilliland, L.U., Kandasamy, M.K., Pawloski, L.C. and Meagher, R.B. (2002) Both vegetative and reproductive actin isovariants complement the stunted root hair phenotype of the *Arabidopsis act2-1* mutation. *Plant Physiol.*, **130**, 2199-2209.

Gilliland, L.U., Pawloski, L.C., Kandasamy, M.K. and Meagher, R.B. (2003) *Arabidopsis* actin gene *ACT7* plays an essential role in germination and root growth. *Plant J*, **33**, 319-328.

Grierson, C.S., Roberts, K., Feldmann, K.A. and Dolan, L. (1997) The COW1 locus of arabidopsis acts after RHD2, and in parallel with RHD3 and TIP1, to determine the shape, rate of elongation, and number of root hairs produced from each site of hair formation. *Plant Physiol*, **115**, 981-990.

Hannon, G.J. (2002) RNA interference. *Nature*, **418**, 244-251.

Jones, M.A., Shen, J.J., Fu, Y., Li, H., Yang, Z. and Grierson, C.S. (2002) The Arabidopsis Rop2 GTPase is a positive regulator of both root hair initiation and tip growth. *Plant Cell*, **14**, 763-776.

Kandasamy, M.K., McKinney, E.C. and Meagher, R.B. (1999) The late pollen-specific actins in angiosperms. *Plant J*, **18**, 681-691.

Kandasamy, M.K., Gilliland, L.U., McKinney, E.C. and Meagher, R.B. (2001) One plant actin isovariant, ACT7, is induced by auxin and required for normal callus formation. *Plant Cell*, **13**, 1541-1554.

Kandasamy, M.K., McKinney, E.C. and Meagher, R.B. (2002) Functional nonequivalency of actin isovariants in Arabidopsis. *Mol Biol Cell*, **13**, 251-261.

Kandasamy, M.K., Burgos-Rivera, B., McKinney, E.C., Ruzicka, D.R. and Meagher, R.B. (2007) Class-specific interaction of profilin and ADF isovariants with actin in the regulation of plant development. *Plant Cell*, **19**, 3111-3126.

Kerschen, A., Napoli, C.A., Jorgensen, R.A. and Muller, A.E. (2004) Effectiveness of RNA interference in transgenic plants. *FEBS Lett*, **566**, 223-228.

Ketelaar, T., Allwood, E.G. and Hussey, P.J. (2007) Actin organization and root hair development are disrupted by ethanol-induced overexpression of Arabidopsis actin interacting protein 1 (AIP1). *New Phytol*, **174**, 57-62.

Kobayashi, H., Fukuda, H. and Shibaoka, H. (1987) Reorganization of actin filaments associated with the differentiation of tracheary elements in *Zinnia* mesophyll cells. *Protoplasma*, **138**, 69-71.

Kost, B., Lemichez, E., Spielhofer, P., Hong, Y., Tolias, K., Carpenter, C. and Chua, N.H. (1999) Rac homologues and compartmentalized phosphatidylinositol 4, 5-bisphosphate act in a common pathway to regulate polar pollen tube growth. *J Cell Biol*, **145**, 317-330.

Mackay, D.J. and Hall, A. (1998) Rho GTPases. *J Biol Chem*, **273**, 20685-20688.

McGinnis, K., Chandler, V., Cone, K., Kaeppler, H., Kaeppler, S., Kerschen, A., Pikaard, C., Richards, E., Sidorenko, L., Smith, T., Springer, N. and Wulan, T. (2005) Transgene-induced RNA interference as a tool for plant functional genomics. *Methods Enzymol*, **392**, 1-24.

Meagher, R.B. and Williamson, R.E. (1994) The Plant Cytoskeleton. In *Arabidopsis*, Vol. 38 (Meyerowitz, E. and Somerville, C., eds). Cold Spring Harbor: Cold Spring Harbor Laboratory Press, pp. 1049-1084.

Miller, D.D., de Ruijter, N.C.A., Bisseling, T. and Emons, A.M.C. (1999) The role of actin root hair morphohgenesis: studies with lipochito-oligosaccharide as a growth stimulator and cytochalasin as an actin perturbing drug. *Plant J*, **17**, 141-154.

Murashige, T. and Skoog, F. (1962) A revised medium for rapid growth and bioassays with tobacco tissue culture. *Plant Physiol.*, **15**, 473-497.

Paavilainen, V.O., Bertling, E., Falck, S. and Lappalainen, P. (2004) Regulation of cytoskeletal dynamics by actin-monomer-binding proteins. *Trends Cell Biol*, **14**, 386-394.

Pollard, T.D., Blanchoin, L. and Mullins, R.D. (2000) Molecular mechanisms controlling actin filament dynamics in nonmuscle cells. *Annu Rev Biophys Biomol Struct*, **29**, 545-576.

Ramachandran, S., Christensen, H.E., Ishimaru, Y., Dong, C.H., Chao-Ming, W., Cleary, A.L. and Chua, N.H. (2000) Profilin plays a role in cell elongation, cell shape maintenance, and flowering in *Arabidopsis*. *Plant Physiol*, **124**, 1637-1647.

Ringli, C., Baumberger, N., Diet, A., Frey, B. and Keller, B. (2002) ACTIN2 is essential for bulge site selection and tip growth during root hair development of Arabidopsis. *Plant Physiol*, **129**, 1464-1472.

Ruzicka, D.R., Kandasamy, M.K., McKinney, E.C., Burgos-Rivera, B. and Meagher, R.B. (2007) The ancient subclasses of Arabidopsis Actin Depolymerizing Factor genes exhibit novel and differential expression. *Plant J*, **52**, 460-472.

Ryan, E., Grierson, C.S., Cavell, A., Steer, M. and Dolan, L. (1998) TIP1 is required for both tip growth and non-tip growth in Arabidopsis. *New Phytologist*, **138**, 49-58.

Schiefelbein, J., Galway, M., Masucci, J. and Ford, S. (1993) Pollen tube and root-hair tip growth is disrupted in a mutant of Arabidopsis thaliana. *Plant Physiol*, **103**, 979-985.

Schiefelbein, J.W. and Somerville, C. (1990) Genetic control of root hair development in *Arabidopsis thaliana*. *Plant Cell*, **2**, 235-243.

Schiefelbein, J.W. (2000) Constructing a plant cell. The genetic control of root hair development. *Plant Physiol*, **124**, 1525-1531.

Sheahan, M.B., Staiger, C.J., Rose, R.J. and McCurdy, D.W. (2004) A green fluorescent protein fusion to actin-binding domain 2 of Arabidopsis fimbrin highlights

new features of a dynamic actin cytoskeleton in live plant cells. *Plant Physiol*, **136**, 3968-3978.

Staiger, C.J. (2000) Signaling to the actin cytoskeleton in plants. *Annu. Rev. Plant Physiol. Plant Mol. Biol.*, **51**.

Swarbreck, D., Wilks, C., Lamesch, P., Berardini, T.Z., Garcia-Hernandez, M., Foerster, H., Li, D., Meyer, T., Muller, R., Ploetz, L., Radenbaugh, A., Singh, S., Swing, V., Tissier, C., Zhang, P. and Huala, E. (2008) The Arabidopsis Information Resource (TAIR): gene structure and function annotation. *Nucleic Acids Res*, **36**, D1009-1014.

Valster, A.H., Pierson, E.S., Valenta, R., Hepler, P.K. and Emons, A.M.C. (1997) Probing the plant actin cytoskeleton during cytokinesis and interphase by profilin microinjection. *Plant Cell*, **9**, 1815-1824.

Vidali, L. and Hepler, P.K. (2001) Actin and pollen tube growth. *Protoplasma*, **215**, 64-76.

Vidali, L., McKenna, S.T. and Hepler, P.K. (2001) Actin polymerization is essential for pollen tube growth. *Mol Biol Cell*, **12**, 2534-2545.

Wasteneys, G.O. and Galway, M.E. (2003) Remodeling the cytoskeleton for growth and form: an overview with some new views. *Annu Rev Plant Biol*, **54**, 691-722.

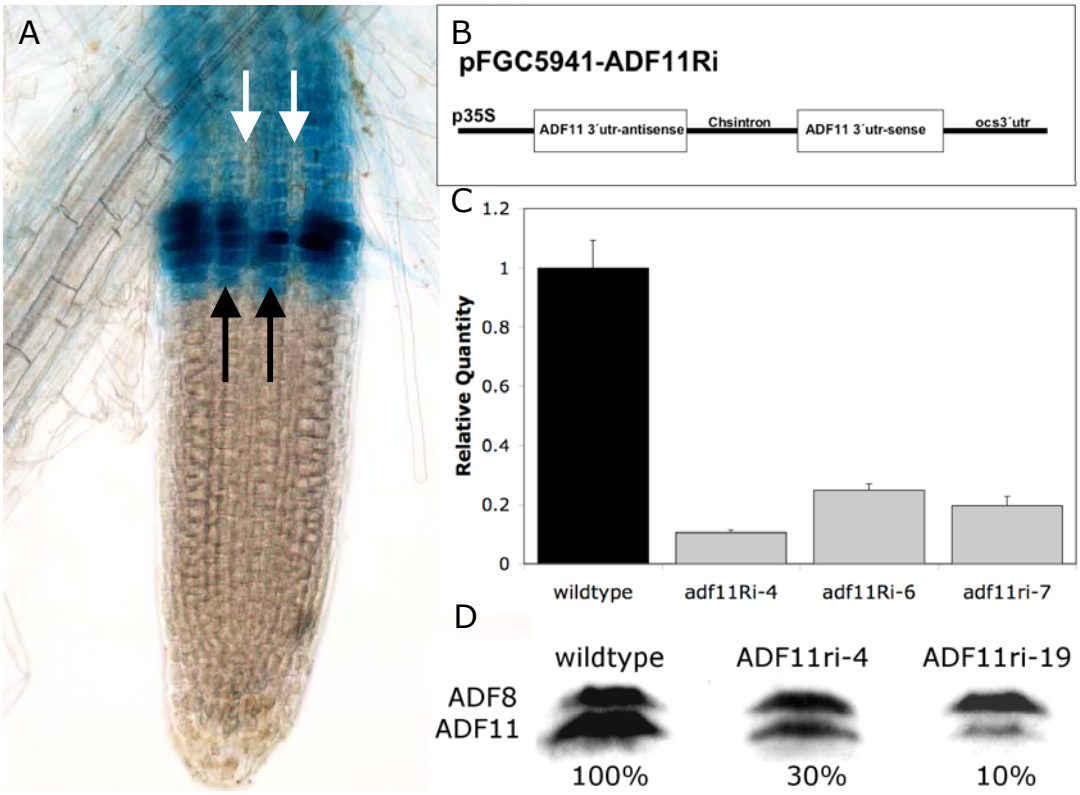

Figure 4.1 The *ADF11* RNAi (*ADF11Ri*) silencing allele results in a significant decrease in ADF11 mRNA and protein. As detailed in chapter 2, the ADF11pi:GUS reporter shows staining exclusively in the rows of trichoblast cells (black arrows) (A). Note the rows of atrichoblast cells are not significantly stained (white arrow). The *ADF11* RNAi construct was designed to arrange the *ADF11* 3´UTR in antisense and sense orientations with a loop-forming linker separating the two complementary regions (B). Under the control the constitutive 35s promoter system, this RNAi precursor stem-loop RNA is expressed ubiquitously and is processed into small RNAs that target *ADF11* mRNA. qRT-PCR was used to determine the relative quantity of *ADF11* and *ADF8* mRNA in wild-type and multiple *ADF11Ri* root tissue samples (C). ADF11 protein

levels were analyzed in a western blot using the ADF8mAb on root tissue (D). The top band is ADF8 protein and the lower band ADF11 protein, indicating that the ADF11 protein levels are reduced in the *ADF11Ri* lines, in agreement with the qRT-PCR data.

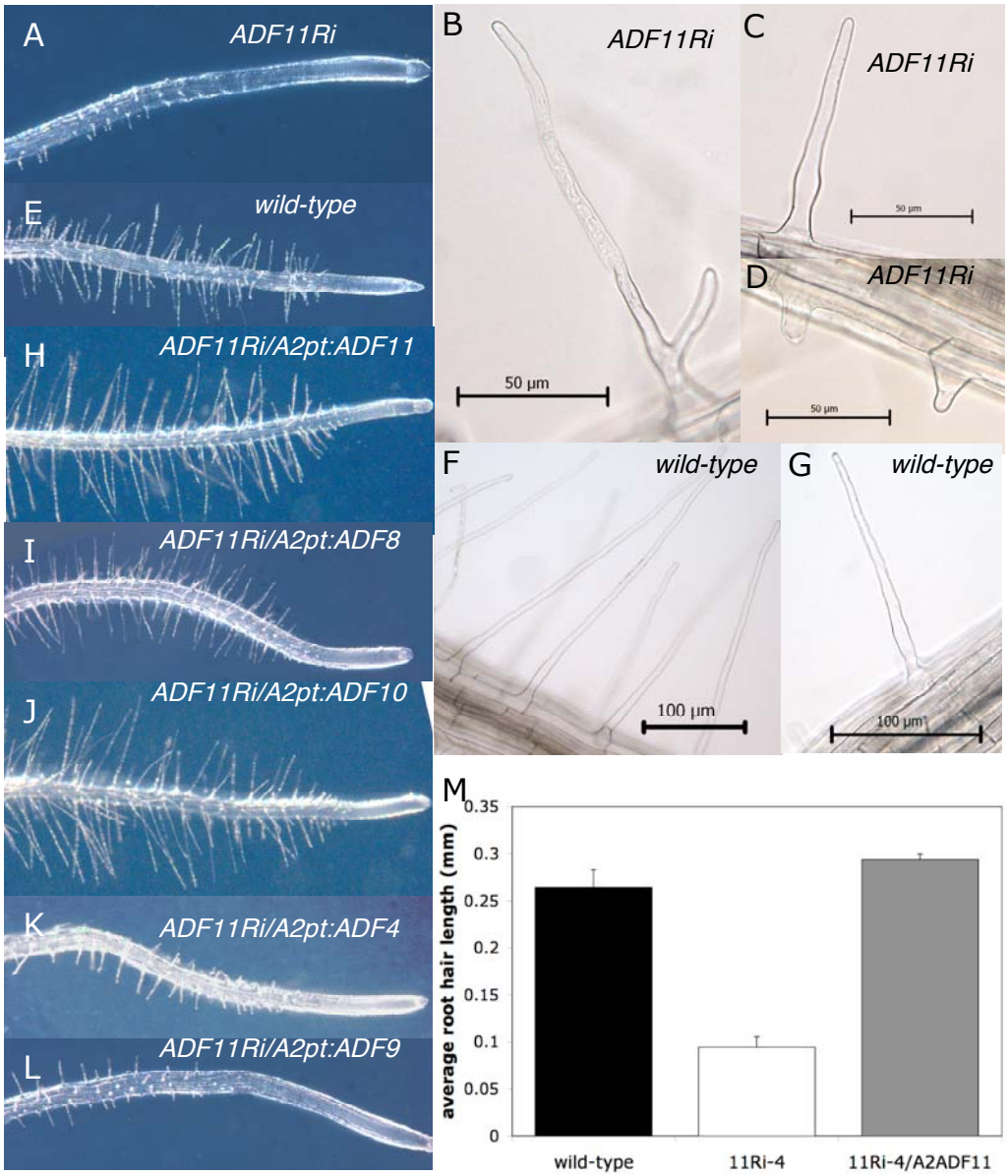

Figure 4.2 ADF11 is required for proper root hair development The primary root of 12 day old *ADF11Ri* (A, B, C, and D) and wild-type (E, F, and G) seedlings showing a root hair elongation defect and branching. An *ADF11Ri* allele was transformed with complementation transgenes comprised of *ADF11* (H), subclass II *ADF8* (I), subclass II *ADF10* (J), subclass I *ADF4* (K), or subclass III *ADF9* (L) cDNAs expressed under the constitutive *ACT2* promoter/terminator. Subclass II ADFs can complement the defect in

ADF11, but not subclass I ADF4 or subclass III ADF9, indicating a significant difference in isovariant function between the Arabidopsis ADF subclasses. The root hair length was quantified for wild-type, *ADF11Ri*, and *ADF11Ri/A2:ADF11* (M).

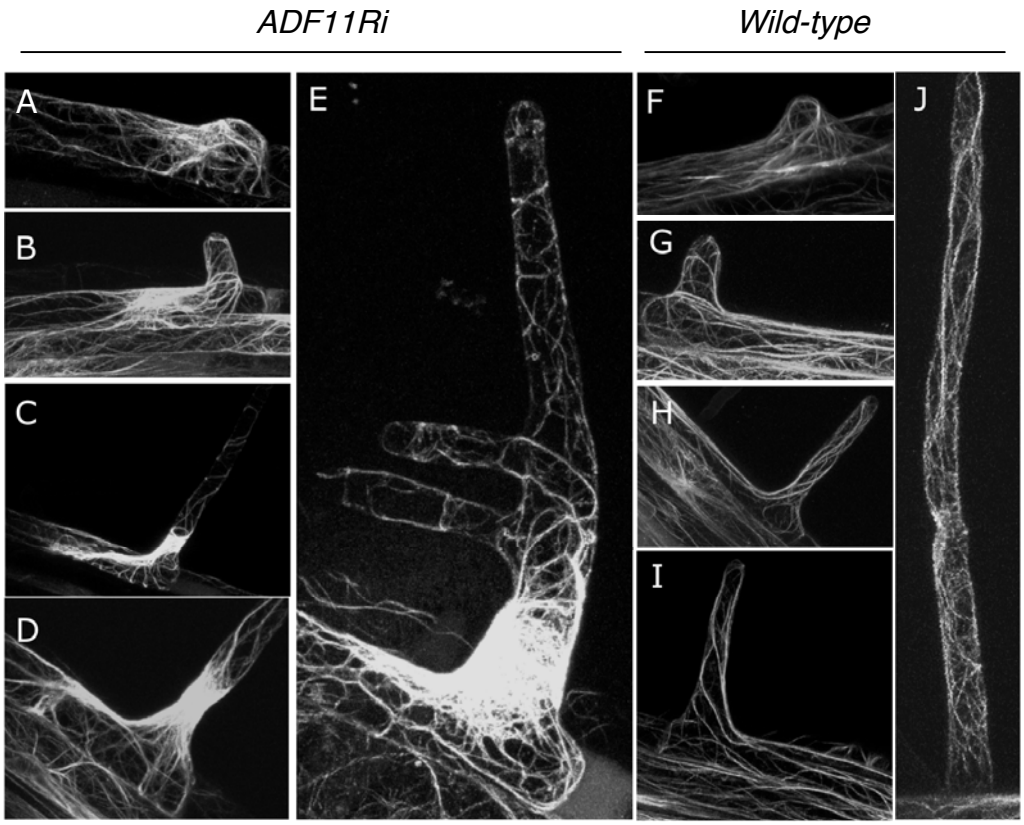

Figure 4.3 *ADF11Ri* root hairs exhibit defective actin cytoskeleton organization and structure. ADF11Ri and wild-type plants containing the fimbrin actin binding domain 2 / GFP reporter were analyzed using confocal microscopy. During early root hair development, the *ADF11Ri* (A) actin cytoskeleton appears similar to wild-type (F). As root hair elongation proceeds, however, gross accumulations of actin filaments form in the root hair cells (B). The *ADF11Ri* mature shortened root hairs exhibit accumulations of actin rings transversely arrayed near the base of the root hair structure (C and D). This morphology is also present in branched *ADF11Ri* root hairs (E). The wild-type actin cytoskeleton is comprised of longitudinally arrayed actin filaments and bundles throughout root hair elongation (G-J).

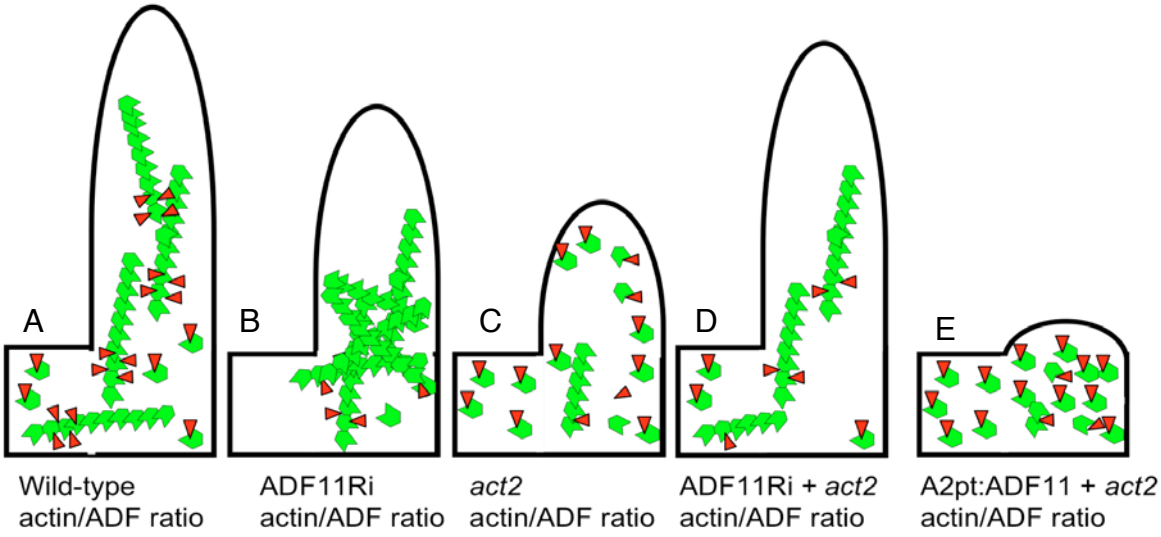

Figure 4.4 Model of the stoichastic balance between G- and F- actin in the *ADF11Ri*, *act2*, and *A2pt:ADF11* alleles. Wild-type trichoblast cells contain longitudinally arrayed F-actin filaments undergoing active remodeling and treadmilling, and have a balanced F- to G- actin ratio (A). *ADF11Ri* trichoblasts exhibit transversely arrayed actin rings near the base of the root hair due to over-polymerization of F-actin and contain a lower concentration of G-actin (B). The *act2* mutant trichoblast cells are also defective in tip elongation because there is too little F-actin (C). By combining the *ADF11Ri* and *act2* alleles, it may restore the balance of G- to F- actin by reducing the relative excess depolymerization seen in the *act2* mutant (D). Similarly, by combining the *A2pt:ADF11* over-expression allele with *act2*, we might expect an additive phenotype (bald roots) because the balance is even further skewed to favor G-actin, thus reducing the F-actin cytoskeleton even further (E).

CHAPTER 5

CONCLUSIONS AND PERSPECTIVES

The actin cytoskeleton sits at the proverbial crossroads of the cell. Essential for a wide range of cell functions, the dynamic remodeling of actin filaments facilitates cell proliferation, growth, and development. The actin cytoskeleton is organized and remodeled by a range of actin binding proteins (ABPs) that each perform diverse functions. The ABP Actin Depolymerizing Factor (ADF) binds to actin filaments, alters the filament's helical twist, and promotes depolymerization and severing. To better understand the regulation of the actin cytoskeleton and its role in multicellular development, we embarked on an in-depth study of the Arabidopsis ADF gene family. At the beginning of this study, our understanding of ADF was limited to detailed biochemical analyses of ADF's actin depolymerizing and severing functions, and more limited looks at ADF's role in cell and organismal development (Bamburg, 1999; Dong *et al.*, 2001a; Dong *et al.*, 2001b). With eleven distinct members, we proposed that ADFs should exhibit differential expression patterns and/or isovariant functions, accounting for their ancient conservation. To test this hypothesis, we characterized the expression

patterns of all eleven Arabidopsis *ADFs* using multiple molecular tools, and also characterized the role of individual ADF isovariants in plant development using mutant alleles and complementation transgenes.

Before committing to an extensive series of experiments to determine the expression patterns of the eleven genes in the Arabidopsis ADF family, we constructed a phylogeny of the ADF protein sequences. By adding putative rice and poplar ADF sequences to the alignment, we concluded that the Arabidopsis ADFs group into four ancient subclasses, each predating the monocot/dicot split approximately 150 million years ago. With this phylogeny in hand, we proposed that the ADFs would exhibit conserved expression patterns among the ancient subclass members. The Arabidopsis genome also encodes large Actin and profilin gene families, and their members exhibit differential expression patterns between anciently conserved vegetative and reproductive subclasses, providing a model for our proposal (Gilliland *et al.*, 2002; Kandasamy *et al.*, 2002).

We explored the expression patterns of the Arabidopsis *ADFs* using qRT-PCR to measure *ADF* transcript levels, developed monoclonal antibodies for western blot analysis of ADF protein localization, and characterized promoter-reporter fusion transgenes of each of the eleven *ADF* genes (Ruzicka *et al.*, 2007). We concluded that the eleven Arabidopsis *ADFs* exhibit differential expression patterns and that these patterns correlate with the evolutionary relationships among the ADF protein sequences. Furthermore, while subclass I and IV *ADFs* were expressed ubiquitously in all tissues throughout plant development, subclass II and III *ADFs* exhibited highly

specific or regulated expression patterns. Subclass III ADFs were expressed in most tissues assayed, and were also highly regulated by phytohormones (*ADF9*) and environmental stresses (*ADF5*). Subclass II *ADFs* split into pollen-specific and root hair-specific subgroups, indicating that their expression patterns may encompass a conserved functional role in polar tip growth. We demonstrated that the ancestral subclass II ADF was likely expressed in both root hairs and pollen by determining that *Oryza sativa's* subclass II ADF genes, *OsADF1* and *OsADF6*, were dually expressed in roots and anthers. We reasoned that the two patterns subfunctionalized into root hair specific and pollen specific expression somewhere within the Arabidopsis lineage. Future endeavors could study the expression patterns of subclass II ADFs in a range of dicot plant species to narrow the evolutionary time window of this subfunctionalization event.

Next, we wanted to explore the functional differences among the various Arabidopsis ADF protein isovariants to address the second objective of our hypothesis. Specific Aims 2 and 3 focused on this objective by characterizing the function of individual Arabidopsis ADFs and also by testing whether various Arabidopsis ADFs could complement the loss of function of an ADF from a different ancient subclass. To start, we characterized a null insertion mutant in *ADF5* (*adf5-1*) and discovered it exhibited multiple pleotropic phenotypes. These phenotypes included defects in F-actin cytoskeleton dynamics and organization, defects in organ and cell development, and also an increase in cold tolerance. Previous studies have shown that the *CBF* transcription factors are induced in response to cold temperatures, and are

subsequently required for the up-regulation of multiple factors required for freeze tolerance. The loss of *ADF5* caused a de-repression of the *CBF* cold-signaling response transcription factors during normal temperatures, resulting in this physiological freeze-tolerance phenotype. To probe the mechanism of ADF5's role in *CBF* gene regulation, we used nuclease protection and chromatin immunoprecipitation assays to detail the changes to the *CBF1* promoter chromatin structure in the *adf5-1* mutant. In summary, ADF5 represses *CBF* expression through a novel pathway, independent of cold-stress regulation. Furthermore, we demonstrated that ADF5 is induced by cold temperatures by the CBFs, and may play a role in a feedback loop repressing the CBFs after returning to normal temperatures.

Importantly, the *adf5-1* freeze-tolerance phenotype appears unique among the numerous reports on mutants in various actin cytoskeleton components, and the overexpression of subclass I *ADF4* or subclass III *ADF9* were unable to complement the *adf5-1* mutant phenotypes. While further studies are required to define the mechanism by which ADF5 affects plant development and gene regulation, the literature supports two important models. First, ADF5 may effect the nuclear localization of actin, and subsequently control actin's participation in various nuclear activities including chromatin remodeling and basal transcription (Miralles and Visa, 2006). Alternatively, ADF5 may modulate cytoskeleton dynamics in the cytosol under very specific conditions, resulting in the activation or repression of high-level transcription factors that interact with F- or G- actin (Ruegg *et al.*, 2004; Balasubramanian *et al.*, 2007). Future work by the Meagher lab will focus on understanding the mechanisms behind the ADF

gene regulation phenotypes. Ultimately, it will be interesting to advance our understanding of how a single member of a large actin binding protein gene family can have such a significant and specific effect on plant development and cold-stress signaling.

To further address the function of Arabidopsis ADF isovariants, we constructed an RNA interference epiallele targeting the root-hair specific subclass II *ADF11* (*ADF11Ri*). Mutants in multiple actin and actin binding protein genes cause diverse root hair phenotypes including defects in cell specification, hair initiation, buldge formation, and tip growth (Ramachandran *et al.*, 2000; Gilliland *et al.*, 2003). Furthermore, root hair development provides a simple model for the effects of coordinated actin cytoskeleton remodeling on cell growth and development. Independent *ADF11Ri* epialleles showed significant levels of RNA silencing, and resulted in a specific decrease in the levels of ADF11 protein. In contrast to the ADF5 study, the *ADF11Ri* knockdown plants exhibited a much more significant F-actin cytoskeleton phenotype. Specifically, *ADF11Ri* root hairs showed a loss of longitudinal filaments and bundles in root hairs and the ectopic formation of transversely arrayed actin rings near the base of the root hair. Following from this cytoskeletal defect, root hair development was also altered in the *ADF11Ri* plants. Root hairs were significantly shorter, and frequently branched, demonstrating that ADF11 is required for the elongation and maintenance (stages 3 and 4) of root hair development (Schiefelbein, 2000). Furthermore, it appears that the *ADF11Ri* root hair phenotype can be rescued by the over-expression of subclass II *ADFs* (*ADF8* and *ADF10*), but cannot be rescued by the over-expression of

subclass I *ADF4* or subclass III *ADF9*. This result argues that functional redundancy may still exist among the subclass II isovariants, but not between the various subclasses. This result supports our earlier proposal that the subclass II *ADFs* had undergone subfunctionalization of expression patterns but have retained a conserved functional role in polar tip growth.

In reflection, I think it is fair to state that no one expected the Arabidopsis ADF gene family to contain so many interesting facets. The field of developmental biology rarely gives the actin cytoskeleton more than a passing consideration, but I believe we have begun to uncover just the tip of an iceberg with ADF and the actin cytoskeleton controlling multicellular development and gene regulation. It is hard to imagine the Arabidopsis ADFs evolving novel functions among its eleven members within the evolution of plants. More likely, the distinct functions of ADF5, ADF11, and ADF9 (see appendix 1) have evolved from an ancestral plant ADF that already exhibited the ability to regulate cellular development and gene regulation. Therefore, the Arabidopsis ADFs are an excellent model to further study the mechanism by which ADF controls gene regulation because this function may be conserved across eukaryotes. Finally, this study began as a test of the theory of isovariant dynamics where large families of cytoskeleton proteins that exhibit various expression patterns and isovariant functions ultimately expands the buffering and regulation of actin cytoskeleton dynamics. Taken one step further, we can now include gene regulation as an additional consequence of isovariant dynamics where specific actin cytoskeleton components may regulate the activity of specific high-level transcription factors and developmental pathways.

REFERENCES

Balasubramanian, R., Karve, A., Kandasamy, M., Meagher, R.B. and Moore, B. (2007) A role for F-actin in hexokinase-mediated glucose signaling. *Plant Physiol*, **145**, 1423-1434.

Bamburg, J.R. (1999) Proteins of the ADF/cofilin family: essential regulators of actin dynamics. *Annu Rev Cell Dev Biol*, **15**, 185-230.

Dong, C.H., Kost, B., Xia, G. and Chua, N.H. (2001a) Molecular identification and characterization of the Arabidopsis AtADF1, AtADFS and AtADF6 genes. *Plant Mol Biol*, **45**, 517-527.

Dong, C.H., Xia, G.X., Hong, Y., Ramachandran, S., Kost, B. and Chua, N.H. (2001b) ADF proteins are involved in the control of flowering and regulate F- actin organization, cell expansion, and organ growth in *Arabidopsis*. *Plant Cell*, **13**, 1333-1346.

Gilliland, L.U., Kandasamy, M.K., Pawloski, L.C. and Meagher, R.B. (2002) Both vegetative and reproductive actin isovariants complement the stunted root hair phenotype of the *Arabidopsis act2-1* mutation. *Plant Physiol.*, **130**, 2199-2209.

Gilliland, L.U., Pawloski, L.C., Kandasamy, M.K. and Meagher, R.B. (2003) *Arabidopsis* actin gene *ACT7* plays an essential role in germination and root growth. *Plant J*, **33**, 319-328.

Kandasamy, M.K., McKinney, E.C. and Meagher, R.B. (2002) Functional nonequivalency of actin isovariants in Arabidopsis. *Mol Biol Cell*, **13**, 251-261.

Meagher, R.B., McKinney, E.C. and Kandasamy, M.K. (1999) Isovariant dynamics expand and buffer the responses of complex systems: the diverse plant actin gene family. *Plant Cell*, **11**, 995-1006.

Miralles, F. and Visa, N. (2006) Actin in transcription and transcription regulation. *Curr Opin Cell Biol*, **18**, 261-266.

Ramachandran, S., Christensen, H.E., Ishimaru, Y., Dong, C.H., Chao-Ming, W., Cleary, A.L. and Chua, N.H. (2000) Profilin plays a role in cell elongation, cell shape maintenance, and flowering in *Arabidopsis*. *Plant Physiol*, **124**, 1637-1647.

Ruegg, J., Holsboer, F., Turck, C. and Rein, T. (2004) Cofilin 1 is revealed as an inhibitor of glucocorticoid receptor by analysis of hormone-resistant cells. *Mol Cell Biol*, **24**, 9371-9382.

Ruzicka, D.R., Kandasamy, M.K., McKinney, E.C., Burgos-Rivera, B. and Meagher, R.B. (2007) The ancient subclasses of Arabidopsis Actin Depolymerizing Factor genes exhibit novel and differential expression. *Plant J*, **52**, 460-472.

Schiefelbein, J.W. (2000) Constructing a plant cell. The genetic control of root hair development. *Plant Physiol*, **124**, 1525-1531.

APPENDIX A

ARABIDOPSIS ACTIN DEPOLYMERIZING FACTOR *ADF9* PARTICIPATES IN CYTOPLASMIC AND NUCLEAR PROCESSES[1]

[1] Brunilís Burgos-Rivera[2], Daniel R. Ruzicka[2], Roger B. Deal, Elizabeth C. McKinney, Lori King-Reid, and Richard B. Meagher

[2]These two authors made equivalent contributions to the manuscript

ABSTRACT

Actin depolymerizing factor (ADF) modulates the rate of actin filament turnover and assists in actin nuclear transport. Plant and animal genomes encode families of diverse ancient ADF isovariants. One weak, but constitutive member of the Arabidopsis (*Arabidopsis thaliana*) family, *ADF9,* is moderately expressed in the shoot apical meristem (SAM). *ADF9* was dramatically induced by phytohormones. Mutant alleles *adf9-1* and *adf9-2* showed a 95% and 50% reduction in transcript levels, respectively. Compared to wild-type, mutant seedlings and plants were significantly smaller and adult mutant plants had decreased numbers of lateral branches, a reduced ability to form callus, and contained excessive F-actin bundles within cells. The mutants flowered early during long-day light exposure, but not during short days. *adf9-1* showed a several-fold lower expression of *FLOWERING LOCUS C (FLC)*, a master repressor of the transition to flowering, and increased expression of *CONSTANS* an activator of flowering. *FLC* chromatin from *adf9-1* plants contained reduced levels of histone H3 lysine 4 trimethylation and lysine 9 and 14 acetylation, as well as increased nucleosome occupancy consistent with a less active chromatin state. The likelihood that ADF9 mediates both nuclear and cytoplasmic processes within the SAM is discussed in the context of a simple model.

INTRODUCTION

The actin-based cytoskeleton plays an essential role in plant and animal development (Jacinto and Baum, 2003; Mathur, 2004; Pawloski et al., 2006). Actin filaments and bundles dynamically contribute to the programming of organ, tissue, and cell development by facilitating the assembly of various cellular structures. Actin's role in cell polarity and division plane determination is particularly important in plants, where cells do not migrate during multicellular organ development. Actin also has alternative nuclear roles controlling gene expression at the levels of chromatin remodeling and transcription (Bettinger et al., 2004; Visa, 2005; Miralles and Visa, 2006). Control of actin function is complicated by the expression of hundreds actin-binding proteins (ABPs) (Cvrckova, 2000; Meagher and Fechheimer, 2003), some of which participate in actin's nuclear activities (Bettinger et al., 2004).

The actin depolymerizing factors (ADFs) and closely related cofilins in vertebrates are among the most highly expressed ABPs that regulate actin dynamics. In the cytoplasm, ADFs bind F-actin to alter its helical twist and bind actin monomers in response to diverse stimuli, with the overall effects of enhancing actin filament turnover and actin filament assembly (Bamburg, 1999). ADFs and Cofilins also can be found in the nucleus and participate in the nuclear import of actin (Bamburg, 1999; Ruzicka et al., 2007). Via their role of shuttling actin into the nucleus, ADFs might participate in the chromatin-level control of gene expression and perhaps in the epigenetic determination of cell fate. A theme emerging from data on nuclear activities for actin and ABPs like ADF is that there may be essential "crosstalk" between the nuclear and cytoplasmic

compartments (Minakhina et al., 2005). This communication could provide both compartments with important dynamic cues as to the status of expanding and dividing cells and the developing organism.

In both plants and mammals the ADFs are encoded by an ancient gene family. The Arabidopsis ADF family is comprised of 11 gene members in several divergent classes (Maciver and Hussey, 2002). Arabidopsis *ADF9* (At 4g34970) is weakly expressed in all vegetative tissues, but is stronger in shoot apical meristem (SAM) and root sub-apical region, trichomes, and callus (Ruzicka et al., 2007). Herein, we have characterized strong and weak knockdown alleles of *ADF9* and shown the defective plants had dramatic alterations in multicellular development. Most of the observed phenotypes might be ascribed to altered cytoplasmic cytoskeletal activities affecting the meristem and shoot development. However, both alleles flowered early relative to the wild-type *Arabidopsis thaliana* Columbia ecotype and transcripts for transcription factors known to control the transition to flowering in the apical meristem, such as *FLOWERING LOCUS C (FLC)* and *CONSTANS (CO)* (Putterill et al., 1995; Michaels and Amasino, 1999), were significantly mis-regulated in *adf9-1*. The structure of chromatin at the *FLC* locus was in a more repressed state in *adf9-1*, in terms of both histone modification and nucleosome occupancy. Our data suggest that *ADF9* has both cytoplasmic and nuclear functions affecting development.

RESULTS

ADF9-defective alleles

Two independent *ADF9* insertion mutant alleles, *adf9-1* and *adf9-2,* were isolated in the *Arabidopsis* Columbia ecotype. They each contained a T-DNA insertion that mapped within the second intron as diagrammed in **Figure 1**. The insertion in *adf9-1* was located 78 bp downstream from the splice donor site and deleted 13 bp of downstream sequences from intron 2. The insertion in *adf9-2* was located 114 bp from the splice donor site and deleted 44 bp from intron 2. Hence, the deleted regions in *adf9-1* and *adf9-2* do not overlap. *ADF9* mRNA levels were assayed in the two mutants relative to the levels of *18S* rRNA and normalized to wild-type in multiple plant samples using quantitative Real Time Polymerase Chain Reaction (qRT-PCR). *ADF9* transcript levels were 95% to 99% reduced in *adf9-1,* but only 50% reduced in *adf9-2*. Thus, *adf9-1* is essentially a null allele, while *adf9-2* is a weak knockdown allele. Similar reductions in relative *ADF9* transcript levels were obtained when these qRT-PCR data were normalized to total input RNA or to actin *ACT2* or ubiquitin *UBQ10* mRNAs instead of 18S rRNA.

Developmental phenotypes of *ADF9*-defective alleles

The *adf9-1* and *adf9-2* alleles displayed similar pleiotropic defects in growth and development as shown in **Figure 2**. Fourteen days following germination, homozygous mutant seedlings of the two alleles were reduced 2-fold and 1.5-fold in size and fresh weight, respectively, in comparison to wild-type, as quantified in **Figure 3**. Both mutants

showed increased apical dominance, revealed by fewer lateral branches (**Figure 2B and 3B**). For example, nine days after bolting the mutants generally had two to three lateral branches, while wild-type had four to five. Although the *adf9* defective lines had fewer lateral branches, the length of individual lateral branches was longer, such that the total length of all lateral branches was nearly indistinguishable among mutants and wild-type (not shown).

The *adf9-1* and *adf9-2* alleles flowered approximately 16 and 18 days after germination, respectively, compared to 22 days for wild-type Columbia controls that were germinated on soil and grown under long-day conditions: 16 hr of light and 8 h of darkness. For the null allele, *adf9-1*, the inflorescence first emerged with only 7 rosette leaves compared to 10 leaves for *adf9-2* and 12 leaves for wild-type Columbia. For the *adf9-1* allele, the accelerated transition to flowering resulted in slightly dwarfed adult plants. Surprisingly, no significant differences in seed set were observed in the mutants relative to wild-type. When *adf9-1* plants were grown under short-day conditions, 9 hr of light and 15 h of darkness, they flowered with the same range of time and with the approximately same leaf number as wild-type (**Figure 2D**). Therefore, the defect in flowering time transition appeared to be photoperiod dependent.

Genetic Complementation and Overexpression

A2pt::ADF9, a construct overexpressing *ADF9* cDNA from a strong constitutive actin *ACT2* expression cassette (**Figure 1B**)was introduced into *adf9-1* plants. This complementation experiment was performed to confirm that the phenotypes observed

for the *adf9-1* allele were due entirely to the disruption of the *ADF9* gene and test the effect of overexpressing ADF9. The *A2pt::ADF9* construct quantitatively complemented all *adf9-1* morphological phenotypes. Seedling size, apical dominance, and flowering time were indistinguishable from wild-type in the complemented lines as quantified for a single representative line in **Figure 3**. The *A2pt::ADF9* transgene produced extremely high levels of the *ADF9* transcript, often several hundred-fold higher than wild-type as shown for one line (**Figure 1C)**. This high expression is consistent with the high levels of expression achieved with the *A2pt* expression cassette in previous studies (Li et al., 2005). This strong overexpression of *ADF9* mRNA did not produce dominant morphological phenotypes that differed from wild-type when expressed in the *adf9-1* or wild-type backgrounds (**Figure 3**).

Alterations to the F-actin cytoskeleton in ADF9 deficient plants

Given ADF's role in remodeling actin filaments, it seemed likely that the structure of the actin-based cytoskeleton would be altered in the *adf9-1* mutant. We transformed wild-type and *adf9-1* mutant plants with an F-actin reporter construct, *ABD2-GFP,* which was produced by a fusion of the fimbrin actin binding domain 2 to green fluorescent protein (Wang et al., 2004). We characterized the morphology and organization of the actin cytoskeleton in trichomes, because the fluorescence of *ABD2-GFP* is visualized with little background in trichomes and *ADF9* is expressed in this cell type (Ruzicka et al., 2007). **Figure 4** shows the actin cytoskeleton in wild-type and *adf9-1.* In wild-type trichomes, the actin cytoskeleton was organized into a network composed mostly of fine

filaments and included some thicker bundles primarily extending longitudinally along the axis of trichome elongation (**Figure 4A and B**). In the trichomes of *adf9-1* plants, the actin cytoskeleton was longitudinally organized, similar to wild-type, but the filaments had a significantly altered morphology. Most of the actin filaments were organized into exceptionally thick bundles (**Figure 4C and D**) and very few fine filaments were detected in comparison to wild-type. We did not observe an altered trichome cell morphology such as altered size or branching in the mutant. Normal trichome development may proceed in *adf9-1* due to the wild-type orientation of the actin filaments and the redundant activities of other ADF family members in trichomes (Ruzicka et al., 2007).

ADF9 expression is induced by hormones

Although weakly constitutive in most vegetative tissues, *ADF9* is more strongly expressed in callus, young seedlings, and the SAM, and *ADF9* transcript levels are dramatically increased by treatment with auxin (www.genevestigator.ethz.ch)(Zimmermann et al., 2004; Ruzicka et al., 2007). These data suggest that *ADF9* expression patterns could be affected by plant growth regulators. An *ADF9* reporter was constructed, *ADF9p::GUS,* fusing the *ADF9* promoter and enhancer intron to b-glucuronidase (*GUS*). *ADF9p::GUS* was transformed into wild-type plants as shown in **Figure 5** (Ruzicka et al., 2007). *ADF9p::GUS* plants were transferred to growth media supplemented with various phytohormones for 20 h and then histochemically stained for GUS expression for 45 min. The *ADF9p::GUS* plants

displayed a strong increase in reported gene expression in the root tip meristem, trichomes, and SAM in response to 2,4-dichlorodiphenoxyacetic acid (2,4-D) and indoleacetic acid (IAA), and a smaller increase in expression in these tissues in response to kinetin, gibberellic acid (GA3), and abscisic acid (ABA). The strong to moderate induction of this reporter in the sub-apical tissues of the root that occurred in response to hormone treatments is shown in **Figure 5B to 5G**. These staining patterns and their intensities are similar to untreated samples stained for 18 h (Ruzicka et al., 2007). These data suggest phytohormones play a role in the regulation of endogenous *ADF9* levels.

Callus induction from *ADF9*-defective tissue

Given that *ADF9* is induced by the application of multiple hormones and that mutants in the phytohormone-induced actin *ACT7* were defective in callus formation, we considered that *ADF9*-defective plants might exhibit growth defects with tissue explants grown on callus-inducing media. To test this proposal, identically sized root sections were removed from vertically grown wild-type and *adf9-1* mutant plants and placed on media containing 2,4-dichlorophenoxyacetic acid (2,4-D) and kinetin. The untreated mutant and wild-type roots were indistinguishable in morphology when examined under a dissecting microscope. After four weeks, the wild-type callus tissue consisted of large clumps of cells, illustrated in **Figure 5H,** that were comprised of multiple cell types (not shown). The *adf9-1* mutant exhibited a significant difference in callus morphology compared to wild-type, with fewer aggregates of large cells and more and longer root

hair-like cells (**Figure 5I**). Additionally, the average fresh weight of the *adf9-1* callus samples was less than half of wild-type callus samples (**Figure 3D**). The *A2pt::ADF9* cDNA expression construct restored the wild-type callus growth rate (**Figure 3D**) and morphology to the *adf9-1* mutant (not shown).

ADF9 is a repressor of flowering under long-day conditions

Given the aberrant F-actin structure observed in the *adf9-1* mutant (**Figure 4**), it was conceivable that the early flowering phenotype was due to defective actin cytoskeleton in the SAM accelerating development of the inflorescence (Meagher et al., 1999; Carraro et al., 2006). However, the early flowering phenotype partially resembled that of several chromatin remodeling mutants negatively affecting *FLOWERING LOCUS C* (*FLC*) transcript expression in the meristem via changes in the structure of chromatin at the *FLC* locus (He and Amasino, 2005). Therefore, we considered an alternative explanation for the early flowering of *ADF9*-defective plants. FLC is a master repressor of the transition from vegetative to reproductive growth in Arabidopsis. FLC represses FT and SOC, which function to activate AP1 and LFY, and advance flowering, as summarized in **Figure 6.** We reasoned that appropriate levels of ADF9 protein might be required to shuttle actin into the nucleus, where actin participates in chromatin remodeling complexes or transcriptional machinery that control the expression of flowering time regulators, like *FLC*. Alternatively, ADF9 might have unknown actin-independent roles in regulating gene expression.

To test the proposal that ADF9 plays a role in controlling gene expression, we examined the *adf9-1* mutant and wild-type plants for the relative expression of *FLC*. We observed that *FLC* transcript levels in 10-day-old seedlings were four-fold lower in the mutant than wild-type (**Figure 6B).** The relative quantities of transcripts in each sample were first measured with respect to 18S rRNA and then normalized to target transcript levels in wild-type. In addition, transcript levels from the downstream flowering activators, *FT*, *SOC1*, and *LFY*, were up-regulated 1.8-, 2- and 4-fold (**Figure 6C**), respectively in *adf9-1,* consistent with loss of FLC expression (He and Amasino, 2005). Mutant lines complemented by the overexpression of *ADF9 cDNA (***Figure 3C)** not only flowered at normal times but they showed *FLC* transcript levels that were restored to those observed in wild-type controls, but not significantly higher than wild-type as show for three complemented lines (**Figure 6B**). Thus, the reduction in *FLC* levels and increases in the downstream flowering activators appear to account for the early flowering phenotype of the *adf9-1* mutant (Michaels and Amasino, 1999; He and Amasino, 2005).

Considering that *ADF9*-defective plants flowered early under long-day but not short-day growth conditions, it was possible that ADF9 also acted in the photoperiod-dependent flowering pathway. The transcription factor CONSTANS (CO) activates *FT* and *SOC* in response to long-day growth conditions (**Figure 6A**). Although there is considerably less evidence than for *FLC*, the *CO* locus also may be controlled at the level of chromatin remodeling (Gaudin et al., 2001). We observed a 1.6-fold increase in the levels of *CO* transcripts in the *adf9-1* mutant in 10-day-old seedling (**Figure 6C**).

These data are consistent with ADF9 functioning as a repressor of *CO* and playing a role in the photoperiod-dependent flowering pathway.

ADF9 is essential to maintain normal chromatin structure at *FLC*

A number of defects in chromatin remodeling machinery cause the down-regulation of *FLC* gene expression (He and Amasino, 2005). Therefore, it seemed reasonable to propose that the reductions in *FLC* expression in *adf9-1* seedlings were due to the inability of ADF9 to contribute to normal chromatin remodeling at *FLC*. We performed a series of Chromatin Immuno-Precipitation (ChIP) assays to look for differences in histone modifications and histone variant subunits deposited in *FLC* chromatin, comparing wild-type and *adf9-1* seedlings grown under long-day conditions. High levels of histone H2A.Z occupancy are observed at the 5´ and 3´ ends of the *FLC* transcript coding region, and mutations that cause significant loss of H2A.Z from these regions are associated with dramatically decreased *FLC* expression and early flowering (Deal et al., 2007). Decreased levels of histone H3 trimethylation at lysine 4 (H3K4Me3) and H3 acetylation at lysine 9 and 14 (H3K9K14Ac) flanking the promoter region of *FLC* are associated with lower levels of *FLC* expression (He and Amasino, 2005; Martin-Trillo et al., 2006).

ChIP assays were performed on formalin fixed and sheared chromatin, using antibodies to H2A.Z, H3K4Me3, and H3K9K14Ac to enrich nucleosome bound DNA. We assayed three sites at the 5´ end of the *FLC* locus located in the promoter (FL1), the transcription start site (FL2), and first intron (FL3) by quantitative PCR (qPCR) of the

precipitated DNA, as shown in **Figure 7**. H2A.Z deposition at the two downstream sites in *FLC* (Primer sets FLC2 and FLC3) was similar to wild-type, while H2A.Z occupancy in the upstream promoter site (Primer set FLC1) was increased 70% above wild-type (**Figure 7B**). In the *FLC* promoter an inverse correlation has been reported between H2A.Z occupancy and gene expression in some genotypes and tissues (Deal et al., 2007). A 30% to 45% drop in the levels of H3K4Me3 was observed at two of the three sites in *FLC* (Primer sets FLC1 and FLC3) (**Figure 7C**). Similarly, a 35% to 50% drop in the levels of H3K9K14Ac was observed at all three sites in *FLC* in the *adf9-1* mutants relative to wild-type (**Figure 7D**).

Increased nucleosome density, particularly in the promoter of a gene, is often associated with decreased rates of transcription. Therefore, we performed an assay of nucleosome occupancy within the *FLC* locus in *adf9-1* and wild-type using quantitative PCR. Nucleosomes prepared from 10-day-old Arabidopsis seedlings and digested with increasing levels of micrococcal nuclease contained DNA fragments of the sizes expected for tri- (450 bp), di- (~300 bp) and mononucleosomes (~150 bp) with a moderate nuclease concentration (**Figure 8**). Primarily monosomal 150 bp DNA was observed at a 15-times higher nuclease concentration. Quantitative PCR primers were designed to amplify 11 nested products of approximately100 bp overlapping by approximately 50 bp from the monosomal preparation giving 50 bp resolution to the assay (**Figure 8B**). The 550 bp region assayed covered the start of transcription (products 8, 9, 10, 11) and extended 350 bp upstream into the promoter. The nucleosome scanning assay of wild-type chromatin (**15 u, Figure 8A**) revealed an

approximately 300 bp nucleosome poor region (i.e., low product amplification) centered 100 bp upstream of the start of transcription (products 4 through 9, **Figure 8C**). This region was flanked by two nucleosome protected regions that amplified efficiently (products 2, 3, 10, 11 in **Figure 8C**). The *adf9-1* mutant revealed 50% to 300% higher levels for five of the six *FLC* products amplified (e.g., products 4, 5, 6, 8, 9) in the nucleosome poor region relative to wild-type. Thus, nucleosome density in the nucleosome poor region appears much higher in the *adf9-1* mutant than in wild-type.

DISCUSSION

Distinct functions for ADF9 in the shoot apical meristem

Defects in organ initiation, growth rates, and flowering time in the *ADF9* mutants are all consistent with a disruption of activities in the SAM (Guyomarc'h et al., 2005; Carraro et al., 2006). Among the 11 diverse members of Arabidopsis *ADF* family there is considerable potential for functional redundancy in the SAM. The *ADF5* and *ADF9* genes comprise class III ADFs, however, the ADF9 isovariant differs from ADF5 in 29 of its 139 amino acids, representing considerable divergence for proteins in the same class (Ruzicka et al., 2007). While both genes are expressed in the SAM, each has its own distinct expression phenotype. *ADF9* is moderately expressed in the SAM and induced by several phytohormones, while *ADF5* is not believed to be hormone responsive and is expressed more broadly in vegetative tissues. In addition to *ADF9* and *ADF5*, four vegetative class I *ADF* genes (*ADF1, 2, 3, 4*) and the constitutive class IV *ADF6* are expressed in the SAM, all more strongly than *ADF9* (Ruzicka et al., 2007).

The expression of seven ADFs from three divergent classes in the SAM suggests there must be redundancy among their activities. However, the strong SAM-dependent phenotypes produced by defects in *ADF9* argue that this isovariant is functionally distinct from the other ADF isovariants expressed in the SAM.

The F-actin cytoskeleton was abnormal in trichomes of the *adf9-1* mutant and is most likely abnormal in other cell types where ADF9 is expressed. Considering the roles that the ADF-controlled actin cytoskeleton plays in elaborating normal pathways of differentiation, loss-of-function mutations in essential SAM-specific ADFs should be expected to cause developmental defects (Jurgens, 2005). The actin cytoskeleton is essential to construction of the preprophase band that positions the division plane and determines cell polarity (Gallagher and Smith, 2000; Smith, 2001). These are arguably the most important factors modulating organ initiation and growth rate. Each of the phenotypes observed for the *adf9-1* allele might be attributed to changes in the cytoplasmic actin cytoskeleton within critical layers of cells in the SAM that determine leaf and stem growth rates and the initiation of lateral branches and the inflorescence (Castellano and Sablowski, 2005; Carraro et al., 2006). Organ initiation and outgrowth from the SAM may be modeled as occurring in three stages (**Figure 9).** ADF9-related defects in the cytoskeleton of SAM cells should be expected to alter stage two, the initiation of organ primorida; and stage three, the establishment the organ polarity and outgrowth. Furthermore, auxin, cytokinin, and GA all affect organ development from the SAM (Castellano and Sablowski, 2005; Carraro et al., 2006), linking the observed hormone-induced expression of *ADF9* with SAM functions. In addition, these hormones

are known to stimulate cytoskeletal dynamics and membrane assembly both in the formation of the cell plate required for cytokinesis and in subsequent cell expansion, leading to outgrowth of new organs (Steps 2 & 3, **Figure 9A**) (Jurgens, 2005). For example, GA stimulates activators of the transition to flowering (**Figure 6A**), and this pathway may ultimately stimulate growth via activities in the cytoskeleton. The stimulation of *ADF9* expression by hormones might be essential to restructuring the cytoskeleton in appropriate meristem cells during organ initiation.

Nuclear roles for actin and ADF

After decades of skepticism, it is now widely accepted that conventional actin and some associated ABPs like ADF/cofilin have distinct functional roles in the nucleus in addition to their cytoplasmic functions (Bettinger et al., 2004; Visa, 2005; Miralles and Visa, 2006). Recent evidence suggests that nuclear actin is a stoichiometric component of most chromatin remodeling complexes isolated from yeast and humans (Olave et al., 2002; Mizuguchi et al., 2004; Ruhl et al., 2006), that it participates in transcriptional initiation via interactions with RNA polymerase (Pol) I, II, and III, that it is localized to Cajal bodies with a likely role in RNA processing, and that it functions in the export of ribonuclear particles (RNPs) and mRNAs. In stressed mammalian cells, the nuclear import of ADF appears to be essential to the nuclear import of actin (**Figure 9B, 9C**) (Ohta et al., 1989; Abe et al., 1993; Nebl et al., 1996; Bamburg, 1999; Pendleton et al., 2003). For example, ADF antibodies microinjected into the cytoplasm block the nuclear import of actin. The phosphorylated form of ADF is thought to be inactive in cytoplasmic

activities, but is preferentially localized to the nucleus, where its activities are poorly defined (Nelb et al., 1996). The phosphorylation state of ADF is highly regulated by specific kinases and phosphatases, and hence, the nuclear import of ADF is highly regulated, perhaps to control the import of actin (Sarmiere and Bamburg, 2004; Tanaka et al., 2005a; Tanaka et al., 2005b). In addition to these interactions with actin, human cofilin 1 also functions as a repressive cofactor regulating the activities of glucocorticoid receptor (Ruegg et al., 2004). We have recently reported that subclass 1 ADF isovariants are localized to the cytoplasm and nucleus of most Arabidopsis leaf interphase cells (Ruzicka et al., 2007). Lacking an ADF9-specific antibody, we have not yet examined the cytoplasmic and nuclear distribution of ADF9. Thus, particular plant ADF isovariants might have full-time nuclear roles, in addition to activities in stressed cells. In summary, data from diverse kingdoms strongly suggest that ADF is essential to nuclear actin import and might have actin-independent nuclear activities. However, these published studies generally lack the genetic evidence needed to demonstrate that ADF nuclear functions are essential to cell viability or development or, with a few exceptions, that they affect the expression of important target genes in the nucleus.

These data on the roles for actin and ADF in the nucleus and our data on the role of ADF9 in development must be considered in light of the mounting evidence that critical steps in leaf, shoot, and floral organ initiation from the SAM are controlled at the level of chromatin remodeling (Guyomarc'h et al., 2005; He and Amasino, 2005; Williams and Fletcher, 2005). The vegetative SAM gives rise not only to leaves, but to inflorescence meristems and floral meristems, and critical steps in each developmental

phase are regulated at the level of chromatin structure. The seedling, lateral branch, and flowering time phenotypes of *ADF9*-defective plants therefore could be ascribed to chromatin remodeling defects that affect the earliest stage of organ development, when morphogenic information is exchanged among cells within the SAM (Stage one, **Figure 9A)**. In other words, it seemed possible that ADF9-dependent developmental signaling and its control by phytohormones might be linked to nuclear activities affecting chromatin structure, gene expression, and morphogenic gradients in the SAM.

We explored the role of ADF9 in chromatin-level control of early flowering, because there are robust data demonstrating epigenetic controls over the activity of the *FLC* locus and FLC's role in the repression of the transition to flowering. In particular, all four measurements of chromatin structure at *FLC* showed differences in the *adf9-1* mutant from WT that may be logically linked to a less permissive chromatin state. Some of these activities may be linked to ADF's role in actin nuclear transport. First, Arabidopsis encodes subunits of a plant counterpart of the yeast SWR1 and human SRCAP complexes, which act to deposit H2A.Z into chromatin (Choi et al., 2005; Deal et al., 2005; Choi et al., 2007; Deal et al., 2007; March-Diaz et al., 2007). The yeast and human SWR1 complexes contain actin subunits, and hence, might require ADF-co-transport of actin for activity (Olave et al., 2002). Defects in some of these subunits result in inefficient histone isovariant H2A.Z deposition within and decreased expression of the *FLC* locus (Deal et al., 2007), arguing that a plant SWR1 complex is essential to normal *FLC* expression. Genotypic differences and developmental states that lower the transcription of *FLC* in wild-type plants can result in increased H2A.Z deposition at the

5´promoter proximal region and 3´end of the *FLC* locus (Deal et al., 2007). A significant increase in H2A.Z deposition was observed for the promoter proximal site examined in the *adf9-1* mutant. This inverse correlation between *FLC* expression and H2A.Z deposition may be indicative of a shift in the balance between SWR1-mediated deposition of H2A.Z and loss of H2A.Z from chromatin as a result of nucleosome disruption by RNA polymerase (Deal et al., 2007). Thus, when the rate of transcriptional initiation is reduced, H2A.Z tends to accumulate to higher levels in chromatin. Second, mutants defective in subunits of the Arabidopsis PAF1-like chromatin-remodeling complex flower early (He et al., 2004; Oh et al., 2004; Kim and Michaels, 2006). It is not known if PAF1 contains an actin subunit, but PAF1 interacts intimately with RNA Pol II and active Pol II protein is tightly associated with nuclear actin (Miralles and Visa, 2006). Among its activities, the PAF1 complex is responsible for trimethylation of histone H3 at lysine 4 (H3K4me3). *FLC* transcript levels are positively correlated with higher levels of H3K4me3 at the *FLC* locus (Oh et al., 2004; He and Amasino, 2005). The levels of H3K4me3 flanking the transcription start site of *FLC* were significantly decreased in *adf9-1* plants, suggesting that ADF9 might play a direct or indirect role in the activity of PAF1 or Pol II to reduce *FLC* expression. Third, *FLC* transcript levels and delayed flowering are also positively correlated with acetylation of histone H3 at lysine 9 and 14 (H3K9/K14Ac) and negatively correlated with deacetylation of H3 within *FLC* nucleosomes (He et al., 2003; Ausin et al., 2004; He and Amasino, 2005). The acetylation and deacetylation of H3 takes place via the activities of several, mostly uncharacterized, complexes. The NUA4 acetyltransferase complex that is known to

carry out H3 and H4 acetylation contains an actin subunit, while other less-well characterized chromatin remodeling complexes controlling acetylation levels are intimately linked with Pol II (Olave et al., 2002; Pederson and Aebi, 2005; Visa, 2005; Miralles and Visa, 2006). There were significant reductions in the level of H3K9/K14Ac at all three sites assayed at the *FLC* locus in *adf9-1* mutant plants, suggesting that ADF9-activities mediate acetylation of H3 in *FLC* chromatin.

Fourth, a 300 bp nucleosome depleted region was identified within the *FLC* promoter located immediately upstream of the transcriptional start site. Mononucleosome enriched preparations from the *adf9-1* mutant showed significantly decreased nuclease sensitivity across this region of the *FLC* locus, but not in flanking sequences, relative to wild-type. These data are consistent with the location established for nucleosome free regions in a large number of expressed yeast genes (Yuan et al., 2005) and increased nucleosome occupancy in these regions in repressed genes (Zhang and Reese, 2007). Decreased nuclease sensitivity of *FLC* DNA in this region in the *adf9-1* mutant likely resulted from increased nucleosome occupancy associated with reduced rates of *FLC* transcription. Hence, all four chromatin assays suggest that in ADF9-deficient plants the structure chromatin at *FLC* is altered and these changes are consistent with decreased *FLC* expression. The precise mechanisms and machinery through which ADF9 contributes to these changes in chromatin structure will be the subject of future studies.

From this evidence, we are proposing that ADF9 might affect the remodeling of chromatin at the *FLC* locus. ADF9 also might play indirect roles in controlling gene

expression that, for example, resulted in changes in the structure of *FLC* chromatin. A simple model for the networked cytoplasmic and nuclear activities of ADF9 within a cell is illustrated in **Figure 9** (Plates B and C). Our data support a model in which ADF9 both remodels actin filaments in the cytoplasm and shuttles actin monomers into the nucleus. By controlling the actin pool in the nucleus, ADF9 might be essential to actin's participating in chromatin remodeling machines, the transcriptional apparatus, and nuclear transport. Left open for consideration is the likely role that the phosphorylation of ADF9 plays in controlling actin nuclear transport and the possibility that ADF9 has its own distinct functions in the nucleus apart from actin. In addition, it is not yet clear how redundant the cytoplasmic and nuclear activities of ADF9 are with those of the other numerous coexpressed Arabidopsis ADF isovariants.

Dissection of the flowering time signaling pathway

Based on flowering time phenotypes and the expression of *FLC, FT, SOC,* and *LFY* transcripts in mutant and/or complemented plant lines, it is logical to model ADF9 as an indirect activator of *FLC*, and hence, a repressor of flowering time (**Figure 6A**). Via the transport of actin into the nucleus, ADF9 might be essential to the activity of chromatin remodeling complexes that activate *FLC* expression. Consistent with this indirect role for ADF9, the overexpression of *ADF9* cDNA in the *adf9-1* complemented lines did not result in the overexpression of *FLC* or late flowering. Note that the overexpression of *FLC* is known to dramatically delay flowering (Michaels and Amasino, 1999). Actin-containing chromatin remodeling complexes are typically composed of ten

or more subunits (Olave et al., 2002). Thus, increasing only the actin concentrations in the nucleus might not be expected to alter the concentration or activities of such complex machines.

Some aspects of the ADF9-deficient early flowering phenotype cannot be reconciled with current knowledge about the flowering time signaling pathway. In particular, the photoperiod-dependent flowering pathway in Arabidopsis is thought to function independent of FLC levels, typically through CO and its downstream targets, *FT* and *SOC1* **(Figure 6A)** (Yanovsky and Kay, 2002; Valverde et al., 2004). Thus, ADF9 is the only known repressor of the photoperiod-dependent flowering pathway that acts at least in part via *FLC*. The levels of *CO, FT, SOC1,* and *LFY* transcripts were significantly increased, while *AP1* levels were unaffected. This complex gene expression pattern may account for the photoperiod dependency of the early flowering time phenotype. Thus, ADF9 may act as a novel repressor of photoperiod-dependent early flowering by networking regulation through both *CO* and *FLC.* Future genetic and biochemical studies will attempt to dissect these activities.

Conclusion

ADF9 is a member of the moderately large Arabidopsis *ADF* gene family that encodes a distinct ADF protein isovariant. *ADF9* deficiency produced morphological and cytoskeletal defects in growth, branching, and F-actin filament structure consistent with its role in remodeling the actin cytoskeleton in the cytoplasm. However, we also demonstrated that ADF9 deficiency produced early flowering and gene expression

phenotypes consistent with defects in nuclear activities in the SAM. Our genetic and biochemical data raise the more general question: Does altering the F-actin cytoskeleton or the concentrations of actin, ADF, and other ABP isovariants in the cytoplasm commonly lead to changes in the control of gene expression in the nucleus and subsequent defects in multicellular development? We present evidence herein that the answer may be "yes," at least for the change in flowering time control in *adf9* mutants, which resulted from reduced expression of the transcription factor *FLC.* This general question creates a serious conundrum for genetic analyses of the cytoskeleton, because it creates doubts about the assumption that other multicellular development phenotypes reported for actin- and ABP-defects result simply and directly from cytoplasmic defects. For example, defects in other plant ABPs and actins that produce phenotypic changes in cell size and cell numbers affecting organ size and shape and defects in organ aging might all result from altered nuclear activities and not defects in the cytoplasmic cytoskeleton (McKinney et al., 2001; Gilliland et al., 2002; Gilliland et al., 2003; Cheung and Wu, 2004; Ketelaar et al., 2004; Deeks et al., 2005; Hussey et al., 2006; Ruzicka et al., In prep). Thus, understanding the networked communication of cytoskeletal proteins between the nuclear and cytoplasmic compartments is imperative to understanding the diverse roles of actin binding proteins like ADF.

MATERIALS AND METHODS

Plant materials and growth conditions

Mutants in the *ADF9* gene (At4g34970) were obtained from TAIR (www.arabidopsis.org) *adf9-1* (SALK_056064) and *adf9-2* (#Garlic_760_A03.b.1.a.Lb3Fa). Both T-DNA insertion mutants were in an *Arabidopsis thaliana* Columbia ecotype genetic background. The mutants were backcrossed twice with wild-type Columbia and examined for a single insertion before phenotypic analysis. Experiments were performed on T4 or T5 generation selfed plants. All controls were performed with the Columbia ecotype. Seeds from wild-type, *adf9-1,* and *adf9-2* plants were sown directly into soil (Fafard). After 2 days at 4ºC, they were moved to growth chambers maintained at 22ºC under long-day (16 h light and 8 h dark) or short-day (9 h light and 15 h dark) photoperiod. Ten days after germination, the seedlings were transferred to 2.5 in. pots and grown under the same conditions. For experiments seeds were sterilized and plated on MS phytoagar (Murashige and Skoog, 1962) supplemented with 1% sucrose, stratified at 4ºC for 2 days, and grown at 22ºC. It should also be noted that an *FLC* null mutant, *flc-3* (Michaels and Amasino, 1999), flowered early under the long-day growth conditions we used in these experiments.

Determination of genotypes by PCR

Allele and gene specific primers were designed to amplify identifying fragments from the wild-type *ADF9*, *adf9-1* or *adf9-2* alleles. A 767 bp fragment for the ADF9 allele was amplified using the sense primer ADF9-5´utrS (5´-GAAAATATTTTGGATGATTGGTATATA) and antisense primer ADF9-3´utrA (5´-

ACGATATAACTCCAGTTATGTGTTGTGA). A 401-bp fragment of the *adf9-1* mutant allele was amplified with a left border T-DNA primer LBaI (5´-TGGTTCACGTAGTGGGCCATCG) and the antisense primer ADF9-3´urtA. A 366 bp fragment of the *adf9-2* mutant allele was amplified with a left border T-DNA primer LB3 (5´-TAGCATCTGAATTTCATAACC) and the sense primer ADF9-5´urtS. The PCR products of both mutant alleles were sequenced to confirm the exact location of the T-DNA insertion. Homozygous mutant plants derived from two backcrosses to wild-type were genotyped by PCR to verify the correspondence of homozygous genotype with various phenotypes. The DNA used as a template for genotype and sequence determination was prepared by a modified rapid alkali DNA screening method (Gilliland et al., 1998) or with CTAB according to Doyle et al. (1990).

Flowering time and inflorescence phenotypes

The total number of rosette leaves at the time in which the first inflorescence could be distinguished from leaf primordia was recorded as a measure of flowering time. At least 24 plants were assayed to determine the flowering time and other phenotypes of each plant line, with four biological replicates to confirm the observations. At 21 days after germination the length of the secondary branches was measured and recorded. At 28 days the number of primary inflorescences was recorded. Gene expression assays to examine the flowering time signaling pathway were performed on 10- and 14-day-old seedlings germinated and grown vertically on MS agar.

Mutant complementation and ADF9 overexpression

Complementation and overexpression studies were carried out by first cloning the 426 bp *ADF9* cDNA protein encoding sequence into the *Nco*I/*Bam*HI replacement region of actin *ACT2* promoter and terminator expression cassette pA2pt (Kim et al., 2005). An *Nco*I site containing the ATG start codon and a *Bam*HI site following the stop codon were introduced to the *ADF9* coding sequence by mutagenic PCR. The fusion between the expression cassette and ADF9 was subcloned into the pCambia binary vector (Hajdukiewicz et al., 1994) using the flanking *Kpn*I and *Sac*I sites to make *pA2pt::ADF9* in *E. coli. pA2pt::ADF9* was transformed into the *Agrobactirium* strain C58C1. Plants were transformed by *Agrobacterium*-mediated vacuum infiltration method (Bechtold and Pelletier, 1998). Complemented plants were selected by plating the seeds on germination medium (0.5x MS, 1% sucrose, phytagar germination medium containing 50 mg^{-1} hygromycin) and after 3 days transferred to soil. Multiple independent T2 lines were generated.

GFP reporter for F-actin

We transformed wild-type and *adf9-1* mutant plants with the F-actin reporter *ABD2-GFP* (Wang et al., 2004). Multiple lines of positive transformants were selected on hygromycin and vertically grown on 0.5 MS agar plates. Microfilaments were visualized in trichomes as described previously (Wang et al., 2004) using a Leica confocal laser-scanning microscope (TCS-SP2, Heidelberg, Germany).

Assays of GUS after treatment with various phytohormones

An *ADF9 promoter-b-glucuronidase (GUS)* reporter fusion (*ADF9pt::GUS)* was transformed into wild-type Columbia and a single insertion homozygous line generated by selfing as described previously. This line was subjected to treatment with various phytohormones and assayed for GUS enzyme expression as modified from Jefferson et al. (1987). Fourteen-day-old seedlings were transferred from vertically grown plates to soft agar plates plus hormones and allowed to grow for an additional 20 h. Hormone stocks were each prepared at 100 mM in DMSO. GUS expression was assayed by incubating seedlings in 50 mM NaPO4 pH 7.0, containing 0.5% Triton X-100, 0.5 mM X-gluc (Jersey Lab Supply, Livingston, NJ), 0.5 mM $K_4(Fe(CN)_6)$ for 45 min at 37ºC. Seedlings were removed from solution and bleached in successive washes of 70% ethanol before being photographed using a Leica dissecting microscope (Leica Microsystems) equipped with a Hamamatsu CCD camera.

Callus phenotype

Wild-type and *adf9-1* seeds were plated on MS media and grown vertically for 2 weeks. Ten leaves (1.5 cm) and ten roots (2.5 cm long sections) of equal size were collected for both wild-type and *adf9-1* seedlings and moved to callus-inducing media supplemented with 4.5 mM 2,4-D and 25 nM kinetin (Kandasamy et al., 2001). The plates were photographed at time zero (not shown), wrapped in foil, and callus was

allowed to grow for 2 and 4 weeks. At 2 and 4 weeks the foil was removed, photographs were taken, and callus fresh weight was measured.

Real time RT-PCR analysis

RNA was isolated from 10-day-old seedlings using the RNeasy Plant Mini Kit (Qiagen, Valencia, CA, USA), and 3 μg of total RNA from each sample was transcribed into cDNA with the Super Script III kit (Invitrogen, Carlsbad, CA, USA) following the manufacturer's instructions except that incubations were performed for only 30 min and at 55ºC using oligo (dT) primer. Aliquots of the cDNA were used as template for the qRT-PCR analysis of triplicate reactions for each of three biological replicates on an Applied Biosystems 7500 Real Time PCR Instrument. Real time PCR reactions consisted of SYBR GREEN PCR Master Mix (Applied Biosystems, Foster City, CA, USA), 0.4 μM of each primer, 1:50 dilution of cDNA in a 25 μl reaction volume. Primer sets used for q RT-PCR assays of transcript levels are as follows: *ADF9* (ADF9-RTS: 5´- CTCAAA ATATAACGAAAGAACAAGAAGACA-3´, ADF9-RTA: 5´-CACTCGTCGCCGTCTTCAA-3´); *18S* rRNA (18s-RT2S: 5´-GGGGGCAATCGTATTTCATA-3´, 18S-RT2A: 5´-TTCGCAGTTGTTCGTCTTTC-3´); *ACT2* (ACT2-RTS: 5´-GATGAGGCAGGTCCAGGAATC-3´, ACT2-RTA: 5´-AACCCCAGCTTTTTAAGCCTTT-3´); *UBQ10* (UBQ-RTS: 5´-AGAAGTTCAATGTTTCGTTTCATGTAA-3´, UBQ-RTA: 5´-GAACGGAAACATAGTAGAACACTTATTCA-3´); *FLC* (FLC-RTS: 5´-CATCATGTGGGAGCAGAAGCT-3´, FLC-RTA: 5´-CGGAAGATTGTCGGAGATTTG-3´);

CO (CO-RTS: 5´-TGGCAAAACTAGACTGCATGCT-3´, CO-RTA: 5´-CCCTATATGCATAAAACCGTGGTAA-3´); *FT* (FT-RTS: 5´-GGCGCCAGAACTTCAACACT-3´, FT-RTA: 5´-CGGGAAGGCCGAGATTG-3´); *SOC1* (SOC1-RTS: 5´-AAAGCTCTAGCTGCAGAAAACGA-3´, SOC1-RTA: 5-GACCAAACTTCGCTTTCATGAGAT-3´); *LFY* (LFY-RTS: 5´-TTGTCGTCATGGCTGGGATATA-3´, LFY-RTA: 5´-GAACATACCAAATAGAGAGACGAGGAT-3´); and *AP1* (AP1-RT-S = 5´-CGCAGCAGC ACCAAATCC-3´. AP1-RT-A 5´-TGAGAAAAGGAGATGGCTGATG-3´). We used the 2^{-ddCt} method (Livak and Schmittgen, 2001) of relative quantification.

Chromatin structure assays at FLC

ChIP assays on H2A.Z deposition at the *FLC* locus were performed on sheared chromatin from 10-day-old shoots grown under long day conditions as described previously (Deal et al., 2007) using the same first three sets of *FLC* PCR primers (FLC1, 2, 3). ChIP assays for histone H3 trimethylation at lysine 4 and H3 acetylation at lysine 9 and 14 were performed identically except that the H3K4Me3 (#07-473) and H3K9K14Ac (#06-599) antibodies from Upstate (Lake Placid, NY) were used in the precipitation assays. The first two ChIP assays were normalized to a region in the *ACT2* 3´UTR and the H3K9K14 assays were normalized to a LINE2 element. The three primer pairs were describe previously (Deal et al., 2007).

Nucleosome occupancy was assayed in the promoter region of *FLC* by a modification of the method described for yeast genes by Sekinger et al. (2005) starting

with 1 g of 10-day-old whole seedlings grown under long-day length conditions. Nucleosomes were prepared by a modification of an older protocol (Vega-Palas and Ferl, 1995). The qPCR assays on nucleosomal DNA were performed using the primer pairs listed in **Table 1**. Relative quantity (RQ) data were normalized first to input DNA concentration by subtracting the raw Cycle Threshold (CT) value for *actin 2* (*ACT2*) from the Target CT value and second the results were normalized to the efficiency of PCR amplification of each primer pair performed on purified Arabidopsis DNA. This latter efficiency of DNA amplification on naked DNA varied by only two-fold among the primer pairs used in this study. qPCR was performed as above for qRT-PCR. The nucleosome preparation, qPCR assays, and calculations are detailed in the Supplemental Section.

ACKNOWLEDGEMENTS

We thank Dr. M. Kandasamy and Gay Gragson for critical reading and discussions of the manuscript and Dr. Richard Amasino for helpful discussions on flowering time experiments. This work was supported by funding from the National Institutes of Health (5RO1GM036397-22) to R.B.M.; an NIH supplement (3RO1GM036397-20S1/C103JD) to B.B; and NIH training grant (GM 07103-29) support to D.R.R., R.B.D., and L.K.-R..

REFERENCES

Abe H, Nagaoka R, Obinata T (1993) Cytoplasmic localization and nuclear transport of cofilin in cultured myotubes. Exp Cell Res **206:** 1-10

Ausin I, Alonso-Blanco C, Jarillo JA, Ruiz-Garcia L, Martinez-Zapater JM (2004) Regulation of flowering time by FVE, a retinoblastoma-associated protein. Nat Genet **36:** 162-166

Bamburg JR (1999) Proteins of the ADF/cofilin family: essential regulators of actin dynamics. Annu Rev Cell Dev Biol **15:** 185-230

Bechtold N, Pelletier G (1998) In planta *Agrobacterium*-mediated transformation of adult *Arabidopsis thaliana* plants by vacuum infiltration. Methods Mol Biol **82:** 259-266

Bettinger BT, Gilbert DM, Amberg DC (2004) Actin up in the nucleus. Nat Rev Mol Cell Biol **5:** 410-415

Carraro N, Peaucelle A, Laufs P, Traas J (2006) Cell differentiation and organ initiation at the shoot apical meristem. Plant Mol Biol **60:** 811-826

Castellano MM, Sablowski R (2005) Intercellular signalling in the transition from stem cells to organogenesis in meristems. Curr Opin Plant Biol **8:** 26-31

Cheung AY, Wu HM (2004) Overexpression of an *Arabidopsis* formin stimulates supernumerary actin cable formation from pollen tube cell membrane. Plant Cell **16:** 257-269

Choi K, Kim S, Kim SY, Kim M, Hyun Y, Lee H, Choe S, Kim SG, Michaels S, Lee I (2005) *SUPPRESSOR OF FRIGIDA3* encodes a nuclear ACTIN-RELATED PROTEIN6 required for floral repression in *Arabidopsis*. Plant Cell **17:** 2647-2660

Choi K, Park C, Lee J, Oh M, Noh B, Lee I (2007) Arabidopsis homologs of components of the SWR1 complex regulate flowering and plant development. Development **134:** 1931-1941

Cvrckova F (2000) Are plant formins integral membrane proteins? Genome Biol **1:** RESEARCH001

Deal RB, Kandasamy MK, McKinney EC, Meagher RB (2005) The Nuclear Actin-Related Protein ARP6 Is a Pleiotropic Developmental Regulator Required for the Maintenance of *FLOWERING LOCUS C* Expression and Repression of Flowering in *Arabidopsis*. Plant Cell **17:** 2633-2646

Deal RB, Topp CN, McKinney EC, Meagher RB (2007) Repression of flowering in *Arabidopsis* requires activation of *FLOWERING LOCUS C* expression by the histone variant H2A.Z. Plant Cell **19:** 74-83

Deeks MJ, Cvrckova F, Machesky LM, Mikitova V, Ketelaar T, Zarsky V, Davies B, Hussey PJ (2005) Arabidopsis group Ie formins localize to specific cell membrane domains, interact with actin-binding proteins and cause defects in cell expansion upon aberrant expression. New Phytol **168:** 529-540

Doyle JJ, Doyle JL, Brown AHD, Grace JP (1990) Multiple origins of polyploids in the *Glycine tabacina* complex inferred from chloroplast DNA polymorphism. Proc. Natl. Acad. Sci. **87:** 714-717

Gallagher K, Smith LG (2000) Roles for polarity and nuclear determinants in specifying daughter cell fates after an asymmetric cell division in the maize leaf. Curr Biol **10:** 1229-1232.

Gaudin V, Libault M, Pouteau S, Juul T, Zhao G, Lefebvre D, Grandjean O (2001) Mutations in LIKE HETEROCHROMATIN PROTEIN 1 affect flowering time and plant architecture in Arabidopsis. Development **128:** 4847-4858

Gilliland LU, Kandasamy MK, Pawloski LC, Meagher RB (2002) Both vegetative and reproductive actin isovariants complement the stunted root hair phenotype of the *Arabidopsis act2-1* mutation. Plant Physiol. **130:** 2199-2209.

Gilliland LU, McKinney EC, Asmussen MA, Meagher RB (1998) Detection of deleterious genotypes in multigenerational studies. I. Disruptions in individual *Arabidopsis* actin genes. Genetics **149:** 717-725.

Gilliland LU, Pawloski LC, Kandasamy MK, Meagher RB (2003) *Arabidopsis* actin gene *ACT7* plays an essential role in germination and root growth. Plant J **33:** 319-328
Guyomarc'h S, Bertrand C, Delarue M, Zhou DX (2005) Regulation of meristem activity by chromatin remodelling. Trends Plant Sci **10:** 332-338

Hajdukiewicz P, Svab Z, Maliga P (1994) The small, versatile pPZP family of *Agrobacterium* binary vectors for plant transformation. Plant Mol Biol **25:** 989-994
He Y, Amasino RM (2005) Role of chromatin modification in flowering-time control. Trends Plant Sci **10:** 30-35

He Y, Doyle MR, Amasino RM (2004) PAF1-complex-mediated histone methylation of *FLOWERING LOCUS C* chromatin is required for the vernalization-responsive, winter-annual habit in *Arabidopsis*. Genes Dev **18:** 2774-2784

He Y, Michaels SD, Amasino RM (2003) Regulation of flowering time by histone acetylation in *Arabidopsis*. Science **302:** 1751-1754

Hussey PJ, Ketelaar T, Deeks MJ (2006) Control of the Actin Cytoskeleton in Plant Cell Growth. Annu Rev Plant Biol **57:** 109-125

Jacinto A, Baum B (2003) Actin in development. Mech Dev **120:** 1337-1349

Jefferson RA, Kavanagh TA, Bevan MW (1987) GUS fusions: beta-glucuronidase as a sensitive and versatile gene fusion marker in higher plants. Embo J **6:** 3901-3907
Jurgens G (2005) Cytokinesis in higher plants. Annu Rev Plant Biol **56:** 281-299

Kandasamy MK, Gilliland LU, McKinney EC, Meagher RB (2001) One plant actin isovariant, ACT7, is induced by auxin and required for normal callus formation. Plant Cell **13:** 1541-1554.

Ketelaar T, Allwood EG, Anthony R, Voigt B, Menzel D, Hussey PJ (2004) The actin-interacting protein AIP1 is essential for actin organization and plant development. Curr Biol **14:** 145-149

Kim SY, Michaels SD (2006) *SUPPRESSOR OF FRI 4* encodes a nuclear-localized protein that is required for delayed flowering in winter-annual *Arabidopsis*. Development **133:** 4699-4707

Kim T, Balish RS, Heaton ACP, McKinney EC, Meagher RB (2005) Engineering a Root-Specific, Repressor-Operator Gene Complex. Plant Biotech **3:** 571-582

Li Y, Dhankher O, Carreira L, Balish R, Meagher R (2005) Engineered overexpression of g-glutamylcysteine synthetase in plants confers high level arsenic and mercury tolerance. Env Tox & Chem **24:** 1376-1386

Livak KJ, Schmittgen TD (2001) Analysis of relative gene expression data using real-time quantitative PCR and the 2(-Delta Delta C(T)) Method. Methods **25:** 402-408

Maciver SK, Hussey PJ (2002) The ADF/cofilin family: actin-remodeling proteins. Genome Biol **3:** reviews3007

March-Diaz R, Garcia-Dominguez M, Florencio FJ, Reyes JC (2007) SEF, a new protein required for flowering repression in Arabidopsis, interacts with PIE1 and ARP6. Plant Physiol **143:** 893-901

Martin-Trillo M, Lazaro A, Poethig RS, Gomez-Mena C, Pineiro MA, Martinez-Zapater JM, Jarillo JA (2006) *EARLY IN SHORT DAYS 1 (ESD1)* encodes ACTIN-RELATED PROTEIN 6 (AtARP6), a putative component of chromatin remodelling complexes that positively regulates FLC accumulation in *Arabidopsis*. Development **133:** 1241-1252

Mathur J (2004) Cell shape development in plants. Trends Plant Sci **9:** 583-590

McKinney EC, Kandasamy MK, Meagher RB (2001) Small changes in the regulation of one *Arabidopsis* profilin isovariant, PRF1, alter seedling development. Plant Cell **13:** 1179-1191.

Meagher RB, Fechheimer M (2003) The Cytoskeletal Proteome of *Arabidopsis*. *In* E Meyerowitz, C Somerville, eds, Arabidopsis, Vol www.aspb.org/publications/arabidopsis/toc.cfm. Cold Spring Harbor Laboratory Press, Cold Spring Harbor, NY

Meagher RB, McKinney EC, Vitale AV (1999) The evolution of new structures: clues from plant cytoskeletal genes. Trends Genet **15:** 278-284

Michaels SD, Amasino RM (1999) *FLOWERING LOCUS C* encodes a novel MADS domain protein that acts as a repressor of flowering. Plant Cell **11:** 949-956

Minakhina S, Myers R, Druzhinina M, Steward R (2005) Crosstalk between the actin cytoskeleton and Ran-mediated nuclear transport. BMC Cell Biol **6:** 32

Miralles F, Visa N (2006) Actin in transcription and transcription regulation. Curr Opin Cell Biol **18:** 261-266

Mizuguchi G, Shen X, Landry J, Wu WH, Sen S, Wu C (2004) ATP-driven exchange of histone H2AZ variant catalyzed by SWR1 chromatin remodeling complex. Science **303:** 343-348

Murashige T, Skoog F (1962) A revised medium for rapid growth and bioassays with tobacco tissue culture. Plant Physiol. **15:** 473-497

Nebl G, Meuer SC, Samstag Y (1996) Dephosphorylation of serine 3 regulates nuclear translocation of cofilin. J Biol Chem **271:** 26276-26280

Oh S, Zhang H, Ludwig P, van Nocker S (2004) A mechanism related to the yeast transcriptional regulator *Paf1c* is required for expression of the *Arabidopsis FLC/MAF MADS* box gene family. Plant Cell **16:** 2940-2953

Ohta Y, Nishida E, Sakai H, Miyamoto E (1989) Dephosphorylation of cofilin accompanies heat shock-induced nuclear accumulation of cofilin. J Biol Chem **264:** 16143-16148

Olave IA, Reck-Peterson SL, Crabtree GR (2002) Nuclear actin and actin-related proteins in chromatin remodeling. Annu Rev Biochem **71:** 755-781

Pawloski LC, Kandasamy MK, Meagher RB (2006) The late pollen actins are essential for normal male and female development in Arabidopsis. Plant Mol Biol **62:** 881-896

Pederson T, Aebi U (2005) Nuclear actin extends, with no contraction in sight. Mol Biol Cell **16:** 5055-5060

Pendleton A, Pope B, Weeds A, Koffer A (2003) Latrunculin B or ATP depletion induces cofilin-dependent translocation of actin into nuclei of mast cells. J Biol Chem **278:** 14394-14400

Putterill J, Robson F, Lee K, Simon R, Coupland G (1995) The *CONSTANS* gene of *Arabidopsis* promotes flowering and encodes a protein showing similarities to zinc finger transcription factors. Cell **80:** 847-857

Ruegg J, Holsboer F, Turck C, Rein T (2004) Cofilin 1 is revealed as an inhibitor of glucocorticoid receptor by analysis of hormone-resistant cells. Mol Cell Biol **24:** 9371-9382

Ruhl DD, Jin J, Cai Y, Swanson S, Florens L, Washburn MP, Conaway RC, Conaway JW, Chrivia JC (2006) Purification of a human SRCAP complex that remodels chromatin by incorporating the histone variant H2A.Z into nucleosomes. Biochemistry **45:** 5671-5677

Ruzicka D, Burgos-Rivera B, Kandasamy MK, McKinney EC, Meagher RB (In prep) An ancient subfamily of plant actin depolymerizing factors with roles tricoblast development and pollen tube tip growth.

Ruzicka D, Kandasamy MK, McKinney EC, Bursos-Rivera B, King-Reid L, Meagher RB (2007) The ancient subclasses of *Arabidopsis* actin depolymerizing factor genes exibit novel and differential expression. Plant J. **Accepted with Revisions**

Sarmiere PD, Bamburg JR (2004) Regulation of the neuronal actin cytoskeleton by ADF/cofilin. J Neurobiol **58:** 103-117

Sekinger EA, Moqtaderi Z, Struhl K (2005) Intrinsic histone-DNA interactions and low nucleosome density are important for preferential accessibility of promoter regions in yeast. Mol Cell **18:** 735-748

Smith LG (2001) Plant cell division: building walls in the right places. Nat Rev Mol Cell Biol **2:** 33-39.

Tanaka K, Nishio R, Haneda K, Abe H (2005a) Functional involvement of *Xenopus* homologue of ADF/cofilin phosphatase, slingshot (XSSH), in the gastrulation movement. Zoolog Sci **22:** 955-969

Tanaka K, Okubo Y, Abe H (2005b) Involvement of slingshot in the Rho-mediated dephosphorylation of ADF/cofilin during *Xenopus* cleavage. Zoolog Sci **22:** 971-984

Valverde F, Mouradov A, Soppe W, Ravenscroft D, Samach A, Coupland G (2004) Photoreceptor regulation of CONSTANS protein in photoperiodic flowering. Science **303:** 1003-1006

Vega-Palas MA, Ferl RJ (1995) The Arabidopsis Adh gene exhibits diverse nucleosome arrangements within a small DNase I-sensitive domain. Plant Cell **7:** 1923-1932

Visa N (2005) Actin in transcription. Actin is required for transcription by all three RNA polymerases in the eukaryotic cell nucleus. EMBO Rep **6:** 218-219

Wang YS, Motes CM, Mohamalawari DR, Blancaflor EB (2004) Green fluorescent protein fusions to *Arabidopsis* fimbrin 1 for spatio-temporal imaging of F-actin dynamics in roots. Cell Motil Cytoskeleton **59:** 79-93

Williams L, Fletcher JC (2005) Stem cell regulation in the *Arabidopsis* shoot apical meristem. Curr Opin Plant Biol **8:** 582-586

Yanovsky MJ, Kay SA (2002) Molecular basis of seasonal time measurement in Arabidopsis. Nature **419:** 308-312

Yuan GC, Liu YJ, Dion MF, Slack MD, Wu LF, Altschuler SJ, Rando OJ (2005) Genome-scale identification of nucleosome positions in *S. cerevisiae*. Science **309:** 626-630

Zhang H, Reese JC (2007) Exposing the core promoter is sufficient to activate transcription and alter coactivator requirement at RNR3. Proc Natl Acad Sci U S A

Zimmermann P, Hirsch-Hoffmann M, Hennig L, Gruissem W (2004) GENEVESTIGATOR. *Arabidopsis* microarray database and analysis toolbox. Plant Physiol **136:** 2621-2632

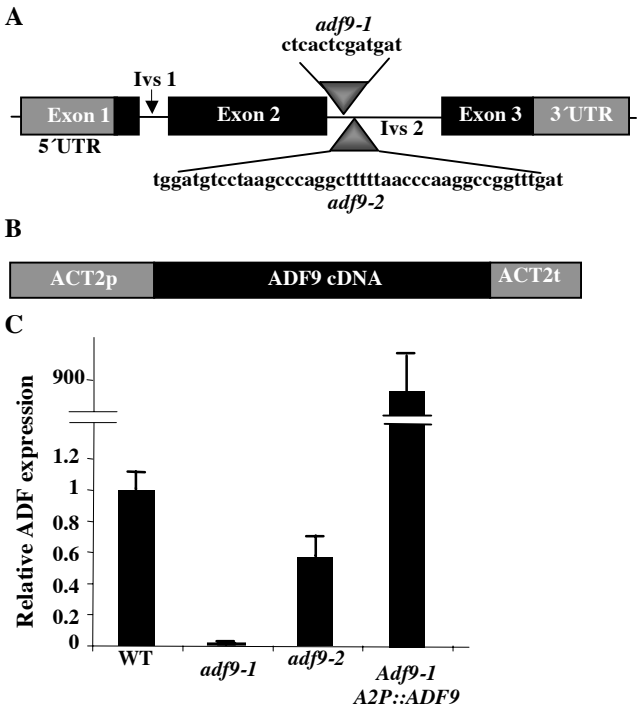

Figure A1.1 Gene constructs and reduced mRNA expression in *adf9-1* and *adf9-2* mutants. A, The T-DNA insertions in *adf9-1* and *adf9-2* were both located within intron 2, were separated at their 5´ ends by 37 bp, and were not overlapping. The intron sequences deleted from each intron and replaced by T-DNA are shown for each insertion. B, The cDNA encoding region of *ADF9* was cloned within the actin *ACT2* constitutive expression cassette *A2pt*. *A2pt::ADF9* was used to complement *adf9-1*. C, The *adf9-1* and *adf9-2* mutations produced a 95% and 50% drop in levels of transcript relative to wild-type, respectively. One possibility is that the *adf9-1* insertion disrupts an important enhancer. Complementing *adf9-1* with *A2pt::ADF9* resulted in an approximately 900-fold increase in ADF9 transcript levels over wild-type.

Figure A1.2 Morphological phenotypes for *adf9-1* and *adf9-2*. A, Twelve-day-old *adf9-1* and *adf9-2* mutant seedlings are smaller compared to wild-type. B, Mutants have an increase of apical dominance in the inflorescence as revealed by a decrease number of secondary branches and longer branches compared to wild-type. C, *adf9-1* and *adf9-*

2 mutants flower earlier with fewer rosette leaves than wild-type under long-day growth. D, *adf9-1* flowers at same time as wild-type under short-day growth conditions.

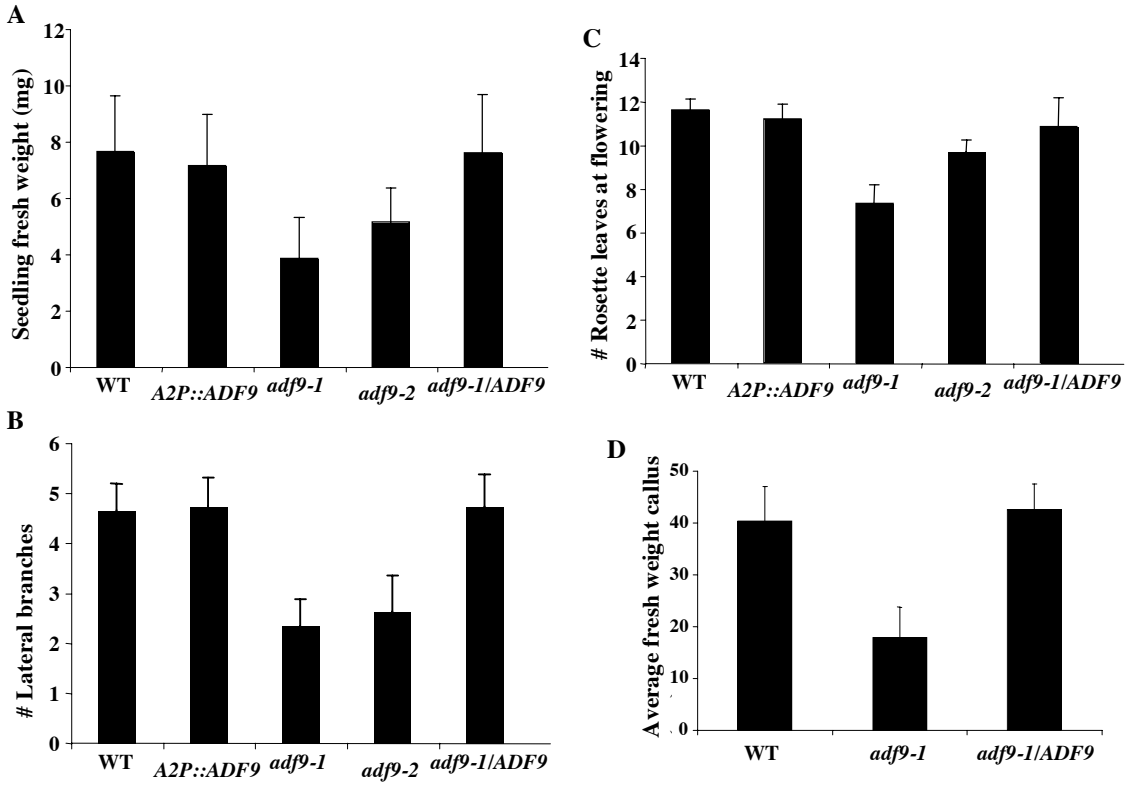

Figure A1.3 Quantification of *adf9-1* and *adf9-2* mutant phenotypes and complemented lines. A, The weight of 12-day-old *adf9-1* and *adf9-2* mutant seedlings was compared to wild-type and *adf9-1* mutant line complemented with the cDNA expression clone *A2p::ADF9*. B, A comparison was made of the number of secondary branches and longer branches compared to wild-type and *adf9-1* complemented with the ADF9 cDNA. C, Early flowering was assayed as the number of rosette leaves at the time the inflorescence first emerges is compared. D, The average fresh weight of callus was measured after two weeks on callus induction media. Ten or more seedlings or plants or root callus samples were measured for each assay. Error bars represent the standard error from the mean.

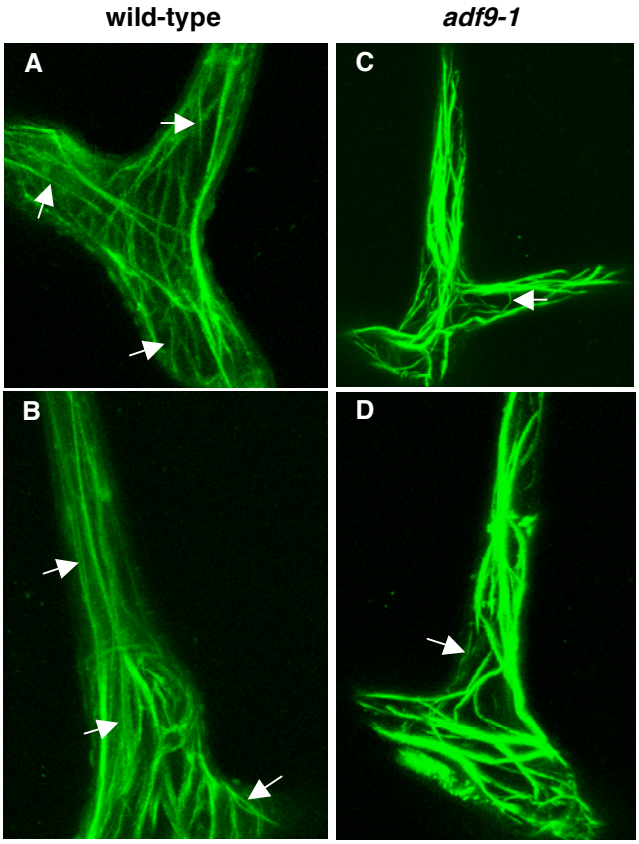

Figure A1.4 F-actin structure in the *adf9-1* mutant trichomes. The GFP/fABD2 construct was used as a fluorescent reporter of actin filaments and bundles. A and B, Wild-type trichomes. C and D, *adf9-1* trichomes. Arrows indicate fine filaments.

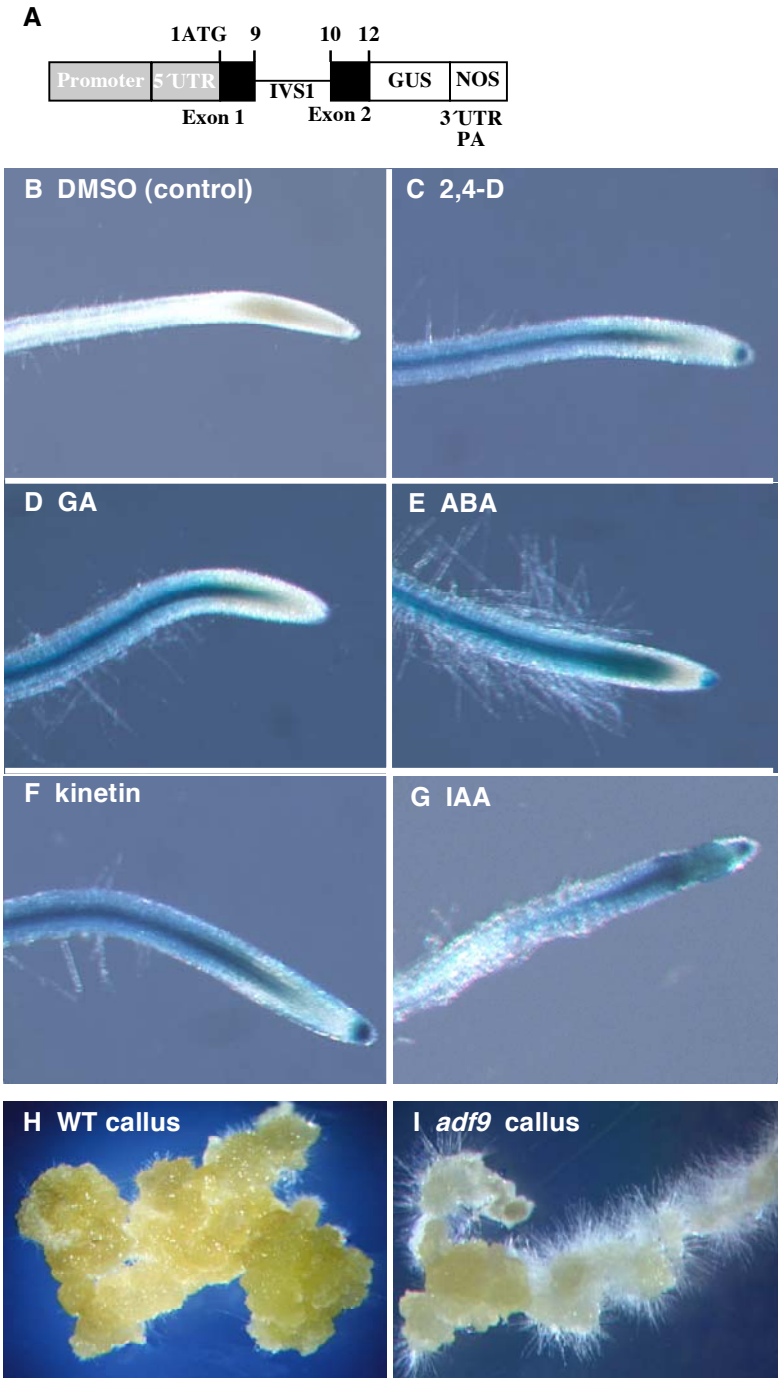

Figure A1.5 Hormone induction of ADF9p::GUS expression and *adf9-1* defective callus formation. A, *ADF9pi:GUS* is the reporter for *ADF9* promoter activity. The fusion is composed of the ADF9 promoter, first exon, first intron (ivs), and first codon of exon 2

fused in frame to *b-glucuronidase (GUS),* and a 3´ UTR and polyadenylation region from *Nopaline Synthase (NOS)* (Ruzicka et al., 2007). B to G,12-day-old seedlings containing the *ADF9p::GUS* promoter-reporter fusion were subjected to 24 hr treatment with phytohormones indicated, assayed briefly for b-glucuronidase (GUS) activity, and compared to seedlings treated only with DMSO, the solvent for each hormone. B, DMSO control (~1 mM). C, 10 mM 2,4,-dichlorophenoxyacetic acid (2,4,-D). D, 10 mM gibberellic acid (GA); E, 10 mM abscisic acid (ABA); F, 10 mM kinetin; G, 10 mM indolacetic acid (IAA). H & I. Samples of callus formed from root tissue are compared between wild-type (H) and *adf9-1* (I). See **Figure A.3** for quantification of this phenotype.

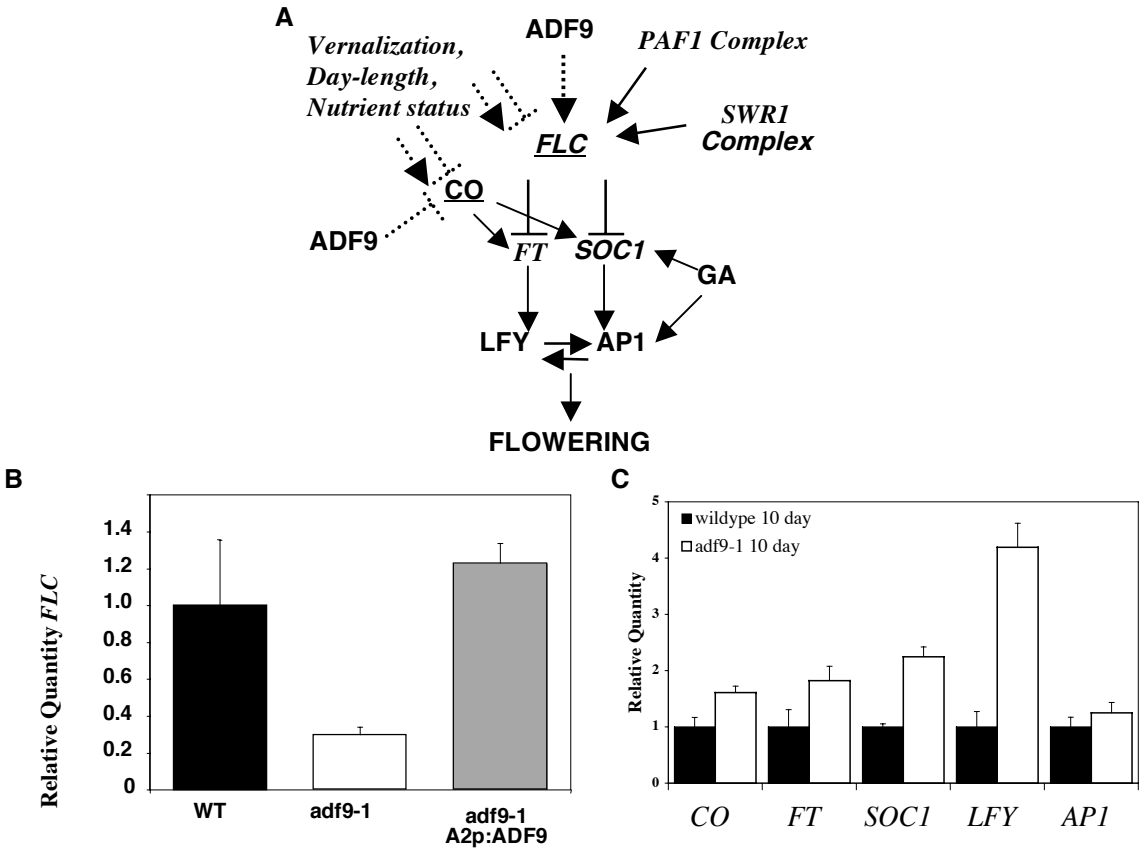

Figure A1.6 ADF9 alters expression of genes controlling flowering time. A, Model for the signaling that occurs in the transition to flowering, and the role of ADF9. FLC is a central repressor of this transition controlled by numerous environmental cues and factors that act via diverse changes in chromatin structure at the *FLC* locus. B, The *adf9-1* line had decreased levels of transcript encoding *FLC* relative to wild-type as assayed by qRT-PCR. FLC levels were restored in several independent lines complemented with *A2pt:ADF9*. C, qRT-PCR assays of transcript levels for several other activators of flowering.

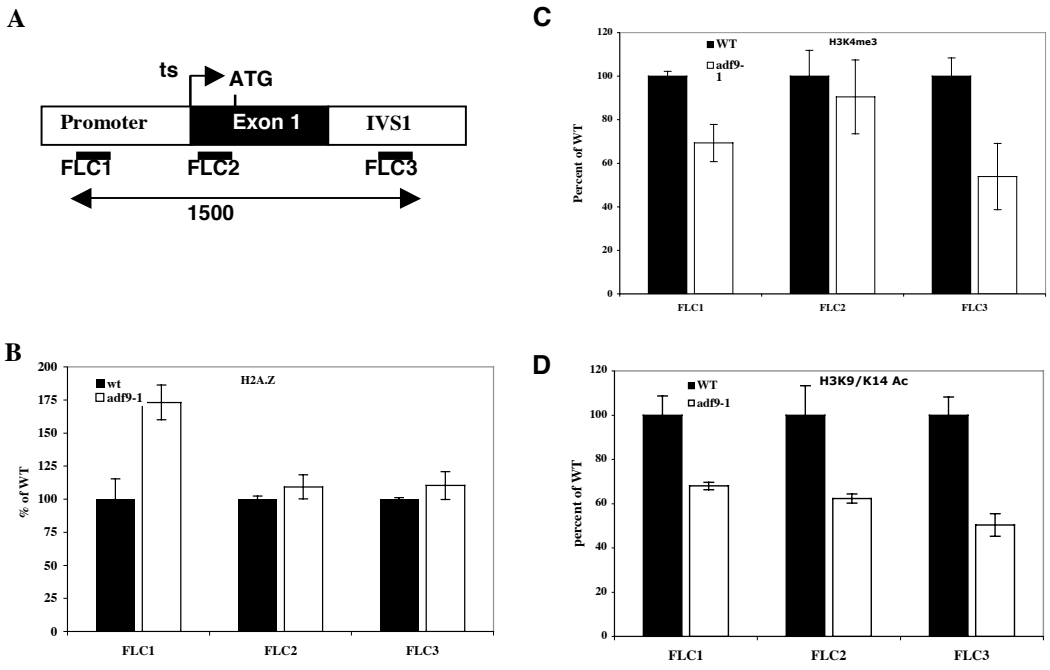

Figure A1.7 Chromatin remodeling phenotypes of *adf9-1* at the *FLC* locus. ChIP assays were performed on sheared *FLC* chromatin. A, qPCR was used to amplify products within the promoter (FLC1), at the start start of transcription (ts, FLC2), and in the first intron (ivs, FLC3). ChIP assays were performed to examine: B, H2A.Z deposition; C, histone H3 trimethylation at lysine 4 (H3K4Me3); and D, H3 acetylation at lysine 9 and 14 (H3K9K14Ac).

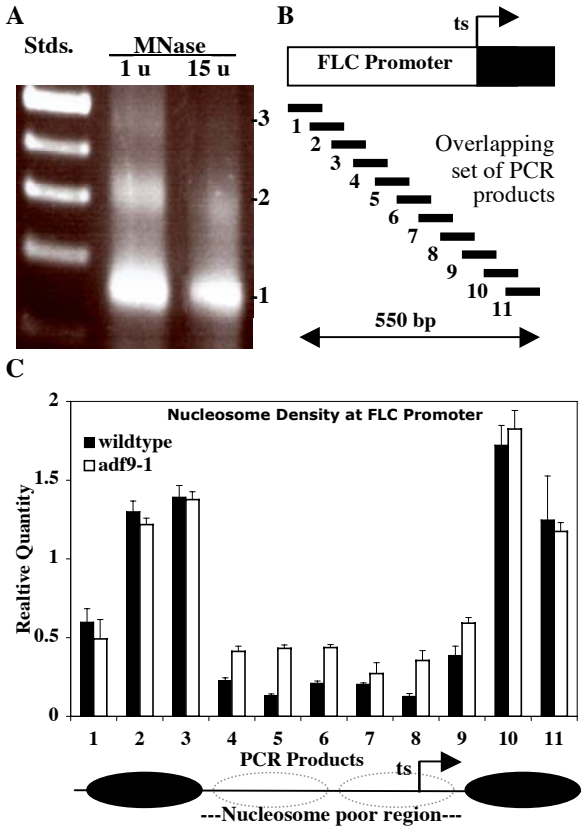

Figure A1.8. Nucleosome occupancy in the *FLC* promoter region. A, Arabidopsis nucleosomal DNA separated on an agarose gel and fluorescently stained with ethidium. Size standard ladder (Stds.); The two samples of DNA were prepared from nucleosomes digested with micrococcal nuclease (MNase) at 1 unit (u) and 15 units per 300 ml reaction. The position of mono- (1), di- (2), and tri-nucleosomes (3) are indicated. DNA from the 15 u digestion was examined in plate C. B, Location of qPCR primers used to assay nucleosome protected DNA relative to a map of the *FLC* promoter region. C, Nucleosome scanning assay the promoter region of *FLC* in wild-type and the *adf9-1* mutant presented as the Relative Quantity of PCR amplification of

the 11 products mapped in A. Standard errors are indicated for three replicate experiments. The normalized RQ values for purified gDNA = 1 for all products and are not shown. Possible nucleosome positions and the nucleosome poor region are indicated below the graph.

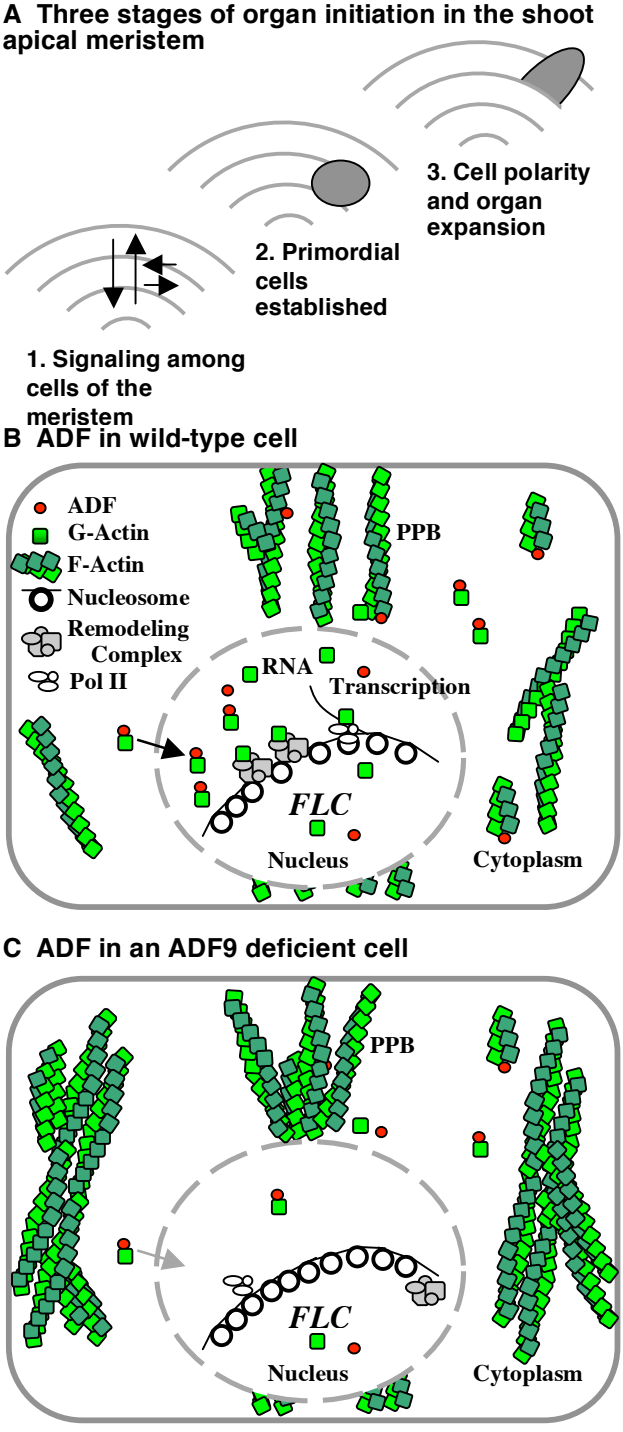

Figure A1.9 Model for the cytoplasmic and nuclear activities of ADF9 in the meristem. A, A model for the development of organs from the shoot apical meristem is

divided into three stages: (1) morphogenic signaling among cells; (2) establishment of primordial cells; and (3) determination of cell polarity and organ expansion. B, Cellular model of ADF9 participating in division plane determination in the cytoplasm and in nuclear chromatin remodeling at the FLC locus. The actin cytoskeleton is essential to cell polarity and development, because of its role in the early positioning of the preprophase band (PPB) of actin filaments upon which the division plane is assembled. ADF also shuttles actin into the nucleus where it participates in the majority of chromatin remodeling machines that have been described so far. The *FLC* gene is regulated by diverse chromatin remodeling activities, and most remodeling machines have an actin subunit. C, ADF9 deficiency (i.e., in the *adf9-1* mutant) results in altered actin polymerization in the cytoplasm affecting PPB formation and altered development (stages 2 and 3 above); it also results in reduced levels of actin in the nucleus result in changes in chromatin structure, changes in gene expression, and altered development (stage 1 above). One particular interpretation of the data in this manuscript is that loss of ADF9 function resulted in lower *FLC* expression due to defect in *FLC* chromatin structure.

Appendix 1 Supplemental Section A1.S1 Micrococcal Nuclease Protection Assay Experimental Protocol

Nucleosomal DNA preparation – This protocol for nucleosome preparation was modified from Vega-Palas and Ferl (1995). The nuclear scanning assay of nucleosome occupancy uses PCR amplification of nested products of MNase digested nucleosomal DNA as first reported by Sekinger et al. (2005).

1. Collect 0.75 grams of leaf or seedling tissue and freeze in liquid nitrogen
2. Grind frozen tissue with mortar/pestle in liquid nitrogen, transfer to fresh mortar/pestle with 5 ml HBM buffer (below) and regrind thawed tissue.
3. Filter through two layers of Miracloth into 15 ml Falcon Tube on ice.
4. Spin at 2000g 4°C for 10 minutes
5. Carefully remove and discard supernatant, and resuspend pellet in 1 mL of HBB buffer (below).
6. Spin at 200g 4° C for 2 min
7. Carefully remove and discard supernatant, and resuspend crude nuclear pellet in 300 μL TNE Buffer.
8. Add 15 units of Micrococcal nuclease (MNase) per 300 ml reaction and digest at 37° C for 3 minutes. Using nucleosomes from leaf tissue this condition produced the nearly complete digestion to mononucleosomes presented in Figure 8A. (MNase from Roche Scientific, Inc., #10107921001 from *Staphylococcus aureus*, 1 mg/15,000 units, Stock 15 u/ul in 50% glycerol and PBS)

9. Add 2.5 μL 0.5M EDTA to stop the reaction and spin at max for 3 minutes
10. Keep supernatant and discard pellet, add 1 μL RNaseA (boiled) to solution and incubate at room temp for 20 minutes.
11. Add 1 vol. phenol/chloroform/isoamyl alcohol to solution, vortex, and spin max 3 minutes
12. Remove aqueous phase to a fresh tube and add 1/10 vol. 3M sodium acetate (pH 5.2), 2 vol. 95% ethanol, and 2 μL glycogen (20 mg/ml in d-water, Roche Cat. 901393). Chill at -80° C for at least 20 minutes.
13. Spin at 4° C max speed for 15 minutes, wash pellet with cold 1 ml 75% ethanol, and spin at 4° C max speed for 15 minutes.
14. Carefully remove ethanol and dry on bench for 5 minutes. Resuspend pellet in 40mL dH_2O.
15. Run 10 mL on 2% agarose gel to confirm mono-nucleosome purity.

Real Time qPCR amplifications

1. Quantitative PCR control reactions for primer amplification efficiency on purified non-nucleosomal DNA.
    a. DNA was purified using a CTAB protocol (Doyle et al., 1990).
    b. DNA concentration (1 ng/reaction) and primer concentration of 0.5 mM following the protocol for SYBR green detection chemistry recommended by ABI.
2. Quantitative PCR reactions on nucleosomal DNA

a. From the 40 ml of resuspended nucleosomal DNA dilute the DNA 1/25 to 1/50 fold for qPCR reactions. Use 5 ml of that dilution per reaction. Primer concentrations of 0.5 mM. Again follow SYBR green detection chemistry.

Real Time qPCR calculations of the Relative Quantity (RQ) of nucleosome-protected DNA in *adf9-1* vs wild-type.

1. We will consider the PCR primer product #5 within the *FLC* locus in Figure 8 in the text as an example: where the product for #5 is P5 and for actin *ACT2* is A2; where plant samples for wild-type nucleosomal DNA is WT and for *adf9-1* is *a9*; where genomic wild-type DNA is gDNA; Nucleosomal is Nuc.; and where CT is the cycle threshold value.
2. Relative Quantity calculation for P5 amplification based on a calculation of the ddCT of dCT values.
    a. dCT for gDNA of P5 is measured relative to actin A2
        i. dCT of $P5_{gDNA} = CT_{gDNAp5}\text{-}CT_{gDNAA2} = 24.216\text{-}23.949 = 0.267$
    b. dCT for nucleosomal P5 DNA is measured relative to actin in the WT sample and the experimental a9 sample.
        i. dCT of $P5_{WT} = CT_{WTp5}\text{-}CT_{WTA2} = 24.601\text{-}21.418 = 3.183$
        ii. dCT of $P5_{a9} = CT_{a9p5}\text{-}CT_{a9A2} = 22.801\text{-}21.32 = 1.481$
3. RQ is estimated from the ddCT
    a. gDNA $P5_{gDNA}$ $RQ_{ddCT} = 2^{-ddCT} = 2^{-(dCT_{gDNA}\text{-}dCT_{gDNA})} = 2^{-(0.267\text{-}0.267)} = 1.0$
    b. Nuc. $P5_{WT}$ $RQ_{ddCT} = 2^{-ddCT} = 2^{-(dCT_{WTP5}\text{-}dCT_{gDNA})} = 2^{-(3.183\text{-}0.267)} = 0.132$

c. Nuc. $P5_{a9}$ $RQ_{ddCT} = 2^{-ddCT} = 2^{-(dCT_{a9P5}-dCT_{gDNA})} = 2^{-(1.481-0.267)} = 0.431$

d. These RQ_{ddCT} values for P5 in WT and a9 samples are the same as those shown in Figure 8 in the main text. The normalized RQ for all gDNA products = 1 and are not shown.

Buffers:

HBM

25 mM Tris pH 7.6
0.44 M Sucrose
10 mM $MgCl_2$
0.1% Triton-X
2 mM Spermidine
10 mM B-mercaptoethanol

HBB

Same as HBM except no spermidine and increase Triton-X to 0.5%

TNE

10 mM Tris pH 8.0
100 mM NaCl
5 mM $MgCl_2$
1 mM EDTA
4 mM $CaCl_2$

PCR Primer Design

To obtain primers with the specific spacing and specificity needed for the nucleosomal scanning assay, oligonucleotide were designed to have estimated $tm_{1/2}$ values of 58 to 62°C based on the summation of 2°C/AT bp and 4°C/GC bp suggested for short oligonucleotides (Maniatis et al., 1989) or estimated $tm_{1/2}$ values of 50 to 54°C following the primer design program at Oligo Analyzer (www.IDTDNA.com). When

possible the primer locations were moved up or downstream a few nucleotides to position A or T residues on the 3´end of each primer following the observation that this improves target specificity and lowers background amplification of inappropriate products (Crameri and Stemmer, 1993).

REFERENCES

Crameri A, Stemmer WP (1993) 10(20)-fold aptamer library amplification without gel purification. Nucleic Acids Res **21:** 4410

Doyle JJ, Doyle JL, Brown AHD, Grace JP (1990) Multiple origins of polyploids in the *Glycine tabacina* complex inferred from chloroplast DNA polymorphism. Proc. Natl. Acad. Sci. **87:** 714-717

Maniatis T, Fritsch EF, Sambrook J (1989) Calculating melting temperatures for perfectly matched hybrids between oligonucleotides and their target sequences. *In* Molecular cloning: A laboratory Manual, Vol 2. Cold Spring Harbor laboratory Press, Cold Spring Harbor, New York, p 11.46

Sekinger EA, Moqtaderi Z, Struhl K (2005) Intrinsic histone-DNA interactions and low nucleosome density are important for preferential accessibility of promoter regions in yeast. Mol Cell **18:** 735-748

Vega-Palas MA, Ferl RJ (1995) The Arabidopsis Adh gene exhibits diverse nucleosome arrangements within a small DNase I-sensitive domain. Plant Cell **7:** 1923-1932